

TRANSPORTATION RESEARCH  
**RECORD**

No. 1440

*Soils, Geology, and Foundations*

---

**Design and Performance of  
Stabilized Bases, and  
Lime and Fly Ash  
Stabilization**

*A peer-reviewed publication of the Transportation Research Board*

**TRANSPORTATION RESEARCH BOARD  
NATIONAL RESEARCH COUNCIL**

**NATIONAL ACADEMY PRESS  
WASHINGTON, D.C. 1994**

**Transportation Research Record 1440**

ISSN 0361-1981

ISBN 0-309-05521-0

Price: \$24.00

**Subscriber Category**

IIIA soils, geology, and foundations

Printed in the United States of America

**Sponsorship of Transportation Research Record 1440**

**GROUP 2—DESIGN AND CONSTRUCTION OF  
TRANSPORTATION FACILITIES**

*Chairman: Charles T. Edson, Greenman Pederson, Inc.*

**Geomaterials Section**

*Chairman: J. M. Hoover, Iowa State University*

**Committee on Cementitious Stabilization**

*Chairman: Mumtaz A. Usmen, Wayne State University*

*Richard L. Berg, William N. Brabston, Dave Ta-Teh Chang, James L. Eades, Donald G. Fohs, Harry L. Francis, K. P. George, J. M. Hoover, Khaled Ksaibati, Harold W. Landrum, Dallas N. Little, Larry Lockett, Kenneth L. McManis, Raymond K. Moore, Peter G. Nicholson, Robert G. Packard, Thomas M. Petry, Lutfi Raad, C. D. F. Rogers, Roger K. Seals, Doug Smith, Sam I. Thornton, Samuel S. Tyson, LaVerne Weber, Anwar E. Z. Wissa*

**Transportation Research Board Staff**

*Robert E. Spicher, Director, Technical Activities*

*G. P. Jayaprakash, Engineer of Soils, Geology, and Foundations*

*Nancy A. Ackerman, Director, Reports and Editorial Services*

*Alison G. Tobias, Editor*

The organizational units, officers, and members are as of December 31, 1993.

# Transportation Research Record 1440

---

## Contents

<b>Foreword</b>	<b>v</b>
<b>High-Strength Stabilized Base Thickness Design Procedure</b> <i>Marshall R. Thompson</i>	<b>1</b>
<b>Performance Evaluation of a Cement-Stabilized Fly Ash Base</b> <i>D. H. Gray, E. Tons, and T. R. Thiruvengadam</i>	<b>8</b>
<b>Field Performance Evaluation of Cement-Treated Bases With and Without Fly Ash</b> <i>Khaled Ksaibati and Travis L. Conklin</i>	<b>16</b>
<b>Cement-Stabilized Open-Graded Base Strength Testing and Field Performance Versus Cement Content</b> <i>Michael Hall</i>	<b>22</b>
<b>Estimating the Design Life of a Prototype Cement-Stabilized Phosphogypsum Pavement</b> <i>D. M. Gerrity, J. B. Metcalf, and R. K. Seals</i>	<b>32</b>
<b>Selection of Design Strengths of Untreated Soil Subgrades and Subgrades Treated with Cement and Hydrated Lime</b> <i>Tommy C. Hopkins, David Q. Hunsucker, and Tony Beckham</i>	<b>37</b>
<b>Long-Term Performance of Flexible Pavements Located on Cement-Treated Soils</b> <i>Tommy C. Hopkins, David Q. Hunsucker, and Tony Beckham</i>	<b>45</b>
<b>Drained Shear Strength of Lime-Clay Mixes</b> <i>C. D. F. Rogers and S. J. Lee</i>	<b>53</b>

---

**Deep-Slope Stabilization Using Lime Piles**

**63**

*C. D. F. Rogers and S. Glendinning*

---

**Lime and Fly Ash Admixture Improvement of Tropical  
Hawaiian Soils**

**71**

*Peter G. Nicholson, Vinai Kashyap, and Clint F. Fujii*

---

# Foreword

This volume is dedicated to James M. Hoover, who was the Chair of the Geomaterials Section. Professor Hoover died on January 30, 1994, in Des Moines, Iowa. He was internationally known for his extensive research in soils and materials and had been associated with the Transportation Research Board since the 1950s.

The 10 papers in this volume cover design and performance of stabilized bases, and lime and fly ash stabilization of soils. Presented in these papers is information that is based on both laboratory and field investigations.

Thompson describes a pavement thickness design procedure that relates to high-strength stabilized bases, such as cement-aggregate mixtures and pozzolanic-stabilized material. Gray et al. provide information on the performance of a 7-year-old compacted, cement-stabilized fly ash base and Ksaibati and Conklin present the results of a field evaluation of pavement bases, which were with or without fly ash, treated with cement. The topic of Hall's paper is performance of the cement-stabilized open-graded base as a drainage layer and construction platform for concrete pavements. Gerrity et al. describe the performance of cement-stabilized phosphogypsum mixtures, and provide information on life-cycle costs of such mixtures. The two papers by Hopkins et al. describe a scheme developed using a mathematical model based on limit equilibrium for selecting design strengths of soil subgrades and subgrades treated with lime or cement; the second paper provides data on the performance of 6- to 30-year-old flexible pavements constructed over cement-treated soils.

The next two papers by Rogers et al. present the results of tests on lime-stabilized clay slopes, and laboratory and field investigation of lime piles emplaced in clay soils. In the last paper, Nicholson et al., describe how lime and fly ash admixtures affect properties of tropical soils.



# High-Strength Stabilized Base Thickness Design Procedure

MARSHALL R. THOMPSON

The basic concepts and the development of a high-strength stabilized-base (HSSB) thickness design procedure are presented. Cement-aggregate mixtures and pozzolanic-stabilized substances are typical HSSB materials. The proposed procedure is based on resilient soil and material testing procedures, the ILLI-PAVE stress-dependent modulus structural model, and design algorithms developed from an extensive ILLI-PAVE HSSB pavement response (stress, strain, deflection) data base. Required inputs are subgrade resilient modulus ( $E_{Ri}$ , ksi), HSSB modulus ( $E$ , ksi), asphalt concrete (AC) thickness ( $T_{AC}$ , in.) and modulus ( $E_{AC}$ , ksi), HSSB Design Compressive Strength (psi), and HSSB thickness ( $T$ , in.). The AC modulus and the HSSB modulus are used to convert the AC thickness ( $T_{AC}$ ) to an equivalent HSSB thickness. The thickness design criterion is FATIGUE of the HSSB pavement layer. The HSSB FATIGUE relation is based on the HSSB stress ratio, which is equal to HSSB design flexural stress/HSSB flexural strength. Traffic is considered in terms of 18-k equivalent single-axle loads (SAL). Simplified design charts are presented for routine HSSB design.

High-strength stabilized base materials are "cementitiously stabilized" coarse-grained materials characterized by high-strength and modulus properties. Typical HSSB materials are pozzolanic stabilized mixture (PSM), cement aggregate mixture, and similar types of high-quality cementitiously stabilized materials. Most HSSB materials are capable of developing cured compressive strengths in excess of 5 MPa (750 psi).

HSSB materials are generally used as base layers in pavement sections with minimum AC surface thicknesses. In some low traffic volume situations, surface treatments or lower quality asphalt-type surface courses are used. Cementitious stabilizers typically increase compressive strength, shear strength (large increase in cohesion), tensile strength (flexural and split tensile), and modulus of elasticity. Freeze-thaw and moisture resistance are significantly enhanced by stabilization. HSSB material durability is an important property and should be carefully considered in the HSSB mixture design process (in fact, durability requirements may control the mixture design proportions).

A summary of the strength, modulus, and fatigue properties for cementitiously stabilized materials has been presented in a previous University of Illinois project report (1). That report emphasized those areas of HSSB technology particularly relevant to thickness design considerations. Other recent references (2-5) are more comprehensive in scope.

## HSSB DESIGN: PERFORMANCE CONSIDERATIONS

Costigan and Thompson (6) summarized and analyzed the response and performance of nine cement-stabilized structural sec-

tions subjected to channelized traffic. Longitudinal cracking (starting at a transverse crack) indicated the initiation of structural failure. Wang and Kilaeski (7) noted similar cracking patterns in cement-stabilized sections trafficked in the Pennsylvania State University Test Track. American Association of State Highway Officials' Road Test cracking progression studies for thin and structurally inadequate nonreinforced jointed portland cement concrete sections also indicated that structural failure initiated with longitudinal cracking in the wheel path.

A recent Transport and Road Research Laboratory (TRRL) study (8) based on extensive field survey data for "lean concrete roads" also indicated that structural failure begins with "longitudinal cracks in the wheel path." TRRL suggests, "it is preferable for heavily trafficked roads to use a design that is sufficiently strong to resist longitudinal cracking." The TRRL study substantiated the validity of using flexural stress and flexural strength as indicators of the potential for developing "cracking"-type distress.

It is apparent that the critical thickness design consideration for the HSSB layer is longitudinal cracking based on edge-corner wheel loading conditions. For HSSB materials, the controlling thickness design criterion is the flexural stress at the bottom of the stabilized material layer.

## HSSB DESIGN CONCEPTS

The structural response and fatigue performance of the HSSB layer (for a given wheel loading) are influenced by the flexural strength, modulus, and thickness of the stabilized layer, the modulus and thickness of the AC surface course layer (if it is used), and the subgrade resilient modulus. HSSB materials of the same quality (strength, modulus) display similar structural responses. Thus HSSB thickness design concepts are independent of material type.

HSSB layer thickness can be established using an "intact layer" structural analysis approach (the HSSB layer is considered to be an "elastic layer," not an incompressible slab) and design concepts based on HSSB layer fatigue consumption (1,9). This approach is valid even though the HSSB layer may initially develop transverse shrinkage cracks. An adequate HSSB layer thickness prevents significant additional cracking [particularly the longitudinal outer wheel path cracking indicative of fatigue failure (6-8)] under traffic loading. HSSB fatigue life is estimated from the calculated stress ratio (SR). ( $SR = \text{HSSB flexural stress at the bottom of the layer-HSSB modulus of rupture}$ .) The mechanistic thickness design option in the American Coal Ash Association Flexible Pavement Manual (5) is based on these concepts and principles.

University of Illinois at Urbana-Champaign, Newmark Civil Engineering Laboratory MC-250, 205 North Mathews Avenue, Urbana, Ill. 61801-2397.

## HSSB DESIGN PROCEDURE DEVELOPMENT

### General

The proposed HSSB thickness design procedure is predicated on the fatigue failure of an "intact" HSSB layer with a nominal AC surface course [maximum of approximately 10 cm (4 in.)]. In this type of pavement structure, the AC radial strains are compressive and subgrade stresses are low. Thus, AC fatigue and subgrade rutting are not significant design criteria. The only thickness design criterion is fatigue consumption in the HSSB layer for considering longitudinal crack formation.

The HSSB fatigue algorithm (SR versus log number load applications to cracking) proposed for use in the Illinois DOT HSSB thickness design procedure (9) is shown in Figure 1. [Additional fatigue algorithms are given by Thompson (1)]. The HSSB thickness requirement is very sensitive to the fatigue algorithm selected. The proposed procedure can easily accommodate other fatigue algorithms considered appropriate by the user agency.

### Stress Ratio Calculations

The flexural stress at the bottom of the HSSB layer ( $\sigma$ ) can be estimated from an algorithm developed by Thompson (1) from a comprehensive ILLI-PAVE HSSB data base. The ILLI-PAVE analyses were based on a 9,000-lb circular load (80 psi pressure)

as a representation of one dual-wheel of the standard 18-kip (18,000-lb) single axle load. The ILLI-PAVE HSSB data base includes many representative HSSB pavement configurations, AC moduli, and HSSB moduli. The AC surface course thickness ranged from 0 (surface treatment) to 4 in. and HSSB thickness varied from 6 to 12 in.

The algorithm for estimating  $\sigma$  is

$$\log \sigma = 2.49 - 0.07 \text{ TEQ} + 0.0001 E - 0.0083 E_{Ri}$$

$$R^2 = 0.95$$

$$\text{SEE} = 0.059 \quad (1)$$

(Note: The AC surface plus HSSB layer pavement section is converted to an "equivalent" HSSB thickness, TEQ.)

$$\text{TEQ} = T + T_{AC} (E_{AC}/E)^{0.33} \quad (2)$$

Required inputs for Equations 1 and 2 are AC modulus ( $E_{AC}$ , ksi) and AC thickness ( $T_{AC}$ , in.); HSSB modulus ( $E$ , ksi) and HSSB thickness ( $T$ , in.); and subgrade resilient modulus ( $E_{Ri}$ , ksi). (NOTE:  $\sigma$  is in psi.)

AC modulus is significantly influenced by pavement AC temperature. Various procedures for estimating  $E_{AC}$ -mix temperature relations are presented in Appendix C4 of National Cooperative Highway Research Program (NCHRP) Project 1-26 (10). The Asphalt Institute AC modulus prediction procedure (11,12) is frequently used.

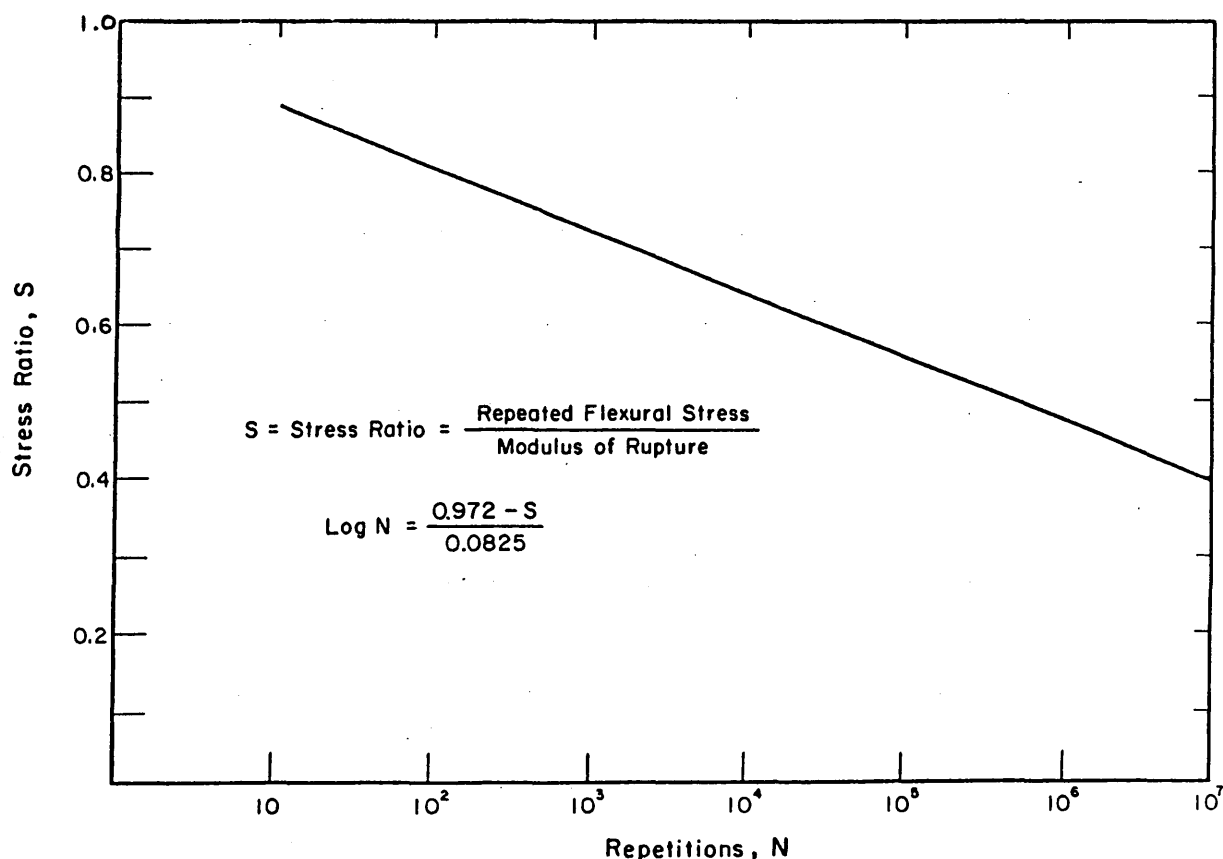


FIGURE 1 High-strength stabilized base fatigue algorithm (9).



A plot of  $E_{AC}/E$  versus  $(E_{AC}/E)^{0.33}$  is shown in Figure 2. For typical AC mixtures and pavement temperature fluctuations representative of a temperate climate (such as the midwestern United States), an  $(E_{AC}/E)^{0.33}$  value of 0.5 is recommended for general HSSB design calculations, although at times a higher value would be indicated. Portland Cement Association recommendations (13) support the general validity of the 0.5 "equivalency." Thus Equation 2 becomes

$$TEQ = T + 0.5 T_{AC} \quad (3)$$

For routine a priori thickness design purposes, approximate HSSB unconfined compressive strength—HSSB modulus and HSSB compressive strength—HSSB modulus of rupture relations are adequate (1). HSSB flexural strength can be estimated as 20 percent of the compressive strength. The HSSB modulus-compressive strength relation recommended for use in the proposed Illinois DOT procedure (9) is

$$E \text{ (ksi)} = 500 + \text{Compressive Strength (psi)} \quad (4)$$

Note: 1 ksi = 6.9 MPa.

Other HSSB modulus-HSSB strength relations are presented by Thompson (1).

Subgrade soil resilient behavior is characterized by the "resilient modulus," defined as

$$E_R = \text{DEV}/\epsilon_r$$

where

$E_R$  = resilient modulus,  
DEV = repeated deviator stress, and  
 $\epsilon_r$  = recoverable axial strain.

Repeated unconfined compression or triaxial testing procedures are often used to evaluate the resilient moduli of fine-grained soils

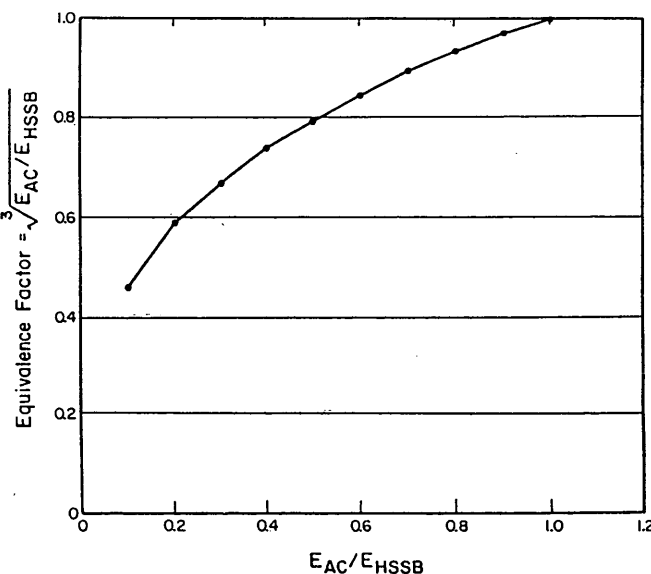


FIGURE 2 Equivalence factors for asphalt concrete surface.

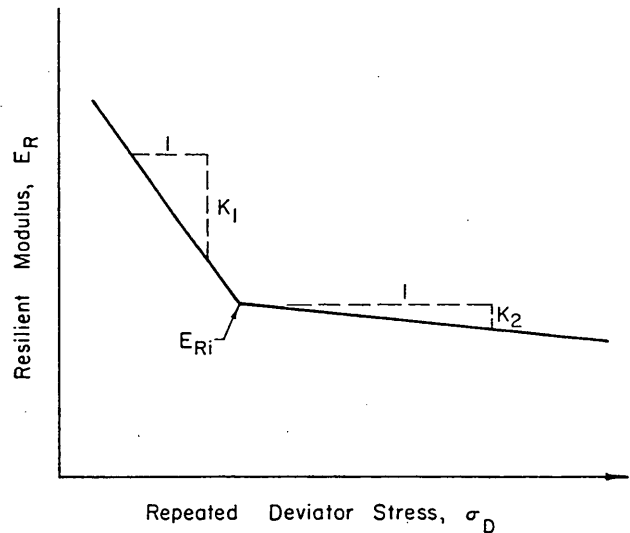


FIGURE 3 ILLI-PAVE stress-dependent fine-grained soil subgrade model.

and granular materials. Resilient moduli are stress dependent: fine-grained cohesive soils experience resilient modulus decreases with increasing stress, whereas granular materials stiffen with increasing stress level.

The arithmetic stress-dependent behavior model for fine-grained soils was used in developing the ILLI-PAVE HSSB data base (1). The model is shown in Figure 3. Extensive resilient laboratory testing, nondestructive pavement testing, and pavement analysis and design studies at the University of Illinois have indicated that the arithmetic model is adequate for flexible pavement analysis and design activities.

In the arithmetic model, the value of the resilient modulus at the break-point [at approximately 42 kPa (6 psi)] in the bilinear curve,  $E_{Ri}$  (see Figure 3) is a good indicator of a soil's resilient behavior. The slope values,  $K_1$  and  $K_2$ , are less variable and influence pavement structural response to a smaller degree than  $E_{Ri}$ .

Subgrade  $E_{Ri}$  can be established from laboratory testing, local experience and information, nondestructive testing, or estimated from soil classification data. Note that the flexural stress estimate is not sensitive to the  $E_{Ri}$  input.

Thompson and Robnett (14) developed a simplified procedure for estimating the resilient behavior of Illinois fine-grained soils. A regression equation for predicting  $E_{Ri}$  at optimum water content and 95 percent of maximum dry density AASHTO (American Association of State Highway and Transportation Officials) T-99 is

$$E_{Ri} \text{ (OPT)} = 4.46 + 0.098 (\% \text{CLAY}) + 0.119 (\text{PI})$$

where

$E_{Ri} \text{ (OPT)}$  =  $E_{Ri}$  (ksi) at optimum moisture content and 95% AASHTO T-99 maximum dry density,

% CLAY = Clay content (< 2 micron)

PI = Plasticity Index

Note: 1 ksi = 6.9 MPa.

Based on the extensive Illinois soils resilient testing data base Thompson and LaGrow (15) established typical " $E_{ri}$  decrease/1 percent moisture content increase" for various U.S. Department of Agriculture (USDA) textural classifications. The following values are useful for a priori pavement design activities:

USDA Textural Classification	$E_{ri}$ Decrease/1% Moisture Increase (ksi/%)
Clay, silty clay, silty clay loam	0.7
Silt loam	1.5
Loam	2.1

Note: 1 ksi = 6.9 MPa.

The  $E_{ri}$  (OPT) estimate should be adjusted to reflect in situ moisture conditions. For the high water table conditions that predominate in Illinois, the in situ subgrade soil moisture content is almost always in excess of AASHTO T-99 optimum, and frequently is near 100 percent saturation.

The general  $E_{ri}$  relationships shown in Table 1 were proposed by Thompson et al. (16) for the design of low-traffic volume air-field pavements. Various approaches that have been proposed for considering subgrade soil moduli are summarized in Appendix C5 of National Cooperative Highway Research Program Project 1-26 (10).

Examination of Equation 1 indicates that  $\sigma$  is primarily controlled by TEQ. Assuming a typical value for  $E_{ri}$  of 3 ksi and estimating  $E$  from compressive strength (see Equation 4), Equation 1 is simplified to

$$\text{Log } \sigma = 2.515 + 0.0001S - 0.07 \text{ TEQ} \quad (5)$$

where

TEQ = Equivalent thickness (in.),  
 $\sigma$  = HSSB flexural stress (psi), and  
 $S$  = HSSB compressive strength (psi).

Note: 1 psi = 6.9 kPa.

Considering the precision with which HSSB field strength can be estimated, the general variability of traffic loading conditions and field subgrade  $E_{ri}$  values, and so on, Equation 4 is considered to be acceptable for routine a priori pavement design activities. A

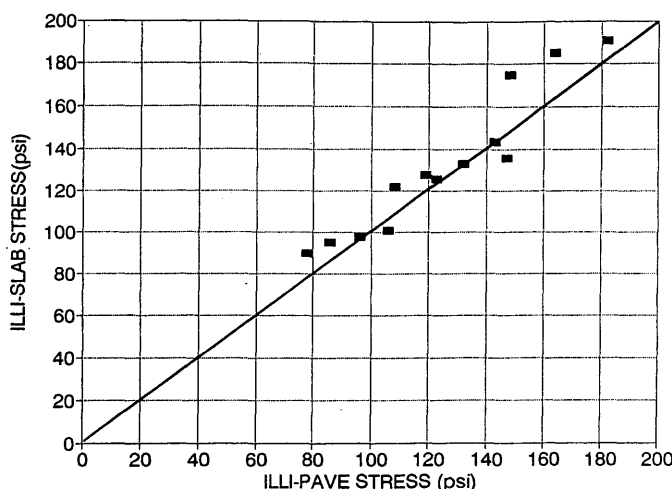


FIGURE 4 ILLI-SLAB/ILLI-PAVE stress calculation comparisons.

highway agency may select different typical values for  $E$  and  $E_{ri}$  from those used previously or elect to apply Equation 1 to each particular set of project design conditions.

The interior flexural stress (Equation 1 or 5) is increased by 50 percent to account for edge loading and HSSB transverse cracking effects (1). ILLI-SLAB analyses (for the condition of no load transfer between adjacent slabs) were conducted in NCHRP 1-26 (Calibrated Mechanistic Structural Analysis Procedures for Pavements) for some typical HSSB sections (TEQ from 8 to 12 in.) to further consider the multiplier factor. An "equivalent  $k$ " ( $k$ —modulus of subgrade reaction—is the subgrade support input for ILLI-SLAB) was established for each section by analyzing the ILLI-PAVE load-displacement data for the "interior" loading condition. The comparison, see Figure 4, indicates the stresses estimated by applying the 50 percent multiplier factor to Equation 1 compared favorably with ILLI-SLAB stresses for a location 18 in. from the pavement edge.

In a prepared discussion of *Transportation Research Record 1095* (6), Ioannides considered the multiplier factor approach

TABLE 1 Estimated Subgrade Resilient Modulus Values (16)

AASHTO Soil Class	Design Subgrade $E_{ri}$ , ksi			
	High Water Table*		Low Water Table**	
	With Frost	W/O Frost	With Frost	W/O Frost
A-4; A-5; A-6	2.0	4.0	3.0	6.0
A-7	2.0	5.0	3.5	7.0

\* Water table seasonally within 24 inches of subgrade surface

\*\* Water table seasonally within 72 inches of subgrade surface

NOTE: 1 ksi = 6.9 MPa

based on Westergaard analysis procedures. For typical HSSB highway pavement sections (radius of loaded area/radius of relative stiffness = 0.15), his recommended value for the multiplier would be about 65 percent.

Because the HSSB design is based on an "early life" compressive strength (a conservative approach) and some load transfer will occur between adjacent slabs, it is recommended that for an a priori pavement design, the 50 percent multiplier factor be used for increasing the HSSB interior stress to estimate the edge stress.  $\sigma_F$ , the "design flexural stress" ( $\sigma_F = 1.5 \sigma$ ) should be used to calculate the SR for HSSB thickness design.

### HSSB Compressive Strength

The proposed design procedure is predicated on the concept that HSSB modulus and flexural strength can be estimated from the cured HSSB compressive strength. HSSB strength development is dependent on many factors (HSSB mixture ingredients and proportions, mixing efficiency, field compaction, curing conditions: time-temperature-moisture, etc.). Freeze-thaw action typically effects an HSSB strength decrease. It is not possible to accurately predict (in a typical a priori design scenario) HSSB strength as a function of time after construction.

Examination of the input parameters in Equation 1 indicates the significant effect of HSSB modulus. In addition to the constantly changing (particularly in the early life of a HSSB pavement) HSSB strength and modulus, the AC modulus fluctuates with temperature. Thus the load-related HSSB flexural stresses also change with time. Cumulative damage accumulation for a range of SRs can be considered by using Miner's procedure:

$$\text{Fatigue damage (\%)} = P_i \quad (6)$$

$$P_i = (N_i/N_{Ti})100 \quad (7)$$

where

$P_i$  = percent fatigue life consumption for  $SR_i$ ,

$N_i$  = number of 18k SAL applied at  $SR_i$ ,

$N_{Ti}$  = number of load applications to failure for  $SR_i$  from Figure 1, and

$n$  = number of SRs considered.

Failure is assumed when the cumulative fatigue damage is 100 percent.

It is difficult to calculate an SR for a particular time and accurately predict the pavement life for several years hence. The application of load repetitions at a high SR (which may occur in the early curing stages when HSSB strength is low) will effect considerable fatigue consumption.

Although an "iterative procedure," which considers that HSSB strength-modulus-time relations for the field-cured HSSB mixture is conceptually and theoretically sound, it is not practical for inclusion in an a priori HSSB thickness design procedure. To simplify the procedure and facilitate the practical application of mechanistic-based concepts, HSSB layer fatigue consumption is calculated on the basis of the HSSB properties (compressive strength and modulus) for specific mixture design procedures, curing conditions (temperature, time, etc.), and construction practices. The compressive strength associated with these conditions is the "Field Design Compressive Strength" (CS).

CS is the field strength equal to (or in some instances greater than) the strength at the time the pavement is subjected to traffic loadings. The design procedure is considered applicable to HSSB materials with CS greater than about 5 MPa (750 psi). CS is the most important design input. It is necessary for a highway agency to establish procedures and guidelines for selecting CS for the thickness design determination.

Some typical examples illustrating various approaches to selecting CS are

1. The American Coal Ash Association (5) suggests that for PSM base, CS is the compressive strength based on 56-day curing at 73°F (100 percent relative humidity).

2. The Portland Cement Association (13) indicates the 28-day strength is appropriate for soil-cement thickness design.

3. In the 1986 AASHTO Guide (17), a structural coefficient 7-day compressive strength relation is shown for cement-treated bases. (Note: Many cement-treated material mixture design approaches are predicated on 7-day moist curing.)

The criteria for establishing CS are not necessarily the same for all HSSB materials. For example, the 28-day cured strength of cement-treated materials is typically about 50 percent greater than the 7-day moist cured strength. PSM frequently do not show the initial rapid strength development with curing characteristic of cement-treated materials, but PSM-cured strength normally continues to increase for a significant time period after construction. There is considerable variability in the rates of cement-treated material and PSM strength increase with curing (time and temperature). The development of "Cured Strength-Degree Day" (DD) data and relations for typical mixtures used by a highway agency are helpful in selecting realistic and appropriate CS values. In the Illinois Department of Transportation (DOT) mix design procedure [see *Flexible Pavement Manual* (5)] for PSM (lime-fly ash-aggregate, cement-fly ash-aggregate), a strength-DD relation is established for each mixture design. The degree days are calculated on the basis of temperatures above 40°F. A typical PSM strength-DD relation is shown in Figure 5.

### SIMPLIFIED HSSB THICKNESS DESIGN PROCEDURE

The information, concepts, and principles previously presented can be used to develop a simplified HSSB thickness design procedure. The procedure is based on Equation 5 and the assumption that the HSSB Field Design CS can be used to estimate the HSSB modulus (see Equation 4) and flexural strength (modulus of rupture =  $CS/5$ ). Equation 5 was used to develop the HSSB Thickness Design Chart shown in Figure 6. Equation 1 and different estimates of the inputs (HSSB modulus, modulus of rupture, and subgrade  $E_{Ri}$ ) can be used to develop more refined design charts.

To select the SR design value (see Figure 1), the estimated design equivalent single axle loads may be increased to attain an increased "design reliability" level. An AASHTO-type "Traffic Multiplier" approach concept (17) is a procedure that might be used. The required HSSB thickness is relatively insensitive to the design reliability factor. A 25-mm (1-in.) HSSB thickness increase is sufficient to increase the design reliability from 50 percent to a considerably higher level. The typical increase in HSSB long-term cured strength (a phenomenon that is not considered in the HSSB

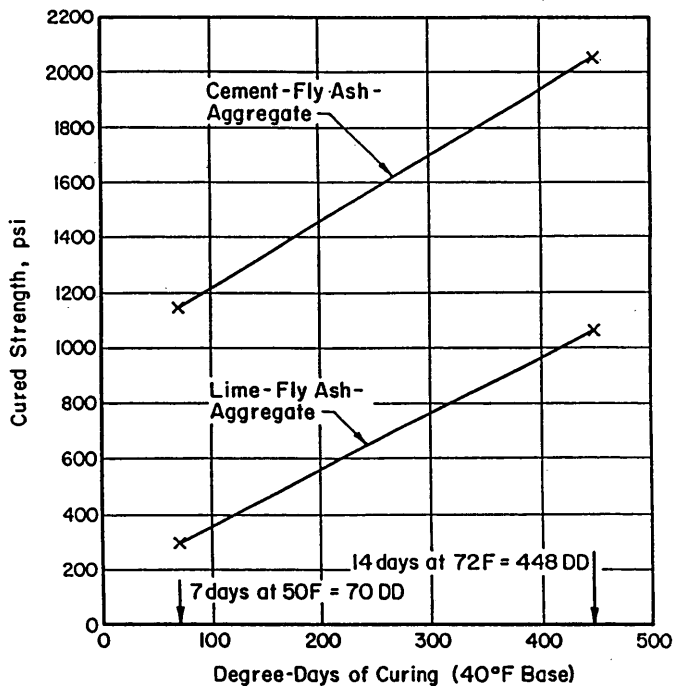


FIGURE 5 Strength-degree day relations for pozzolanic stabilized materials.

thickness determination process based on Field Design Compressive Strength) will effect a significant increase in the design reliability.

To limit early life fatigue consumption (HSSB strengths are low at this time), the HSSB pavement section must be adequate to effect an SR in the HSSB layer less than 0.65 before truck traffic loading. If the section is overloaded or fatigued at an early age, the "intact layer"-type structural behavior of the HSSB layer may be significantly reduced.

#### OTHER FACTORS INFLUENCING HSSB PAVEMENT PERFORMANCE

Historical performance and maintenance data for HSSB pavements should be considered in establishing policies for using HSSB pavements. The proposed HSSB thickness design procedure is based on an intact layer-HSSB flexural fatigue consumption approach. Other factors also influence the overall HSSB pavement performance.

- A TRRL report (8) indicated that, "for best performance, cemented roadbase should be laid in a single layer." The TRRL field survey data indicated the superior performance of "single-layer" versus "two-layer" construction. The degree of bonding achieved between the HSSB layers was probably the key contributing factor. If the required HSSB thickness exceeds the single-lift thickness that can be adequately constructed (primarily a full-depth adequate density consideration), special construction procedures are needed to achieve acceptable bonding between the HSSB layers.

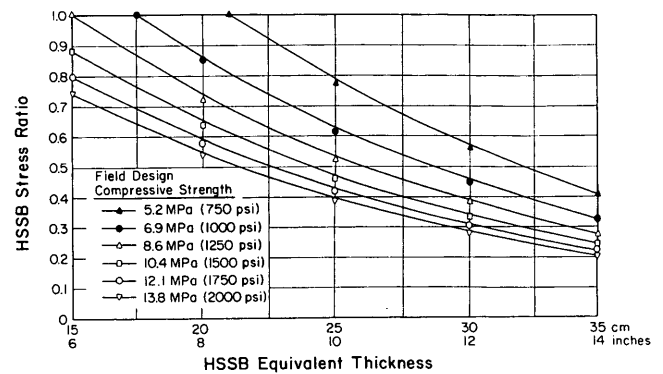
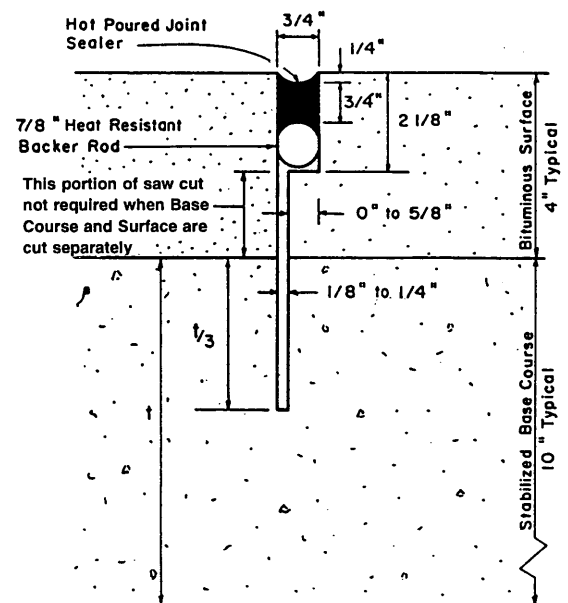


FIGURE 6 High-strength stabilized base equivalent thickness design chart.

- The performance of transverse cracks in the HSSB layer, HSSB material breakdown at transverse cracks, and pumping are major concerns. Increased pavement deflections may contribute to more rapid transverse crack breakdown and accompanying decreased load transfer at cracks, and increased potential for faulting and subgrade erosion or pumping. The Illinois DOT has implemented a policy for "sawing and sealing" joints in lime-fly ash and cement-fly ash base construction to improve joint performance. The Illinois DOT sawing and sealing detail for HSSB construction is shown in Figure 7.



TRANSVERSE CONTRACTION JOINT DETAIL

When base course is constructed adjacent to existing pavement this joint will not be required.

(Recommended joint spacing is 30 feet)

FIGURE 7 Illinois Department of Transportation high-strength stabilized base joint detail.

## REFERENCES

1. Thompson, M. R. *Mechanistic Design Concepts for Stabilized Base Pavements*. Civil Engineering Studies, Transportation Engineering Series No. 46, Illinois Cooperative Highway and Transportation Series No. 214, University of Illinois at Urbana-Champaign, July 1986.
2. Terrel, R. L., J. A. Epps, E. J. Barenberg, J. K. Mitchell, and M. R. Thompson. *Soil Stabilization in Pavement Structures: A User's Manual*. Vol. 2: *Mix Design Considerations*. FHWA-IP-80-2, FHWA, U. S. Department of Transportation, 1979.
3. *Soil and Base Stabilization and Associated Drainage Characteristics*, Vol. 1: *Pavement Design and Construction Considerations*, and Vol. 2: *Mixture Design Considerations*. Prepared for FHWA, U.S. Department of Transportation (Contract DTFH61-88-C-0005) by ERES Consultants, Inc., 1992. (To be published).
4. Little, D. N., M. R. Thompson, R. L. Terrel, J. A. Epps, and E. J. Barenberg. *Soil Stabilization for Roadways and Airfields*. Technical Report ESL-TR-86-19. Engineering and Services Laboratory, Air Force Engineering and Services Center, Tyndall Air Force Base, FL, 1987.
5. *Flexible Pavement Manual*. American Coal Ash Association, Washington, D.C., 1991.
6. Costigan, R. R., and M. R. Thompson. Response and Performance of Alternate Launch and Recovery Surfaces (ALRS) Containing Stabilized—Material Layers. In *Transportation Research Record 1095*, TRB, National Research Council, Washington, D.C., 1986.
7. Wang, M. C., and W. P. Kilareski. Behavior and Performance of Aggregate-Cement Pavements. In *Transportation Research Record 725*, TRB, National Research Council, Washington, D.C., 1979, pp. 67–73.
8. Mayhew, H. C., and J. F. Potter. Structural Design and Performance of Lean Concrete Roads. In *Proc., International Conference on Bearing Capacity of Roads and Airfields*, Plymouth, England, 1986.
9. Thompson, M. R. *A Proposed Thickness Design Procedure for High-Strength Stabilized Base (HSSB) Pavements*. Civil Engineering Studies, Transportation Engineering Series No. 48, University of Illinois at Urbana-Champaign, May 1988.
10. *Calibrated Mechanistic Structural Analysis Procedures for Pavements*. Final Report—Phase 2, Vol. II—Appendices. National Cooperative Highway Research Program Project 1-26. TRB, National Research Council, Washington, D.C., December 1992.
11. *Research and Development of the Asphalt Institute's Thickness Design Manual (MS-1) Ninth Edition*. Research Report No. 82-2. The Asphalt Institute, Aug. 1982.
12. Miller, J. S., J. Uzan, and M. W. Witczak. Modification of the Asphalt Institute Bituminous Mix Modulus Predictive Equation. In *Transportation Research Record 911*, TRB, National Research Council, Washington, D.C., 1983.
13. Packard, R. G. *Thickness Design for Soil-Cement Pavements*. Portland Cement Association, Skokie, Ill., 1970.
14. Thompson, M. R., and Q. L. Robnett. Resilient Properties of Subgrade Soils. *Journal of Transportation Engineering*, ASCE, Vol. 105, No. TE1, Jan. 1979.
15. Thompson, M. R., and T. G. LaGrow. *A Proposed Conventional Flexible Pavement Thickness Design Procedure*. Civil Engineering Studies, Transportation Engineering Series No. 55, University of Illinois at Urbana-Champaign, Dec. 1988.
16. Thompson, M. R., et al. *Development of a Preliminary ALRS—Stabilized Material Analyses System (SPAS)*. Technical Report ESL-TR-83-84. U.S. Air Force Engineering and Services Laboratory, Tyndall Air Force Base, Fla., 1983.
17. *AASHTO Guide for Design of Pavement Structures*. American Association of State Highway and Transportation Officials, Washington, D.C., 1993.

# Performance Evaluation of a Cement-Stabilized Fly Ash Base

D. H. GRAY, E. TONS, AND T. R. THIRUVENGADAM

The performance of a compacted, aggregate-free, cement-stabilized fly ash base beneath a highway shoulder is described. A 2.7-m (9-ft) wide, 457.5-m (1,500-ft) long fly ash test section was placed on both sides of State Highway M-54 near Grand Blanc, Michigan, in May 1987. The test section base was constructed using a high carbon, Class F fly ash that was stabilized with 12 percent by weight portland cement. A number of tests were used to monitor and evaluate the performance of the base. These tests included (a) Clegg impact readings on the compacted surface of the fly ash, (b) moisture-density and unconfined compression tests on core samples, (c) elevation and vertical deflection measurements on the pavement, (d) edge break surveys, (e) a crack pattern analysis, and (f) leachate analyses. The results of monitoring and evaluation tests conducted to date show that in general the fly ash test section has held up reasonably well where design and compaction specifications have been met. No widespread major problems (e.g., crumbling, disintegration, excessive heave or settlement of the pavement) have occurred during the 5-year period since construction in these areas. Problems with heave and cracking of the pavement on top of the fly ash have so far been restricted to a few local areas. Heaving and cracking in these areas occur mainly during the winter and are associated with frost effects. The presence of a joint that was purposely cut in the surface wearing course between the road shoulder and traveled way on one side of the highway greatly exacerbated arcuate cracking that developed next to the joint.

The Michigan Department of Transportation, which is responsible for 15456 km (9,600 mi) of federal and state trunkline highways, expects to complete 225 km (140 mi) of road shoulder replacement annually. This shoulder replacement program could use 300,000 tons of fly ash annually, or 1/8 of the total annual production in southern Michigan's lower peninsula. Use of fly ash in a roadway base course requires careful design of a fly ash-cement mix suitable for Michigan's demanding traffic loads and winter climate.

Previous research (1) has shown that raw fly ash exhibits unsatisfactory freeze-thaw characteristics, thus requiring stabilization with cement. Results of tests on a high-carbon fly ash (2) showed that a cement content of 12 percent by dry weight of solids would be sufficient to meet strength-durability criteria and minimize frost heaving. Design thickness calculations indicated that the required thickness of a compacted and trimmed base course was 2.54 cm (10 in.). This design was based on achieving an in-place density of 98 percent of the maximum dry density based on the Modified Proctor test. Protocols (2) were also developed for mixing, handling, and placement of the fly ash mixture in the field. The laboratory work indicated the importance of thorough mixing of cement and fly ash to achieve uniform properties and satisfactory performance. Laboratory findings showed that uniform cement

dispersion could be achieved by pre-blending a dry 40:60 fly ash and cement mixture. This mixture was then proportioned with fly ash and water to produce the desired base course product containing 12 percent cement by weight of dry solids. A full-scale field trial confirmed the need for this pre-blended concentrate to achieve uniform dispersion.

Fly ash used for this project was a high-carbon, Class F, dry hopper ash from Consumers Power Company's D.E. Karn Plant located at Essexville, Michigan, 80.45 km (50 mi) north of the demonstration site. The site selected for the demonstration was a new construction project: a four-lane state highway connecting I-75 directly south of the city of Flint. The trial road shoulder base course was placed on both sides of 457.5-m- (1,500-ft-) long section of the four-lane highway.

The cement-stabilized fly ash base course, mixed on-site using pre-blended 40:60 fly ash-cement mix and conditioned fly ash, was placed and compacted in two lifts. Control of compaction was critical. The first passes on each lift were made with a 10-ton steel wheel roller without vibration, whereas subsequent passes used vibration. A rubber tire roller was then used to close all cracks, thereby producing a smooth base surface. The final dimension of the base course was 2.54 cm (10 in.) thick by 2.74 m (9 ft) wide. The compacted finished surface was protected from drying and rain by application of a sprayed asphalt emulsion. An asphalt concrete leveling course was placed over the fly ash shoulder 7 days after construction and the surface or wearing course was completed 3 days later. The finished M-54 highway was opened to traffic in June 1987. Details about the field construction of the fly ash base course and preliminary findings are presented elsewhere (2-4).

A 5-year post-construction monitoring and testing program was implemented to evaluate the performance of the base course under operating conditions. These tests included

1. Moisture-density and unconfined compression tests on core samples from the fly ash base,
2. Elevation and vertical deflection measurements on the pavement,
3. Edge break surveys,
4. Crack pattern analysis, and
6. Analysis of samples from both groundwater monitoring wells and a leachate collection system installed beneath the fly ash test section.

The results and findings of this monitoring program are summarized in the following sections.

## TEST SECTION DESCRIPTION

The Michigan Department of Transportation (MDOT) participated actively in the site selection and construction planning phases of

D. H. Gray and E. Tons, Department of Civil Engineering, University of Michigan, Ann Arbor, Mich. 49109. T. R. Thiruvengadam, Consumers Power Co., Jackson, Mich. 49201.

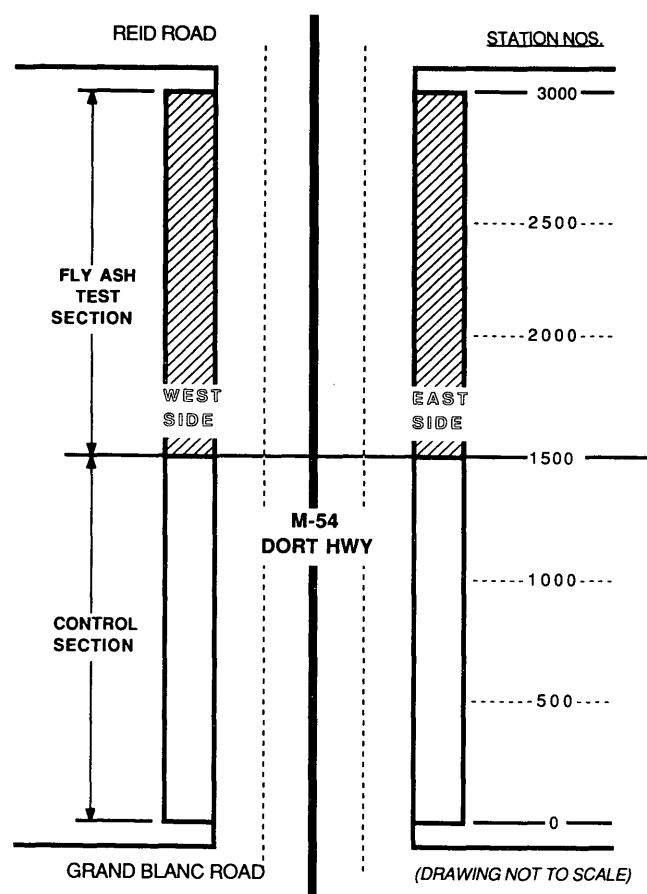


FIGURE 1 Schematic diagram showing plan and layout of road shoulder test.

the project. A new highway construction project on Michigan Route M-54 emerged as the most promising location from a number of candidate sites considered. A 457.5-m- (1,500-ft-) long section between Grand Blanc Road and Reid Road (see Figure 1) was selected for a trial fly ash shoulder. The combined length of the fly ash shoulder on both sides totaled 915 m (3,000 ft). An additional 915-m (3,000-ft) length of shoulder adjacent to the fly ash test section was established as a control section. At present the traffic is of medium intensity, but is expected to grow with time. To accommodate the traffic, the asphalt pavement was made 14.6 m (48 ft) wide with two 3.66-m (12-ft) lanes in each direction. The total width of the roadway, including the 2.7 m (9-ft) shoulders on each side, was 20.1 m (66 ft).

The required thickness of the fly ash base was calculated using the American Association of State Highway and Transportation Officials (AASHTO) design equation. The soil support value was assumed to be 3, which is equivalent to a California Bearing Ratio of about 3, and the minimum required sand subbase thickness was taken as 30.4 cm (12 in.). The final thickness of the compacted cement stabilized fly ash base course for the M-54 shoulder was calculated to be about 25.4 cm (10 in.). This design thickness was reasonable, based on previous experience. The adjacent control section had a standard Michigan Class A design with a 12.7-cm (5-in.) asphalt concrete base, 10.1-cm (4-in.) aggregate base and a 6.3-cm- to 7.6-cm- (2.5 to 3-in.-) thick asphalt surface supported on a sand subbase. A stratigraphic profile of both the fly ash and control section is shown in Figure 2.

## PERFORMANCE EVALUATION TESTS

### Field Moisture-Density Tests

The compacted, cement-stabilized fly ash base course was constructed during the period May 14 to 19, 1987. MDOT drilled 10.1-cm- (4-in.-) diam core samples from the fly ash test section on August 1987, December 1987, and April 1988. These dates correspond approximately to 90-, 180-, and 270-day test samples. The cores were sealed in plastic bags and transferred to the laboratory for determination of their moisture content, density, and unconfined compressive strength.

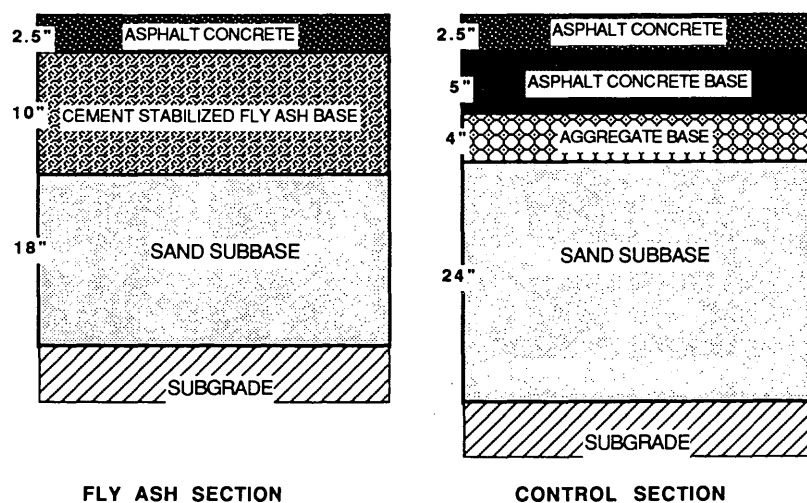


FIGURE 2 Stratigraphic profile of fly ash test section and control section.

Samples were obtained from 9 to 10 coring locations on either side of the highway. The locations were selected randomly, with the exception of two locations that were cored each time in the same vicinity of stations with known high and low Clegg impact readings, respectively; namely, Stations 26+00 (west) and 15+00 (east), respectively. Test specimens were recovered from both the top and bottom portions of the fly ash field cores.

Moisture contents for the 90-day cores samples ranged from 26 to 44 percent (dry weight basis) with an average value of 33.5 percent. With one or two possible exceptions, all of the cores samples exhibited moisture contents well in excess of the Modified Proctor optimum moisture determined in the laboratory investigation to lie between 24 and 26 percent of dry weight for cements contents ranging from 0 to 15 percent dry weight. Moisture contents measured on the 180-day (6-month) cores were even higher, ranging from 29 to 53 percent with an average value of 36.5 percent.

Dry densities for the 90- and 180-day samples averaged 11.0 and 11.5 kN/cu.m (69 and 72 pcf) respectively. These values lie below the target density of 12.4 kN/cu.m (78 pcf), and correspond to a relative compaction of slightly under 90 percent based on the modified AASHTO test. These dry densities were also lower than the dry densities measured on the compacted base using a nuclear gauge [average = 12.8 kN/cu.m (80.2 pcf), range = 11.8 to 14.3 kN/cu.m (74.3 to 89.7 pcf)]. Cement contents in the field cores varied from 2.8 to 19.1 percent dry weight. The target cement content was 12 percent. This variation is consistent with cement contents measured on pugmill samples during construction, which varied from 5.9 to 18.5 percent by weight with an average of 11 percent.

Unconfined compression tests were run on 5.1-cm (2-in.) cube samples that were trimmed from the cores by dry sawing. The average unconfined compressive strength at 90 and 180 days was 3369 and 2825 kPa (489 and 410 psi) respectively. These averages exceed the minimum required 7-day strength of 2756 kPa (400 psi). The average unconfined compressive strength at 270 days was unreliable because the sample population was too small and included samples that were either shattered or too soft, and hence not usable. Although the average strength met or exceeded the minimum value required, there was considerable variation among samples. Strengths ranged from less than 689 kPa to about 6890 kPa (100 to 1,000 psi). Only about half the samples tested met or exceeded the minimum target strength of 2756 kPa (400 psi). No additional strength gain was observed after 90 days of elapsed time.

Correlations were examined among unconfined compressive strength and other soil properties such as density, moisture content, cement content, and Clegg impact readings. The relationship between unconfined compressive strength versus dry density at 180 days is plotted in Figure 3. Fairly good correlations were obtained, with the strength increasing with dry density in an exponential fashion as shown. The coefficient of correlation for 90- and 180-day strength versus dry density was 0.61 and 0.95, respectively.

### Clegg Impact Tests

Impact tests were run on the compacted surface of the fly ash base course using a Clegg impact tester. This device records the deceleration of a standard weight dropped from a fixed distance onto

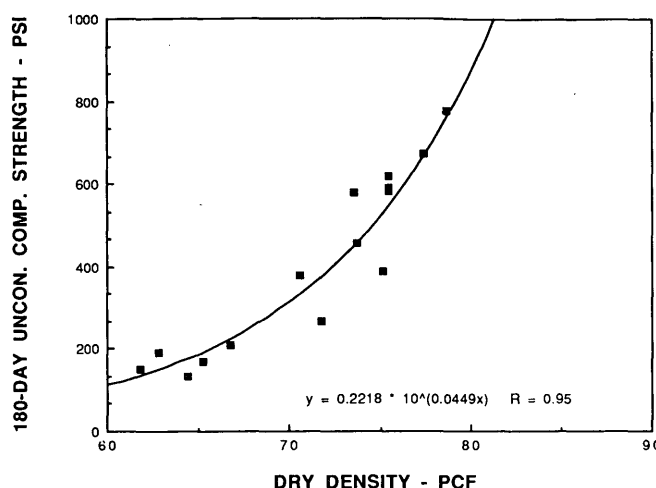


FIGURE 3 Unconfined compressive strength versus dry density: 180-day samples (1 psi = 6.89 kPa).

the base course surface. The Clegg "impact" reading obtained in this way can be correlated (5) with the modulus and strength of a compacted base. This test was run every 15.2 m (50 ft) along the surface and at different elapsed times up to 4 days following compaction. The test is nondestructive, fast, and provides a good record of the spatial variation and development of strength or stiffness with time.

Typical results of the Clegg impact test along the length of the fly ash test section on the west side of the highway are shown in Figure 4. Strength gains tended to be higher on the south end of the project. In addition, east side readings were generally higher than the corresponding west side readings on the opposite side of the highway. A pronounced dip in Clegg impact values was recorded in the vicinity of Stations 26+00 to 27+00 on both sides of the highway. These low values indicated a weaker base at this location and helped to identify an area that required close scrutiny as the study progressed.

There are several possible reasons for the low values at Stations 26+00 to 27+00. Low cement contents are a possible explanation; however, the coincidence of low values at exactly the same location but on opposite sides of the highway suggest other explanations as well. The highway traverses a topographic low at this location. A small amount of standing water was observed in the road shoulder trench before placement of the fly ash base. This moisture may have adversely affected compaction of the fly ash and the cement set, thus explaining a much lower rate of strength increase relative to other locations.

### Edge Break Survey

Another indicator of stability and durability of the road shoulder is the extent of "edge breaking" along the outside edge of the pavement. The extent of edge breaking was assessed along the fly ash and control sections, respectively. Edge breaking was classified as either major or minor. "Major" refers to crumbling, disintegration, or excessive settlement at the edge of the pavement, whereas "minor" refers to a slight cracking or deflection at the edge.



The amount of edge breaking in these two categories was paced off along the entire length of the control and fly ash sections in June of 1989. The results of the survey showed that edge breaking was not as extensive along the fly ash test section compared with the control section. This finding was true for both categories of severity. It is interesting to note the pronounced contrast in major edge breaking along the fly ash test section between the east side (15 paces) versus the west side (109 paces). This difference in resistance to serious disintegration and crumbling at the edge is also consistent with the findings of the Clegg impact tests (see Figure 4) on the surface and unconfined compression tests on core samples. In general, impact readings were much higher on the east than on the west side. The same also holds true for unconfined compression test results.

Vertical Displacement Measurements

During the winter of 1988 to 1989, a visual inspection of the fly ash road shoulder in March appeared to indicate that some vertical heave had occurred at certain locations. The heave was manifest most visibly in the form of a localized, slightly raised crown or mound with an associated cracking pattern on the west side road shoulder in the vicinity of Station 25+00. A slight amount of apparent differential heave also took place over some distance along the joint that had been cut in the pavement between the traveled way and the shoulder. This vertical heave subsided, however, to a very small residual value by May 1989.

In order to study and document this suspected vertical heave more thoroughly, two series of vertical displacement measurements were initiated in the fall of 1989. The first consisted of measuring the vertical separation distance or offset every 7.6 m (25 ft) along the joint. The second consisted of running a line of levels every 30.5 m (100 ft) down the middle of the fly ash test section road shoulder on either side of the highway. Both these measurements were repeated periodically during succeeding years to see if frost heaving was occurring, and if so, its magnitude and extent.

Results of these measurements show that a considerable amount of vertical movement (or heave) has taken place along some por-

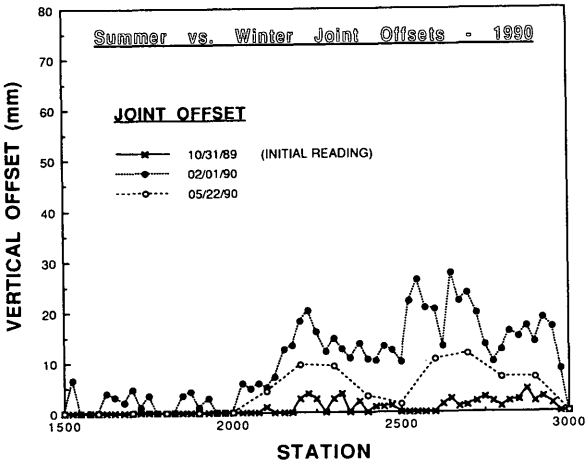


FIGURE 5 Vertical offsets measured in 1990 at joint in pavement between shoulder and traveled way.

tions of the shoulder. Vertical deflections ranged as high as 6.8 cm (2.7 in.) along the joint in some locations after 5 years. The temporal and spatial distribution of vertical heave or offset along the joint are shown in Figures 5 and 6. Compared in Figure 5 are the vertical offsets measured in 1990, some 3 years after construction, and compared in Figure 6 are offsets measured in 1992, approximately 5 years later. Vertical offsets were measured during the winter and in the late spring or early summer. The residual vertical heave along the joint measured in late spring or early summer was approximately half that recorded in February during the height of the winter when the ice lenses in the base course were fully developed. Vertical heaving or deformation increased progressively with time, as can be seen by comparing vertical deflections in 1990 (Figure 5) versus 1992 (Figure 6).

The vertical offset measurements at the joint are a good surrogate for heave-induced elevation changes. This equivalency was demonstrated by a strong correspondence between vertical offset at the joint versus elevation change along the centerline of the shoulder. East and west side elevation changes along the center

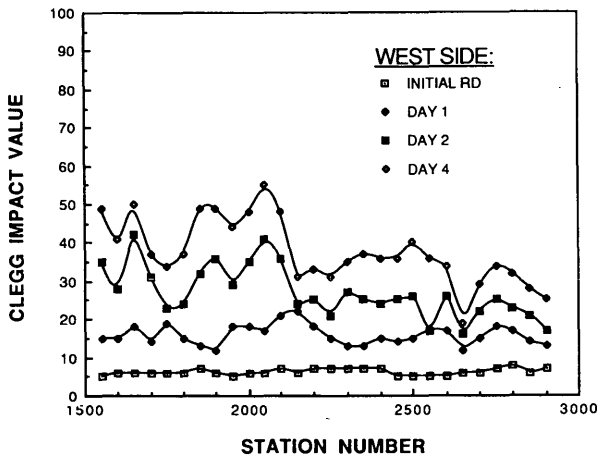


FIGURE 4 Clegg impact readings at different elapsed times and locations along the west-side shoulder.

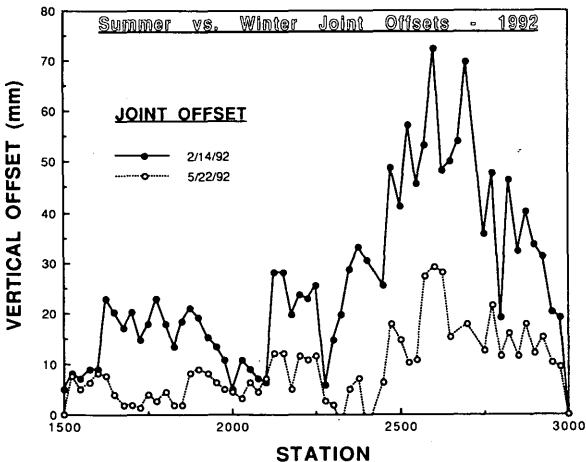


FIGURE 6 Vertical offsets measured in 1992 at joint in pavement between shoulder and traveled way.

of the shoulder measured on February 1, 1990, are compared in Figure 7. The two curves are virtual mirror images, with the exception that vertical heave tends to be greater (approximately 2 times) between stations 15+00 to 24+00 on the west side compared with the east side. This finding is particularly significant because in spite of the generally higher heave on the west side, there is little or no sign of cracking or distress where the shoulder abuts the roadway. In other words, it appears that cutting a joint—the procedure adopted on the east side—has contributed largely to the subsequent vertical offset measured along the joint and associated cracking and deformation problems (discussed in the next section). The presence of the joint has allowed runoff from the roadway to flow down into the subbase. The problem is exacerbated when the shoulder heaves (relative to the roadway) and presents a vertical face that diverts runoff vertically downward directly into the base. This infiltrating water becomes a source of water for ice lense formation in the underlying base during the winter.

Vertical displacement or heave is generally lower from Stations 15+00 to 24+00 compared with the area from Stations 24+00 to 30+00. The stabilized base in the former area tended to have higher cement contents and compacted densities. Analysis of field cores revealed relatively high cement contents in this area (e.g., 19.1 percent at Station 16+36 and 15.4 percent at Station 21+00, respectively). From Stations 25+00 to 28+00, the measured frost heave was virtually the same, but much higher for both shoulders compared with the area between Stations 15+00 to 24+00. This larger frost heave correlated with low cement contents in the base (e.g., 2.8 percent at east side Station 26+07). This is also the same area in which relatively low Clegg impact readings were recorded immediately after construction, as shown previously in Figure 4.

### Crack Pattern Survey

Periodic inspection visits were made to the site following construction of the road shoulder base in May 1987. One of the main purposes of these visits was to look for any crack development in the asphalt pavement cap. The first crack was observed on April 13, 1988, in the vicinity of Station 25+10 on the west side shoulder.

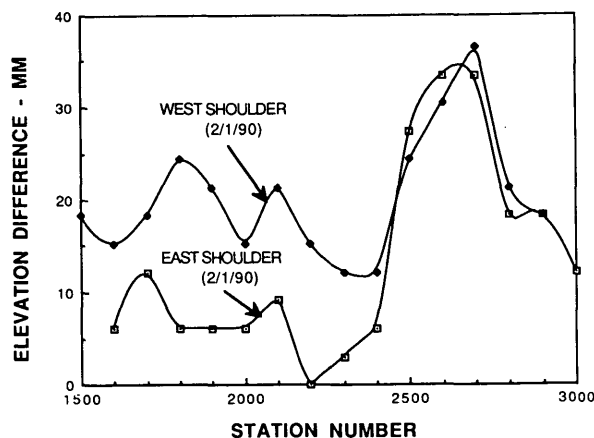


FIGURE 7 Comparison between elevation changes along centerline of east and west shoulders, respectively.

der. The cracking consisted of two narrow approximately parallel cracks with a combined length of 1.82 m (6 ft) at a distance of about 0.91 m (3 ft) from the traveled way pavement. No other structural cracks were observed in either shoulder at that time.

Four major types of cracking patterns have subsequently developed in the pavement overlying the fly ash base course during the 5-year monitoring period. These categories include the following:

Type I: Arcuate-shaped cracks along the joint between the shoulder and traveled way resulting from traffic passing over a raised and weakened portion of the shoulder;

Type II: General, random cracking associated with areas of under compaction or insufficient cement content in the fly ash;

Type III: Cracks originating in and propagating away from core holes in the pavement; and

Type IV: Cracks propagating away from joint corners.

Crack growth tended to progress with time. The character and development of arcuate (Type I) cracking along the joint at Station 25+30 on the east side is shown in Figure 8. The development of random (Type II) cracking at Station 25+10 on the west side is shown schematically in Figure 9. The crack growth versus time at Station 25+10 (west side) is illustrated in Figure 10.

The temporal pattern of crack development at Station 25+10 (west side) shown in Figure 10 indicates that crack growth is most rapid during the winter months and is associated with frost heaving in the base. The density and strength of cores from this area are generally much lower than those at other locations. The cement content of a core from this location was also quite low (2.8 percent by weight). Visual evidence during the winter indicated that localized heaving was occurring here as well. Snow plow striations in the pavement surface were clearly visible here as a result of a slightly raised "mound" in the pavement surface.

### Influence of Pavement Joint

The traveled way wearing or surface course was continued and extended across the shoulder on the west side. A different procedure was followed, however, on the east side. Here a 0.6-cm- (1/4-in.-) wide and 3.8-cm- (1 1/2-in.-) deep groove was cut and sealed right above the construction joint where the traveled way pavement base and the fly ash base (shoulder base) meet. This procedure (grooving) is often specified when two different, adjacent base materials are used. This way the shoulder can move somewhat independently as a result of material and other influences. Unfortunately, the presence of this joint also contributed to localized (Type I) cracking problems observed in the east-side shoulder.

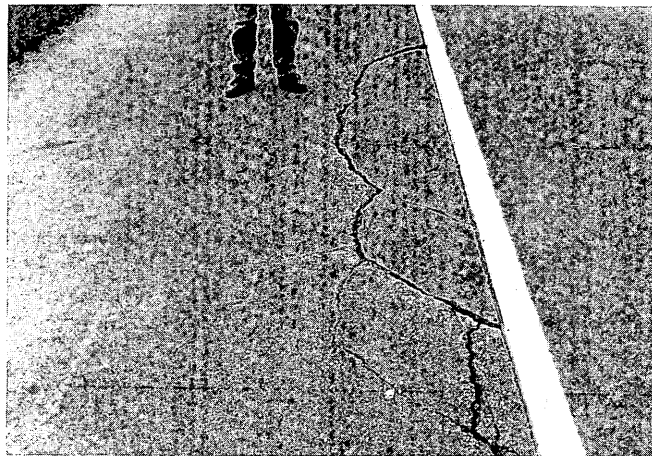
Pronounced arcuate (Type I) cracks developed adjacent to the joint on the east side at Stations 25+30, 26+90, 27+20, and 27+50. The cracks at these locations are crescent-shaped features oriented parallel to the joint. These cracks coincide with areas of maximum joint offset (see Figures 7 and 8) and generally lower strengths (see Figure 4). The cracks most likely developed in response to traffic loads during the spring thaw when the shoulder was raised in a sharp vertical discontinuity at the joint. This problem was not observed in the west-side shoulder in spite of generally higher elevation changes along the west side (see Figure 9). This finding indicates that it would have been advisable not to cut

a joint in the pavement. The presence of the joint not only tended to divert run-off water downward into the fly ash base, it also contributed to the cracking problems observed along the east-side shoulder.

In general, any kind of penetration through the pavement (e.g., grooves, joints, or holes) adversely affected the pavement. Cracks originated in and propagated away from core holes and joint corners as well. The deleterious effect of the core holes was particularly pronounced; these holes were often the locus of major transverse cracks in the fly ash pavement.

ENVIRONMENTAL MONITORING

Both laboratory leaching tests and field monitoring of water quality in observation wells and leachate collection stations were implemented as part of the demonstration project. The purpose of



(a)



(b)

FIGURE 8 Arcuate cracking along joint at Station 25+30 (east side) showing progression of cracking with time: (a) July 19, 1991, and (b) May 5, 1992.

WEST SIDE CRACK #3  
STATION 25+10 05/22/90

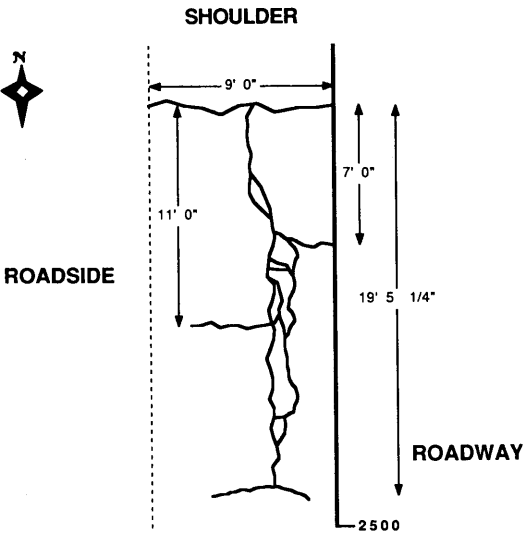


FIGURE 9 Schematic diagram of cracking pattern measured May 22, 1990, in vicinity of Station 25+10 on west-side shoulder.

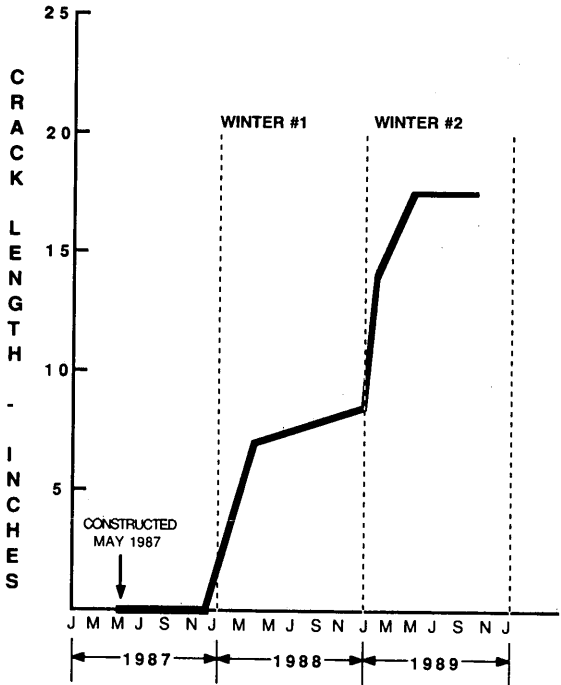


FIGURE 10 Crack growth with time at west-side Station 25+10 (1 in = 25.4 mm).

the laboratory leaching studies was to ascertain the potential for contaminant generation by cemented fly ash under extreme leaching conditions. The field monitoring system was installed in order to determine the impact, if any, of the cemented fly ash base course on water quality.

### Laboratory Leaching Studies

In order to simulate the "worst case" condition, two relatively extreme leaching protocols were followed. In the first, two samples of cemented fly ash were subjected to the leaching procedures established by the Environmental Protection Agency (EPA) under the Resource Conservation and Recovery Act (EPA Method 1310). The analytical results obtained on the resulting leachate are summarized in Table 1. The recommended limits established under the Safe Drinking Water Act (SDWA) are included in this table for reference purposes. In general, the concentration of metal ions and in the leachates from the cement-fly ash samples are below the recommended limits established by the SDWA. Only chromium and selenium slightly exceeded the SDWA standards. Even these exhibit less than an order-of-magnitude concentration above the standards.

### Field Monitoring

The laboratory studies indicated the potential for certain metal ions being released from pulverized, cemented fly ash. Thus, particular emphasis was placed in the field monitoring study on metals analysis. Groundwater monitoring wells were installed adjacent to the roadway in both the fly ash and control sections. Leachate samples were taken from sub drain pipes, placed directly beneath the fly ash base, which discharged into a man hole sampling box. The leachate samples were collected by positioning a carefully pre-cleaned stainless steel bucket at the pipe opening and catching the leachate as it flowed from the pipe.

Results from the groundwater monitoring wells are unremarkable. Insufficient time has elapsed for any leachate to reach the

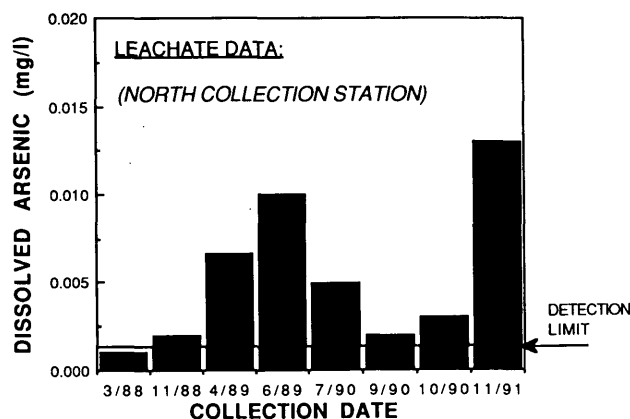


FIGURE 11 Sub drain leachate test results for dissolved arsenic.

wells and no significant differences have been observed to date between the background and test section wells. Leachate samples from the sub drains were analyzed for a number of toxic ions including selenium, arsenic, chromium, and cadmium. Typical results are shown in Figure 11, where dissolved concentrations are plotted versus collection date for arsenic. Results were plotted only for the north collection station, which receives leachate from the fly ash test section. Leachate concentrations for dissolved cadmium and chromium have remained relatively constant over time. On the other hand, selenium and arsenic concentrations have tended to fluctuate over time. The latter trend is particularly noticeable in the case of dissolved arsenic, as shown in Figure 11. Concentrations peaked in June 1989 and again in November 1991. It is important to note, however, that the maximum dissolved arsenic concentration in the leachate is still well below the Safe Drinking Water Standards (SDWS), as shown in the following table:

Parameter	Sub Drain Leachate (mg/liter)	SDWS (mg/liter)
Arsenic (As)	0.013	0.050
Cadmium (Cd)	0.020	0.010
Chromium (Cr)	0.030	0.050
Selenium (Se)	0.015	0.010

Only a limited number of usable samples have been obtained from the south collection station, which services the control section. A comparison of leachate concentrations (Arsenic, Cadmium, Chromium, and Selenium) between the fly ash test section and control sections on three different dates (07/90, 10/90, and 11/91), reveal little difference in concentrations between the two sections. Arsenic and selenium leachate concentrations tended to be slightly higher in the fly ash test section and this difference appeared to increase with the passage of time. These undiluted concentrations are nevertheless still within or near SDWS.

### CONCLUSIONS

Post-construction monitoring of the fly ash-cement base has shown that if the fly ash is mixed correctly with the specified amount of cement and compacted to the specified density, it will

TABLE 1 RCRA Leaching Test Results on Cement-Stabilized Fly Ash

COMPOUND	LEACHATE CONC - MG/LITER		
	SAMPLE "A"	SAMPLE "B"	SDWA LIMITS
Arsenic	0.009	0.005	0.050
Barium	0.070	0.460	1.000
Cadmium	<0.002	<0.02	0.010
Copper	<0.02	<0.02	1.000
Chromium	0.160	0.070	0.050
Lead	<0.02	<0.02	0.050
Mercury	<0.0002	<0.0002	0.002
Selenium	0.024	0.014	0.010
Silver	<0.01	<0.01	0.050
Zinc	<0.02	<0.02	5.000
Cyanide	<.005	<0.005	0.200

#### Notes:

1. Fly ash stabilized with 10% by wt. Portland cement
2. Molding w/c: "A" = 20 %; "B" = 28 % (dry wt. basis)

perform well. Problems with surface heave and pavement cracking have so far been restricted to a few local areas. These localized problems appear to be the result of low density and strength in combination with a low cement content in the fly ash base and a thin asphalt cap.

A groove or joint should not be cut in an asphalt pavement between the shoulder and traveled way. The joint ultimately intercepts and diverts runoff and meltwater into the underlying fly ash base with serious consequences. The presence of a joint was the main cause of severe heave and cracking in sections of pavement on the east side.

Monitoring of groundwater well samples and sub drain leachate has not revealed any adverse impact of the fly ash-cement base on water quality to date.

#### ACKNOWLEDGMENTS

The project was sponsored by the Electric Power Research Institute and Consumers Power Company. The Michigan Department of Transportation funded the incremental cost of fly ash acquisition and placement. The contractors for the research and development work and follow-up environmental monitoring were the University of Michigan, Environmental Control Corporation of Michigan, and Soil and Materials Engineers.

The authors gratefully acknowledge the assistance of individuals at Consumers Power Company, Michigan Department of Natural Resources, GAI Consultants, Michigan Ash Sales, Dundee Cement Company, and the paving construction contractor, Thompson-McCully Company.

#### REFERENCES

1. Gray, D. H., and Y. K. Lin, Engineering Properties of Compacted Fly Ash. *Journal of Soil Mechanics and Foundations Division* (ASCE), Vol. 98, SM4, 1972, pp. 361–380.
2. Berry, W. H., D. H. Gray, U. W. Stoll, and E. Tons. *Use of Coal Ash in Highway Construction: Michigan Demonstration Project. Interim Report*. Electric Power Research Institute, EPRI GS-6155, Palo Alto, Calif., 1989.
3. Gray, D. H., E. Tons, and W. H. Berry. Design and Construction of a Cement-Stabilized Coal Ash Base Course in a Highway Pavement. In *Proc., International Symposium on Utilization of Coal Mining Wastes*, Glasgow, Scotland, Sept. 2–5, 1990.
4. Gray, D. H., E. Tons, and W. H. Berry. Post-Construction Monitoring and Performance Evaluation of a Cement-Stabilized Fly Ash Base. In *Proc., 9th International Ash Use Symposium*, Vol. 2: Stabilization and Aquatic Uses, EPRI GS-7162, Jan. 1991, pp. 45:1–16.
5. Clegg, B. An Impact Testing Device for In Situ Base Course Evaluation, In *Proc., 8th Australian Road Research Board Conference*, Perth, Australia, Vol. 8, No. 8, 1976, pp. 1–6.

# Field Performance Evaluation of Cement-Treated Bases With and Without Fly Ash

KHALED KSAIBATI AND TRAVIS L. CONKLIN

A field evaluation of pavement sections containing cement-treated bases with and without fly ash was undertaken at the University of Wyoming. The study was conducted using historical data from Wyoming Transportation Department (WTD) construction documents and field performance data collected with the WTD road profiler. Pavement performance models were first developed on the basis of the physical attributes of the sections. Another analysis was also conducted to determine if the performance of sections with fly ash in the base was statistically different from the performance of sections without fly ash.

Traffic volumes and the loads associated with them keep increasing on roads and highways throughout the United States. This increase has created a need for stronger pavement structures. Because of these circumstances, the use of cement-treated bases (CTBs) was implemented to increase the strength of roadway sections subjected to heavy loads or where aggregate sources for base materials demonstrated less than optimal characteristics. CTB can be defined as a compacted mixture of fine and coarse aggregate, cement, and water (1). CTB is mixed in a batch plant or in situ depending on the strength, durability, and uniformity requirements of the layer being constructed. Although cement, aggregate, and water are the primary materials used in CTB, there are other materials that can be added to CTB to reduce the quantity of cement required. Fly ash has been shown to accomplish this goal (2).

There are many factors that make the use of fly ash in cement-treated bases attractive. The most important of these considerations is economic. Fly ash is much less expensive than the alternate base materials it replaces. In fact, transportation agencies began using fly ash as a partial replacement for cement in the 1970s because of the dramatic increases in cement prices. Currently, 86 percent of the fly ash produced each year is wasted, and therefore most of the cost associated with fly ash use is the cost of transportation (3). Another positive aspect of using fly ash as a partial replacement for portland cement is that fly ash in cement-treated bases may continue to gain strength for years after placement, thus resulting in higher ultimate strengths (4). Although cement- and fly ash-treated bases have been successfully used in roadway construction for several years, little work has been done to evaluate their field performance. The main objective of this research was to evaluate the field performance of pavement sections containing CTB with and without fly ash.

## DESIGN OF EXPERIMENT

In this experiment, a large number of test sections were first selected in Wyoming. Physical and performance data were then col-

lected on the selected sections. All data were later compiled in a computerized data base and a statistical analysis was conducted. The overall field performance evaluation strategies are shown in Figure 1.

## CTB Construction Requirements in Wyoming

The Wyoming Department of Transportation has extensive experience in the construction of cement-treated bases. All CTBs are mixed in a center mixing plant by either batch or continuous mixing. Mixed materials are then transported to the roadway and spread on a moistened subgrade or base in a uniform layer. Spreading and compacting the CTB is accomplished by using a Jersey spreader in combination with a motor grader followed by rolling. CTB mixtures are normally compacted to at least 100 percent of maximum density determined in accordance with AASHTO (American Association of Highway and Transportation Officials) T-99. After the mixture has been compacted, the surface is reshaped to the required lines, grades, and cross sections. No more than 60 min is allowed between the start of mixing to the time of starting compaction. Finally, in order to ensure proper curing, the air temperature should be 4°C (40°F) in the shade and rising.

## Strength of CTB in Wyoming

In a recent laboratory study performed at the University of Wyoming (2), the most commonly used CTB materials in Wyoming were tested for strength and durability. The aggregate used in this testing was scoria, volcanic ash or cinders composed of basalt. This type of aggregate is incorporated in approximately 50 percent of the CTB projects in the state of Wyoming. Three fly ash sources and Type II cement (moderate sulfate resistance) manufactured by Mountain Cement in Laramie were used in the testing.

The strength of samples were determined by conducting the unconfined compressive test. Samples were prepared with 8 percent cement by weight, 16.5 percent moisture content, and 1.3:1 fly ash to cement replacement ratio. The samples were cured for 7 and 28 days and then loaded to failure. The results from the 7- and 28-day compressive strength tests are shown graphically in Figures 2 and 3, respectively. These figures show that up to 55 percent of the cement can be replaced with fly ash without causing any reduction in the unconfined compressive strength of the samples.

## Selection of Test Sections

The test sections were selected based on data obtained from WTD data files. These files contained important information on a variety

K. Ksaibati, University of Wyoming, P.O. Box 3295, University Station, Laramie, Wyo. 82071. T. L. Conklin, Engineering Associates, P.O. Box 1900, Cody, Wyo. 82414.

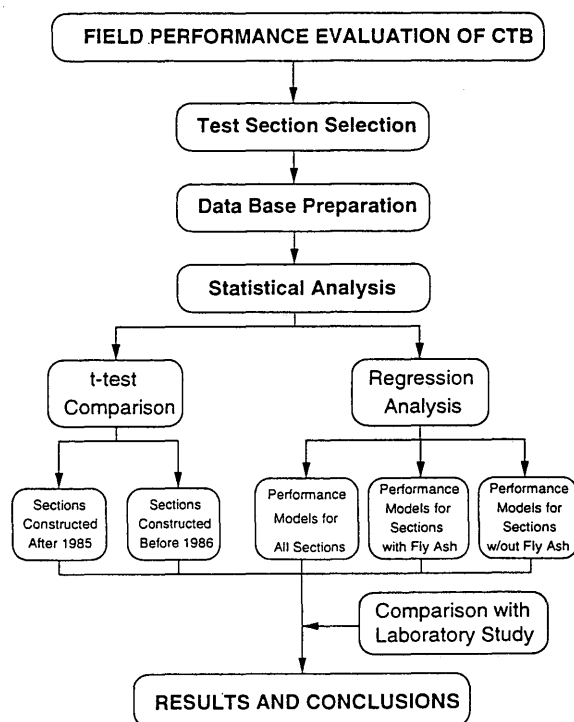


FIGURE 1 Field performance testing strategy.

of parameters that affect pavement performance. The files were reviewed extensively to identify appropriate sections with CTB. Each section was 0.322 km (0.2 mi) long. In total, 29 sections were selected, of which 18 sections contained CTB with fly ash and the other 11 sections contained CTB with no fly ash. The sections without fly ash were included in the experiment to act as control sections. The geographical locations of the sections are shown in Figure 4.

#### Data Collection and Data-Base Preparation

After the test section selection process was completed, detailed information was gathered on each site. The physical characteristics and current condition of all sections are summarized in Tables 1 and 2. The thickness of the asphaltic surface of test sections ranged between 5.0 and 10.2 cm (2 to 4 in.). On the other hand, the base thickness varied from 12.7 to 33 cm (5 to 13 in.). The sections were selected with variable thicknesses to determine the effect of base thickness on the long-term performance of pavement. The soil classifications and  $R$  (resistance) Values were also obtained to account for the effect of subgrade strength on pavement performance. The cement content in the base was about 7 percent in all test sections. In addition, fly ash percentages and types ( $C$  or  $F$ ) were obtained for all sections containing fly ash in the base. It was found that all sections except one contained type  $C$  fly ash. Therefore, fly ash type and source were eliminated as a factor in the analysis. It should be mentioned that fly ash percentages ranged from 18.6 to 40 percent. These percentages reflect the amount of cement replaced with fly ash.

Two factors related to age were also considered in this study. First, the number of years in service, which ranged from 1 to 10

years, were obtained for every section. Second, the accumulated equivalent single axle loads (ESAL) applied since construction were estimated from the WTD data files. The ESALs ranged between 16,000 and 1,012,000. Current field conditions of test sections were determined with two indices: Present Serviceability Index (PSI) and rut depth. The PSI was determined with the WTD road profiler, which is a duplicate of the South Dakota road profiler. The PSI is rated on a 5-point scale on which a rating of 5 indicates a perfect pavement (one that conceivably does not exist) and a rating of 0 means very poor condition. The PSI of the test sections ranged between 2.7 and 4.4. Rut depth measurements were also obtained with the Wyoming road profiler. These measurements ranged between 0.025 and 0.51 cm (0.01 and 0.20 in.). After all the data were obtained, a comprehensive computerized data base was compiled and prepared for data analysis.

#### DATA ANALYSIS

The field performance of pavement sections included in the study was evaluated using two techniques. First, a regression analysis was used in developing performance models to predict the PSI and rut depth based on the physical attributes of test sections (base thickness, fly ash percentage, etc.). The second technique compared the performance of sections containing fly ash with the sections without fly ash. This was accomplished by using the standard  $t$ -test. The sections were first broken down into two age groups and then the  $t$ -test was performed to determine if there was a significant difference in performance between sections with and without fly ash.

#### Regression Analysis

In this analysis, the dependent variables were PSI or rut depth and the independent variables were age, base thickness, asphalt layer thickness, fly ash percentage, and  $R$ -value of the subgrade. The following general regression model was considered in the

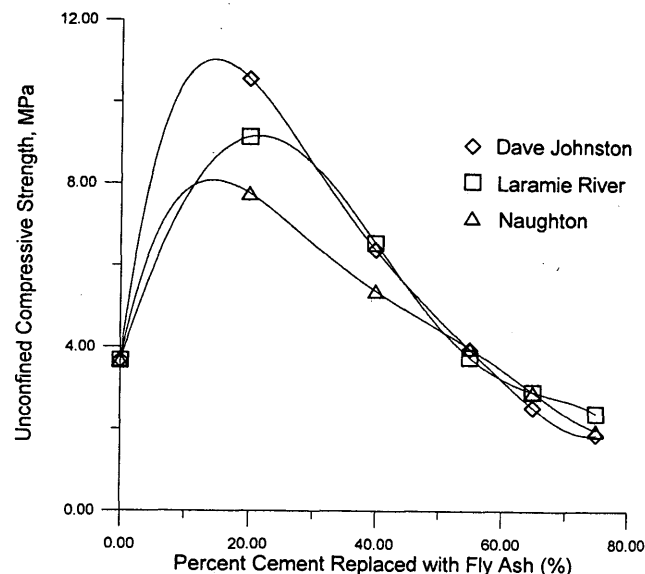


FIGURE 2 Seven-day unconfined compressive strengths.

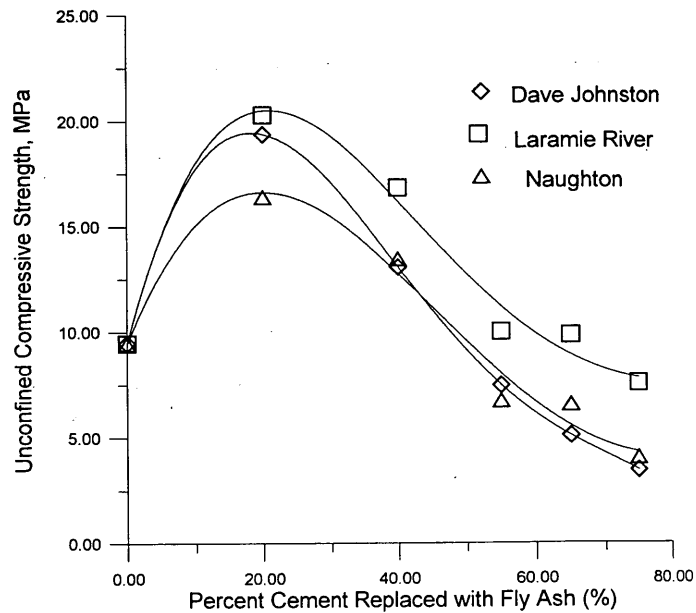
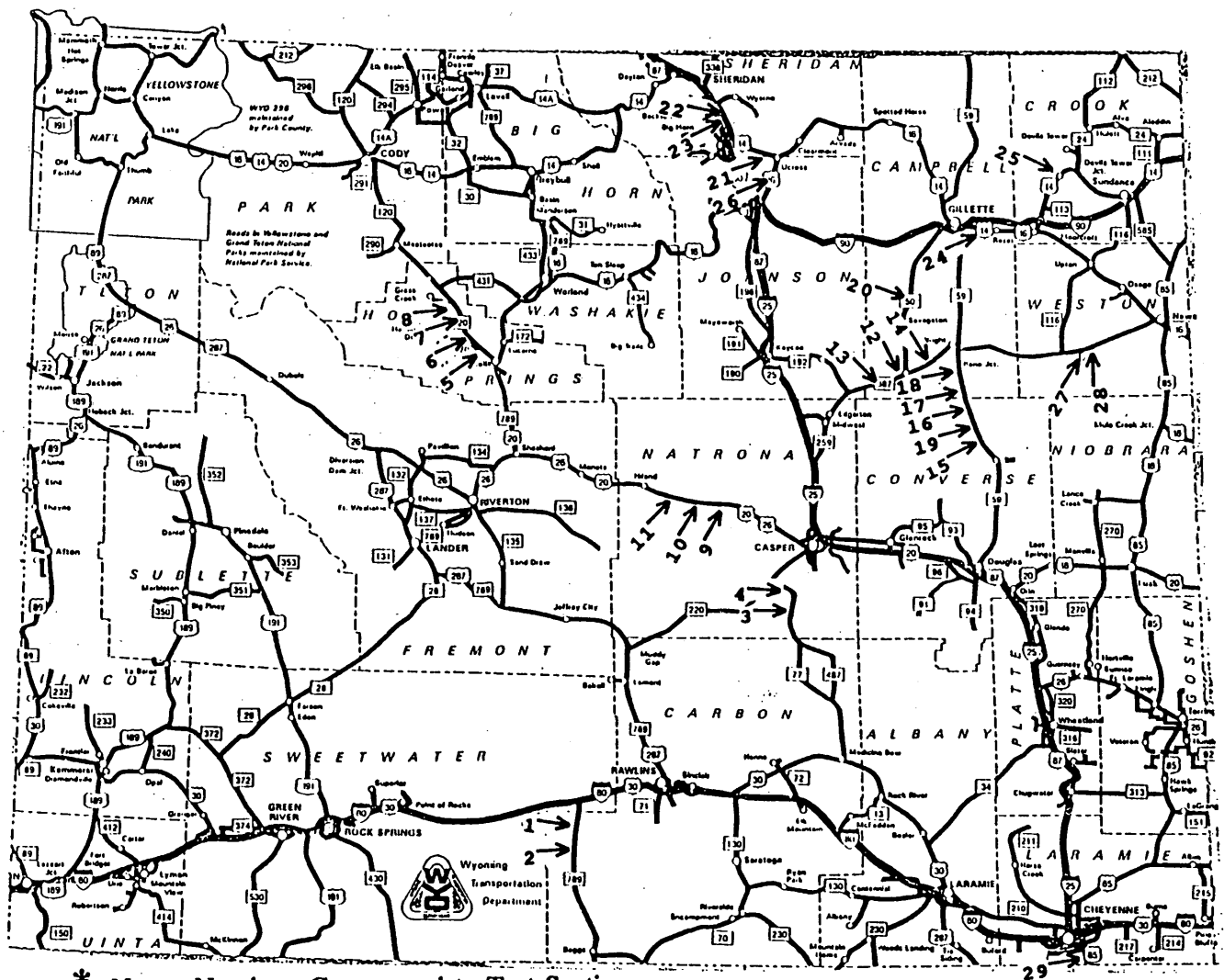


FIGURE 3 Twenty-eight-day unconfined compressive strengths.



\* Note: Numbers Correspond to Test Sections

FIGURE 4 Location of roadway sections.



analysis:

$$y_i = \beta_0 + \beta_1 x_{i1} + \beta_2 x_{i2} + \dots + \beta_j x_{ij} + \epsilon_i \quad (1)$$

where

- $y_i$  = dependent variable (rut depth or PSI);  
 $x_{ij}$  = independent variable (base thickness, fly ash percent, etc.);  
 $\beta_j$  = regression coefficients ( $j = 0$  to  $n$ ); and  
 $\epsilon_i$  = random error.

Initially, performance models were obtained for all test sections with and without fly ash in the base. These models are shown as follows:

Equations	$R^2$ (%)
PSI = 2.10 + 0.116 asphalt + 0.0469 base - 0.0677 age	18.3
Rut = 0.0820 + 0.0282 age	32.8

The coefficients of determination for these models indicate little correlation among the factors involved. The data were then divided into two major sets: one for the 10 sections with no fly ash in the base and another for the 19 sections with variable fly ash percentages. The models developed for the test sections that contained no fly ash are summarized as follows:

Equations	$R^2$ (%)
PSI = 2.16 + 0.0658 base - 0.0661 age	80.5
Rut = 0.033 - 0.00301 base + 0.0476 age	73.3

The coefficients of determination for the PSI and rut depth were 80.5 percent and 73.3, respectively. These models indicate that the thickness of the base layer and the age of the section do have an influence on the PSI and rut depth. PSI decreases with age and increases with increasing base thickness. On the other hand, rut depth increases with age and decreases as the thickness of the base increases. The relatively high  $R^2$  values for these models indicate that pavement sections without fly ash have similar performance.

An analysis similar to the one already described was conducted on all test sections containing variable percentages of fly ash. As shown in the following table, the coefficients of determination for these models were low, indicating that adding fly ash to cement-treated bases will cause some variations in pavement performance.

Equations	$R^2$ (%)
PSI = 3.55 + 0.100 asphalt - 0.0255 base + 0.00685 R-value - 0.0655 age	32.4
Rut = - 0.071 + 0.00847 base + 0.0227 age	25.9

where

- Rut = rut depth (cm),  
 PSI = Present Serviceability Index (0-5),  
 Asphalt = thickness of the asphalt layer (cm),  
 Base = thickness of the base layer (cm),  
 R-value = the R-value of the subgrade material, and  
 Age = the number of years since section was constructed.

TABLE 1 Physical Attributes of Test Sections

Section Number	Pavement Thickness (cm)	Base Thickness (cm)	Year Constructed	Soil Classification	Resistance Value (R-Value)	Percentage of Fly Ash Used
1	7.6	30.5	1987	A-4(2)-(5)	67	30.0
2	7.6	30.5	1988	A-4(1)	25	20.2
3	10.2	20.3	1988	A-7-6(12)	1	20.0
4	10.2	20.3	1987	A-4(3)	40	25.0
5	5.1	30.5	1986	A-1-a(0)	74	0.0
6	7.6	25.4	1987	A-4(0)-(8)	16	20.5
7	7.6	25.4	1988	A-6(11)	10	20.2
8	10.2	25.4	1989	A-2-4(0)	45	0.0
9	10.2	33.0	1985	A-6(12)	6	24.7
10	7.6	25.4	1984	A-4(2)-(6)	43	0.0
11	7.6	15.2	1985	A-2-4(0)	61	20.0
12	10.2	27.9	1984	A-4(3)-(6)	50	0.0
13	7.6	30.5	1983	A-4(5)-(7)	26	0.0
14	7.6	30.5	1982	A-4(1)-(6)	15	0.0
15	5.1	20.3	1989	A-2-4(0)	58	20.0
16	5.1	20.3	1989	A-2-4(0)	51	20.0
17	10.2	25.4	1984	A-2-4(0)	68	40.0
18	10.2	25.4	1985	A-2-4(10)	40	40.0
19	5.1	22.9	1988	A-2-4(0)	63	20.0
20	7.6	22.9	1986	A-4(1)-(4)	30	0.0
21	7.6	17.8	1987	A-2-4(0)	45	0.0
22	5.1	17.8	1987	A-4(2)-(3)	15	25.3
23	5.1	17.8	1987	A-6(1)-(10)	16	0.0
24	7.6	17.8	1987	A-2-4(0)	40	20.3
25	7.6	20.3	1988	A-2-4(0)	7	20.5
26	7.6	12.7	1986	A-2-4(0)	59	0.0
27	5.1	20.3	1982	A-4(8)	7	18.9
28	5.1	20.3	1980	A-4(3)-(6)	15	0.0
29	7.6	20.3	1988	A-6(5)-(6)	6	25.3

### T-Test Comparison

The main objective of this statistical test was to determine whether the field performance of sections with fly ash was significantly different from that of sections without fly ash. A 95 percent confidence level was used in the whole analysis to be within practical limits, and assumptions were made that (a) the population samples are small and (b) both the populations are normal with  $S_1 = S_2 = S$  and the design is completely randomized. The  $t_0$  value was calculated with the following equation:

$$t_0 = \frac{(\bar{Y}_1 - \bar{Y}_2)}{S_p \sqrt{\frac{1}{n_1} + \frac{1}{n_2}}} \quad (2)$$

where

$\bar{Y}_1$  and  $\bar{Y}_2$  = sample means (PSI or rut depth),

$n_1$  and  $n_2$  = sample sizes, and

$S_p$  = estimate of the common variance  $S_1^2 = S_2^2 = S^2$ .

The common variance  $S_p$  was computed with the following equation:

$$S_p^2 = \frac{(n_1 - 1)S_1^2 + (n_2 - 1)S_2^2}{n_1 + n_2 - 2} \quad (3)$$

where  $S_1^2$  and  $S_2^2$  are the two individual sample variances.

The data were first broken down into two age groups to eliminate the effect of age factor from the analysis. One age group contained sections built before 1986 and the second group contained sections built in 1986 or later. Means of PSI and rut depths for both age groups were then calculated. PSI means for sections with fly ash were compared with PSI means for sections without fly ash for both age groups. A similar analysis was conducted on rut depth measurements. The test statistic  $t_0$  was determined by using Equation 2, and finally its absolute value was compared with  $t^* = t_{\alpha/2, n_1+n_2-2}$ . If  $ABS(t_0) > t^*$ , it would be concluded that the two means are statistically different. Four paired comparisons were made on two age groups. The results from the comparisons are summarized in the following table for PSI:

Date Constructed	$t^0$	$t^*$	Statistical Difference
Before 1986	2.08	2.11	Not significant
1986 or later	0.892	2.36	Not significant

and for rut depth measurements:

Date Constructed	$t^0$	$t^*$	Statistical Difference
Before 1986	0.388	2.11	Not significant
1986 or later	0.912	2.31	Not significant

It is clear from examining these tables that there is no significant difference between the field performance of sections with fly ash and those without fly ash. This result indicates that using fly ash as a partial replacement for cement has no significant negative effect on field performance.

TABLE 2 Data Related to Field Performance of Test Sections

Section Number	ESAL's (thousands)	Rut Depth (cm)	Present Serviceability Index
1	299	.254	3.7
2	227	.330	3.3
3	68	.127	3.3
4	89	.178	4.0
5	176	.076	3.8
6	143	.051	4.0
7	112	.152	3.6
8	76	.025	3.9
9	881	.178	3.9
10	1012	.203	3.7
11	1012	.025	4.4
12	270	.203	3.3
13	303	.279	3.6
14	335	.356	3.8
15	99	.127	3.3
16	99	.203	4.3
17	954	.330	3.7
18	847	.254	4.0
19	143	.102	3.8
20	74	.330	3.5
21	36	.025	2.8
22	16	.025	3.5
23	16	.076	3.2
24	469	.203	4.3
25	37	.203	3.5
26	26	.229	2.8
27	81	.330	2.7
28	96	.432	2.8
29	54	.279	4.2

### CONCLUSIONS AND RECOMMENDATIONS

In this research, a field evaluation was performed to examine the factors affecting the performance of pavement sections containing CTB with and without fly ash. The study consisted of selecting previously constructed sections, collecting data, preparing a computerized data base, and finally conducting statistical analysis. Based on the evaluation performed, the following conclusions can be drawn:

1. The field performance of the sections containing CTB without fly ash is affected by the thickness of the base. The thicker the base, the better the performance.
2. The  $R^2$  of fly ash performance models are lower than the  $R^2$  for CTB performance models. This is because fly ash characteristics vary from time to time within a plant, which causes more variations in field performance.
3. There is no significant statistical difference in performance of sections with and without fly ash.

There are several implications associated with these conclusions. First, CTB sections containing fly ash perform as well as sections without fly ash. Therefore, fly ash should be used more often in highway construction because it is an inexpensive waste material. Second, more extensive research needs to be conducted with better control over construction parameters. Specifically, it is recommended that test sections be constructed to provide varying levels of pavement layer thicknesses, base layer thicknesses, fly ash replace-

ment percentages, and cement content. This will ensure that all possible parameters are taken into account and will help improve the reliability of performance models developed in this research.

## REFERENCES

1. Williams, R. *Cement-Treated Pavement Materials, Design, and Construction*. Elsevier Applied Science Publishers, London and New York, 1986.
2. Conklin, T. L., and K. Ksaibati. *Laboratory Evaluation of Cement-Treated Bases with Fly Ash*. Final Research Report, Western Research Institute, Laramie, Wyo., 1993.
3. Boles, W. A. *A Perspective of Potential: Introduction*. Proceedings: Fly Ash in Highway Construction Seminar, Federal Highway Administration Demonstration Project 59, FHWA DP-59-7, Nov. 1985.
4. Collins, R. *Fly Ash in Bases and Subbases*. Proceedings: Fly Ash in Highway Construction Seminar, Federal Highway Administration Demonstration Project 59, FHWA DP-59-7, Nov. 1985.

# Cement-Stabilized Open-Graded Base Strength Testing and Field Performance Versus Cement Content

MICHAEL HALL

Explored in this study is the use of cement-stabilized open-graded base (CSOGB) to provide a drainage system and construction platform for concrete pavements. Objectives were to (a) assess concrete testing methods for CSOGB and (b) examine cement content versus performance under construction traffic. Modified concrete testing methods were used to sample, fabricate, cure, and test cylinders, beams, and cores prepared on site. Large sample sizes were used, specimens were compacted by surface tamping, cylinders were cured in plastic molds, and loading rates were reduced. Laboratory-cured compressive and bending, field-cured compressive and split tensile, and core split tensile and permeability tests were conducted. Strength tests were performed successfully and yielded reasonably consistent results. Permeability was successfully measured using a modified New Jersey falling head permeability apparatus. Low, medium, and high cement content material was placed on grade and used as a haul road during paving. The condition of the CSOGB was monitored during construction and trucks, both loaded with concrete and empty, were counted. Performance under load was found to depend on cement content, truck traffic, sub-layer stability, segregation, and surface irregularities. A cement content of  $1163 \text{ N/m}^3$  ( $200 \text{ lb/yd}^3$ ) was suitable for general use,  $873 \text{ N/m}^3$  ( $150 \text{ lb/yd}^3$ ) was adequate for low trucking volumes, and  $1454 \text{ N/m}^3$  ( $250 \text{ lb/yd}^3$ ) was appropriate for high trucking volumes or poor support conditions.

Research indicates that adequate drainage is an essential component of a pavement system. In Wisconsin this has led to the provision of an open-graded base layer under most new concrete pavements. Typically 10.2 cm (4 in.) of an open-graded coarse aggregate over a dense-graded base layer is specified. This system frequently lacks the stability required to support construction activities. Cement stabilization of open-graded material is an option that simultaneously provides drainage and a stable construction platform.

Paving is safer and more efficient when the grade is used as a haul road. Construction activities can be isolated from regular traffic without the cost of building a temporary road. Full-width paving can be accomplished even when lateral clearance is limited. Pavers equipped with dowel-bar inserters can place material dumped directly on the grade without a spreader in the paving train. These advantages can help the contractor expedite construction and contain costs.

At the time of this project there were no standard testing procedures for cement-stabilized open-graded base (CSOGB) material and little information was available on its ability to support construction traffic. This work represents the collective efforts of the Wisconsin Department of Transportation (WisDOT), the Federal Highway Administration (FHWA), the James Cape & Sons

Company, and the Wisconsin Concrete Pavement Association (WCPA) to evaluate the potential of this material.

The primary objectives of this study were to assess (a) the use of concrete testing procedures to measure mechanical properties of CSOGB and (b) the correlation between the cement content of CSOGB and its performance under construction trucking activities. The research was performed during the 1990 reconstruction of the northbound side of Interstate 90 near Stoughton, Wisconsin, originally opened in 1962. Adjacent southbound lanes carried daily traffic of about 20,000 cars and 5,000 heavy trucks without interruption throughout the course of the project. The old pavement was completely removed and the existing 28-year-old grade was restored. The new structure consisted of 25.4 cm (10 in.) of doweled plain concrete pavement over 10.2 cm (4 in.) of CSOGB over a minimum of 10.2 cm (4 in.) of restored dense-graded base, all over a typically heavy soil subbase.

This job, divided into two portions, was selected because a section of the work was located where an access road would be difficult to construct. The contractor's batch plant was located in the middle of the project to limit haul lengths. Construction proceeded from the ends toward the midpoint. CSOGB placed at each end carried limited trucking whereas that placed nearest the plant carried more trucks.

## SPECIFICATIONS AND PROCEDURES

Cylinders and beams were fabricated using CSOGB from the contractor's batch plant. Flexural specimens and half of the compression specimens were subsequently transported to the WisDOT lab for controlled moist curing and testing. Split tensile specimens and the rest of the compression specimens were field-cured and tested by FHWA on site. A 793-m (2,600-ft) test section was established for material of each of three cement contents designated as low, medium, and high. A 122-m (400-ft)-long divided area was provided within each test section to create separate lanes for loaded and empty trucks. Cores were cut from each test section for split tensile and permeability testing.

Although concrete testing procedures as prescribed by the American Society for Testing and Materials (1) were followed as closely as possible, modifications were made to accommodate special characteristics of the material and unique conditions encountered in the field.

### Specifications

Compositions of the test mixes are tabulated in Table 1. The target dry weight for the 0.19-cm (0.75-in.) top-sized crushed limestone

TABLE 1 Test Mix Compositions

	Component weights (N/m <sup>3</sup> ) <sup>a</sup> for each test mix					
	Lab-Cured			Field-Cured		
	Low	Medium	High	Low	Medium	High
Type I Cement	873 (150)	1163 (200)	1454 (250)	873 (150)	1163 (200)	1454 (250)
Dry Crushed Limestone	14793 (2543)	14909 (2563)	14764 (2538)	14798 (2544)	14909 (2563)	14816 (2547)
Dry Recycled Sand	337 (58)	343 (59)	349 (60)	349 (60)	343 (59)	355 (61)
Net Water	820 (141)	605 (104)	683 (118)	829 (143)	605 (104)	683 (118)
Water/Cement Ratio	0.94	0.52	0.47	0.95	0.52	0.47

<sup>a</sup> Values in parentheses are in lb/yd<sup>3</sup>

coarse-aggregate was 14,793 N/m<sup>3</sup> (2,543 lb/yd<sup>3</sup>), the same quantity used in the concrete on the job. The contractor also added 337 N/m<sup>3</sup> (58 lb/yd<sup>3</sup>) of recycled sand. The resulting total gradation conformed to specifications for American Association of State Highway and Transportation Officials No. 67 stone (2). Cement contents of 873 N/m<sup>3</sup> (150 lb/yd<sup>3</sup>), 1163 N/m<sup>3</sup> (200 lb/yd<sup>3</sup>), and 1454 N/m<sup>3</sup> (250 lb/yd<sup>3</sup>) were used. Water content for each mix was determined from assessment of the material as it was placed to minimize separation of the paste. The water/cement (w/c) ratio thus varied between mixes. Mixing procedures were essentially the same as those used for concrete with mixing time extended from 60 to 70 sec for each 8.4 m<sup>3</sup> (11 yd<sup>3</sup>) batch.

CSOGB was transported in open box dump trucks and agitator trucks and placed with a slightly modified finegrader. Augers spread material laterally and a blade was used to establish the grade. Compaction was provided by a full-width vibratory steel plate. A small vibratory plate was used to resurface the material in the trackline of the finegrader. Plastic sheeting was applied immediately after placement to limit evaporation during a 3- to 4-day curing period. A 92-m (300-ft) section was left uncovered to assess the importance of covering.

Test sections for each cement content were located in areas with no visible subgrade problems. Low-cement material was placed near the beginning of the project where the least amount of trucking would occur. Medium-cement material was placed where significant one-way hauling was done. High-cement material was placed where extensive two-way operation was required. Observations were also made of material placed outside the formal test sections. Several variations were tried, but medium-cement material was used on most of the project.

## Procedures

Samples for controlled laboratory curing were delivered in the contractor's trucks to an indoor casting site on the project and field-cured samples were taken on grade. Large samples were used to minimize evaporation and provide enough material for each series of specimens. About 0.76 m<sup>3</sup> (1 yd<sup>3</sup>) of the 8.4-m<sup>3</sup> (11-yd<sup>3</sup>)

load was discharged onto a plastic sheet. The sheet was folded over the material to prevent moisture loss. Material was taken from different areas of the sample throughout the casting process to ensure uniformity among the specimens. Surface material was continually discarded as it dried out.

Specimens for testing at each age were produced consecutively in groups of three to minimize variability. Cylinders for compression testing at each of four ages (3, 5, 7, and 28 days) and beams for flexural testing at each of three ages (3, 5, and 7 days) were cast for each cement content and marked for laboratory curing. Field curing was specified for compression cylinders cast for testing at 3, 5, and 7 days (low cement) and at 3, 5, 7, and 28 days (medium and high cement). Field-cured split tensile cylinders for each cement content were cast for testing at each of four ages (3, 5, 7, and 28 days).

Specimens were compacted using a tamper consisting of a 11.4-cm (4.5-in.) diam pipe flange on a 4.76-cm (1.88-in.) diam pipe nipple 25.4 cm (10 in.) long. Consistent compactive effort was achieved by dropping the 15.3-N (3.44-lb) tamper from about 2.5 cm (1 in.) above the surface of the material.

Cylinders were cast in 15.2-cm (6-in.) diam × 30.5-cm (12-in.) long plastic molds. Material was placed in 10.2-cm (4-in.) lifts and tamped 25 times/layer. The final layer was overfilled to adjust for subsidence of the material. The surface provided by tamping was superior to that produced if a strike-off was attempted.

Beams were cast in 15.2-cm × 15.2-cm × 53.3-cm (6-in. × 6-in. × 21-in.) steel molds. Material was placed in 7.6-cm (3-in.) lifts and tamped 63 times, once for every 12.9 cm<sup>2</sup> (2 in.<sup>2</sup>) of surface area layer. A darby was used to strike off the beams, with care taken to avoid loss of surface aggregate.

Individual plastic bags were placed on the cylinders. Each group of specimens was covered with plastic sheeting laid down tightly over the surface of each beam. Laboratory-cured specimens were transported to the WisDOT lab after 24 hr. Field-cured cylinders were moved to the on-site FHWA testing facility after 3 days and recovered. Specimens were left in their molds and padded during transportation to avoid damage from early handling.

Controlled moist curing at 22.8°C (73°F) was provided for laboratory-cured specimens. Cylinders were left covered and in

their molds and beams were stripped. Field-cured specimens were stored on site until tested. Material on grade was exposed to drying conditions between removal of the plastic sheeting and the time it was paved over. Corresponding field-cured specimens were uncovered for 3 days to simulate this exposure and were then recovered. Field temperatures fluctuated from day to night but were, on average, within 5 percent of the laboratory value.

Three 15.2-cm (6-in.)-diameter cores were cut from each formal test section and from the uncovered section for split tensile testing. Three 10.2-cm (4-in.)-diameter cores were also cut from the high-cement test section for permeability testing.

ASTM (1) concrete testing procedures, with lower loading rates to avoid early failure, were followed for compression, split tensile, and third-point bending tests. Split tensile tests were also done on 15.2-cm (6-in.)-diameter cores only 10.2 cm (4 in.) long. The 10.2-cm (4-in.)-diameter cores were adapted for testing in a modified New Jersey falling-head permeability apparatus (3).

## RESULTS OF PHYSICAL TESTING

Results of compression, bending, and split tensile tests performed on prepared specimens are shown in Table 2 and split tensile test

TABLE 2 Strength Tests of Prepared Specimens

			Strength (kPa) <sup>a</sup> for each test specimen			
Cement Content		Age (days)	1	2	3	Average
Lab Compression	Low	3	1,220	1,220	1,330	1,256
		5	1,454	1,578	1,557	1,530
		7	1,909	1,585	1,578	1,690
		28	2,246	2,122	1,977	2,115
	Medium	3	1,481	1,612	1,495	1,530
		5	1,647	1,750	1,805	1,734
		7	1,867	1,909	2,060	1,945
		28	2,701	2,584	2,963	2,749
	High	3	5,188	4,837	5,250	5,092
		5	5,464	5,388	5,588	5,480
		7	6,601	5,009	5,043	5,551
		23	6,249	6,601	6,132	6,327
Field Compression	Low	3	1,020	937		978
		5	1,144	1,082	1,164	1,130
		7	1,116	1,068	1,027	1,070
	Medium	3	3,045	3,004	2,832	2,960
		5	2,942	2,963	2,880	2,928
		7	2,894	2,811	2,928	2,878
		28	3,362	3,597	3,796	3,585
	High	3	3,293	3,569	3,500	3,454
		5	4,492	4,127	4,175	4,265
		7	3,824	4,334	4,403	4,187
		28	4,699	5,154	5,360	5,071
	Lab Flexural	Low	3	287	413	316
5			482	431	453	455
7			442	488	460	463
Medium		3	387	425	425	412
		5	396	345	431	390
		7	482	505	505	497
High		3	1,062	1,108	1,189	1,120
		5	1,209	1,177	1,223	1,203
		7	1,120	1,235	1,321	1,225
Field Split Tensile	Low	3	117	123		120
		5	168	156	191	172
		7	212	263	243	239
		28	204	274	251	243
	Medium	3	372	422	389	394
		5	553	570	627	583
		7	601	469	616	562
		28	554	520	487	520
	High	3	588	466	551	535
		5	768	745	686	733
		7	807	588	688	694
		28	898	859	931	896

<sup>a</sup> 1 kPa = 0.145 psi

TABLE 3 Tests of Core Samples

Cement Content	Age (days)	Split tensile strength (kPa) <sup>a</sup> for each test specimen			
		1	2	3	Average
Low	8	391	438	338	389
Medium	7	680	475	531	562
High	7	476	1,038	650	721
High (uncovered)	7	669	457	558	561

Cement Content	Age (days)	Permeability (m/day) <sup>b</sup> for each test specimen			
		1	2	3	Average
High	28	878	1178	766	941

<sup>a</sup> 1 kPa = 0.145 psi<sup>b</sup> 1 m/day = 3.279 ft/day

results of cores are presented in Table 3. Results of falling-head permeability tests performed on cores of the high-cement content material are also presented in Table 3.

### Strength Versus Age Relationships

Laboratory-cured compressive strengths (Figure 1) show a moderate increase from low to medium cement with a much larger increase for high cement. Laboratory-cured flexural strengths (Figure 2) show almost identical results for the low and medium cement with marked improvement for the high cement. Flexural strength curves are extended to 28 days for visual comparison with the other plots but this extrapolation is not intended to predict the strength beyond 7 days. Field-cured compressive and split tensile strengths (Figures 3 and 4) showed a more uniform increase with cement content.

Measured strength depended on the test method and curing condition. The parallel nature of the regression lines shown in Figures 1 through 4 indicates a relatively consistent correspondence among samples. Further testing with multiple replicates for each sample will be required to accurately assess and explain these differences.

### Review of Findings

The unique characteristics of CSOGB led to modification of typical procedures. Observations during fabrication, handling, and testing, and the numerical results suggest that the modifications were effective.

Use of a single large sample to produce all the specimens for each cement content and curing condition helped minimize variability. This approach, however, meant that one bad sample could

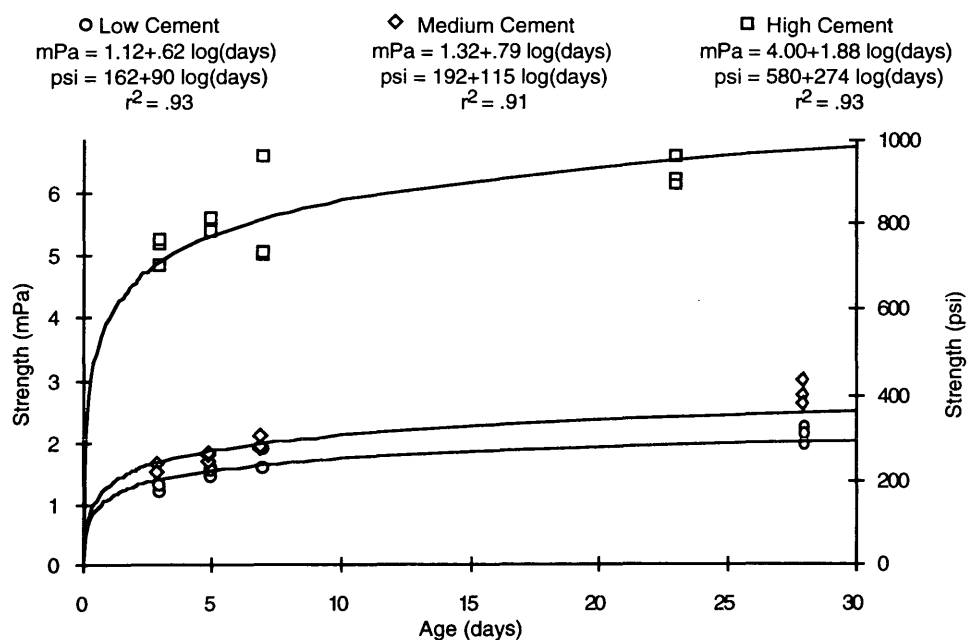


FIGURE 1 Laboratory-cured compressive strength versus age.

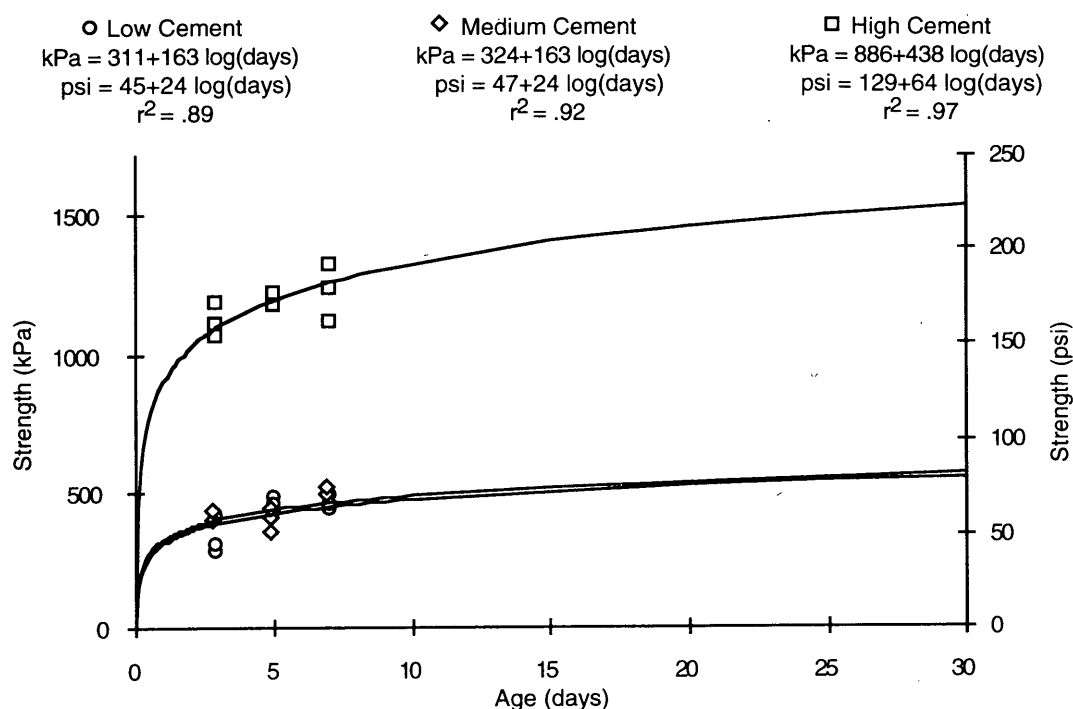


FIGURE 2 Field-cured compressive strength versus age.

jeopardize the validity of several specimens. The usefulness of all the data generated from the laboratory-cured medium-cement sample is thus limited. The relationship between cement and strength for Figures 1 and 2 is consequently obscured.

Examination of strength data and test specimens revealed no significant problems attributable to the fabrication process. Com-

paction was fairly uniform throughout the cylinders. Separate lifts were identifiable in some cases, but did not seem to affect the behavior during testing. The individual test results for each age are generally tightly grouped.

A rectangular tamper should be used for beams to provide for uniform compaction in the corners. Care should be taken to avoid

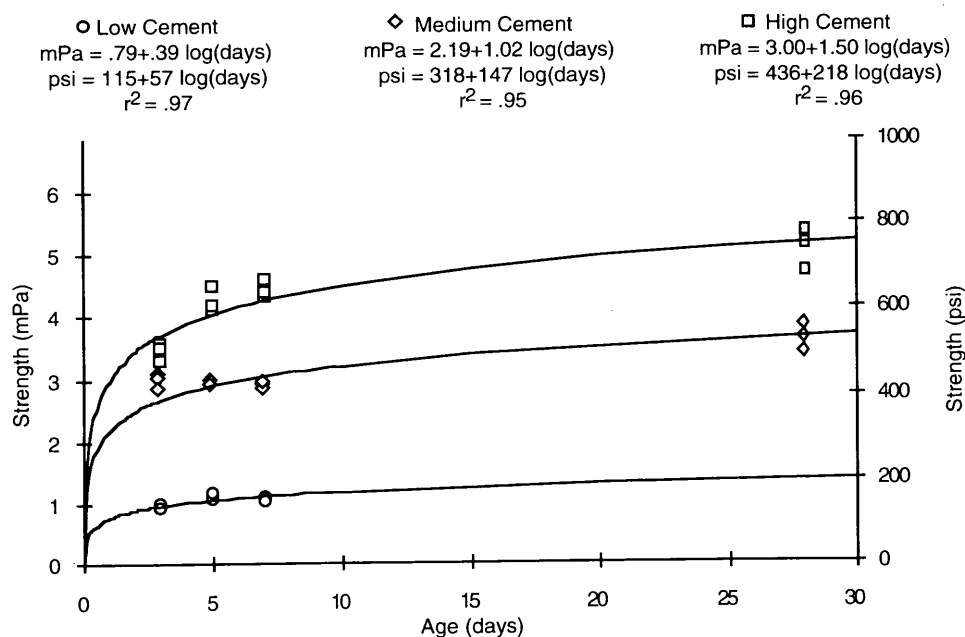


FIGURE 3 Laboratory flexural strength versus age.



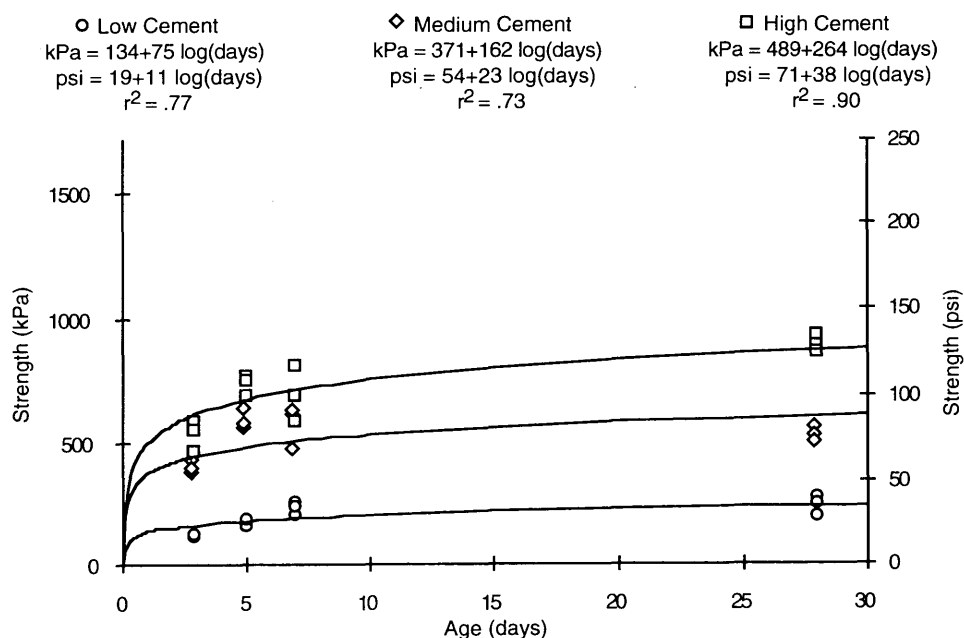


FIGURE 4 Field-cured split tensile strength versus age.

aggregate fracture during tamping. Use of a wooden tamper instead of the steel one employed in this work might be advisable.

No major problems occurred during transportation or handling. However, two low-cement content field-cured cylinders were broken during stripping for the 3-day tests. If precautions are taken, problems associated with excessive drying and mechanical damage can be avoided.

In this work, field-cured specimens were uncovered for 3 days in the middle of their curing period to mimic the exposure of the material on grade. Because field conditions are variable, and for simplicity, specimens should probably be left covered until tested.

Mechanisms observed during failure of CSOGB were similar to those seen with regular concrete. Low-cement content compression and split tensile specimens tended to fail with disintegration of material over the entire cross section, a mechanism common for low-strength concretes. Higher-cement content specimens had shear or cone failures in compression and a surprisingly clean failure plane in split tensile tests. All bending tests had clean fracture surfaces near mid span. These observations tend to support the validity of the testing procedures.

Strength versus age plots for laboratory-cured specimens show a nonuniform increase in strength with cement content, whereas field-cured plots and core strengths indicate a more uniform strength gain. This inconsistency makes it difficult to come to a definitive conclusion about the correlation between strength and cement content. This problem is thought to have been caused by the inclusion of a nonrepresentative sample (outlier) for the laboratory-cured medium cement content.

Marginal effectiveness of cement additions may vary with cement content. Cement at the points of contact between aggregate particles provides bonding, whereas cement coating open surfaces contributes little to the strength. This mechanism could account for some non-uniformity in the cement content versus strength relationship.

The w/c ratio of the low-cement mix (0.94) is substantially higher than that of the medium-cement mix (0.52) and the high-

cement mix (0.47). Based on this, the strength of the low-cement material should be significantly lower than that of the other two materials. This, however, was clearly not the case. Higher w/c may facilitate the migration of the paste toward the points of contact and thus tend to improve the strength of CSOGB material.

Strength development mechanisms for CSOGB are potentially more complicated than those for regular concrete. These mechanisms must be more thoroughly understood before a reliable mix design procedure can be developed. This work implies that cement content instead of w/c is a better indicator of strength for CSOGB. Until data from more tightly controlled testing are obtained, design decisions should probably be based on cement content.

Cores were taken without difficulty for each of the three cement contents. Split tensile tests were undertaken because the cores were too short for a valid compression test. Although more variable, strengths are similar to those obtained for field-cured cylinders. Higher variability is probably caused by segregation during placement and the smaller size of the cores.

Curing, requiring several workers to place and later remove plastic sheeting, was expensive. Cores of material left exposed showed lower average strengths (Table 3) than covered material but there was some overlap in the data. If exposure does not cause significant strength loss, more cement can be used without covering to provide a potentially better product at reduced cost.

Permeability tests (Table 3) indicate that, even with high cement material, CSOGB provides adequate drainage. Core tests show an average flow rate of 930 m/day (3,085 ft/day) whereas WisDOT specifies a minimum of 305 m/day (1,000 ft/day).

## EFFECTS OF CONSTRUCTION TRUCKING OPERATIONS

### Test Section Observations

Observations were made of formal test sections provided for each cement content. Distinction is made between one-way and two-

way trucking. Under one-way conditions, the grade is used primarily for return traffic operating unloaded at relatively high speeds. Loaded trucks are channeled onto the grade at about 0.8-km (0.5-mi) intervals, and operated at lower speeds, primarily in reverse. With two-way hauling, the entire project is trucked, at speed, by both empty and loaded trucks. Passage of about 310 trucks/km (500 trucks/mi) of pavement was required.

The typical empty truck had 44.5 kN (10 kip) on a single front axle with about 66.8 kN (15 kip) on a tandem rear axle. Fully loaded with a 6.88 m<sup>3</sup> (9 yd<sup>3</sup>) batch of concrete, the front axle carried about 89.0 kN (20 kip), with about 151 kN (34 kip) on the rear tandem and an additional 44.5 kN (10 kip) on the auxiliary rear axle.

### *Low Cement Content*

The test section for low-cement material was laid out near the north end of the project to minimize the one-way trucking that it would carry. The condition of the subbase was good, with no significant areas of soft or wet spots. Some segregation was evident with crescent-shaped light and dark streaks characteristic of the placement procedure throughout this project. The center of the placement was somewhat undercompacted, whereas the material near the edges was more stable. The surface was generally smooth, with some roughness caused by worker footprints in the fresh material.

Material subjected to 250 empty trucks running at relatively high speeds sustained only surface damage. Raveling developed quickly with some expansion of initial problem areas but, at the time they were paved over, the worst were no more than 2.5 cm (1 in.) deep. Loose material was dispersed and some aggregate fracture was observed. About 5 percent of the surface, corresponding to the locations of crescent-shaped segregation bands, was affected. Deterioration also showed some correspondence to areas of initial surface roughness.

Under the action of slower-moving, loaded trucks, deterioration tended to be deeper, with loose material confined to damaged areas. Although degradation began more slowly, full-depth damage with up to 2.5-cm (1-in.) ruts developed after passage of 250 loaded trucks. At this point, as CSOGB was paved over, there was no significant infilling or pumping of fines in the ruts. Again there was correlation between the locations of distressed areas and segregation bands. Here, however, the frequency of significant damage was lower, with about 2 percent of the area substantially affected.

One-way construction traffic varied from 74 to 250 trucks over the test section. Performance was characterized as good, with no serious deterioration and no remedial work required before paving.

### *Medium Cement Content*

The test section for medium-cement material began about 5.6 km (3.5 mi) into the northern portion of the project. Although the subgrade was generally dry and stable, there were some soft areas that had been undercut and filled with sand. Again there was minor segregation, surface roughness, and differential compaction.

Damage from 1,800 higher-speed empty trucks was limited to surface erosion. The onset and growth of distress was more grad-

ual than it was with the low-cement material. Loosened material was thrown from raveled areas by the trucks. Deterioration affected about 3 percent of the area and extended to depths of up to 2.5 cm (1 in.). Although not all segregation bands showed distress, surface degradation followed the same pattern. There was little correlation between initial roughness and the development of raveling.

Under 530 loaded trucks, isolated full-depth degradation occurred with 2.5- to 5-cm (1- to 2-in.) ruts over about 2 percent of the total area. There was some infilling of fines, but to a degree that had no appreciable effect on drainability. Loose material was confined to the ruts.

One-way traffic ranged from 1,680 to 1,940 trucks over the test section. Performance was generally good, but there were some isolated areas of more severe distress. These trouble spots were related to poor conditions in the subbase. Damage in these areas was repairable, characterized by dispersion of loose material, cracking, and loss of permeability caused by infill and pumping of fines.

### *High Cement Content*

The test section for high-cement material was located about 6.4 km (4 mi) into the southern portion of the project. Underlying dense-graded material was extremely stable with only isolated soft spots. Segregation and roughness were comparable to the other test sections and there was some differential compaction.

Operation of 2,045 empty trucks caused only minimal aggregate fracture and virtually no erosion of the surface. The only discernible defects were transverse shrinkage cracks at 15- to 30-m (50 to 100-ft) intervals. Operation of up to 1,475 loaded trucks led to only minor deterioration. The only noticeable effects were some aggregate fracture and a limited amount of erosion along some of the shrinkage cracks.

Two-way trucking of 1,250 to 2,060 trucks was sustained over the test section. Performance was excellent. There was some confined full-depth damage directly over a small soft spot in the subgrade.

### *Auxiliary Observations*

Observations of material with varying water contents indicated that, although higher water contents promoted segregation, excessively dry mixes deteriorated faster. This effect became less pronounced as cement content was increased. High-cement content mixes also exhibited increased ability to bridge over soft spots in the subbase. Low-cement content material subjected to extended trucking suffered severe deterioration regardless of water content or subbase support.

A 122-m (400-ft) length of high cement material was left exposed to air cure. When compared with the adjacent material that was covered with plastic for the first 4 days, no significant degradation in truckability was evident.

### *Factors Influencing Performance*

Major factors influencing the performance of the CSOGB were cement content, number of trucks, structural stability of sublayers, and segregation. Surface irregularities played a minor role.

TABLE 4 Performance Index

0 Very poor	Widespread dispersion of material, extensive deep deterioration, and significant infill of fines. Required extensive replacement of material to maintain support and/or permeability.
1 Poor	Extensive dispersion of material, frequent deep deterioration, cracking, and localized infill of fines. Required additional material and regrading.
2 Fair	Some dispersion of material, deep raveling, occasional deep deterioration, and some isolated infill of fines. Required some grading of dispersed material.
3 Good	Isolated dispersion of material, shallow raveling, some deep deterioration, and no appreciable infill of fines. Required only isolated grading of dispersed material.
4 Very good	Minimal raveling, confined deep deterioration with some subsidence, and no infill of fines. Required no significant repairs.
5 Excellent	Deterioration confined to isolated problem areas. Required no significant repairs.

Higher cement content mixes performed better for all subbase conditions. Improvement from medium-to-high cement was markedly greater than that observed from low-to-medium cement in areas with soft support.

CSOGB deteriorated with trucking volume. Problems tended to develop quickly in areas with segregation or poor structural support. The severity of distress increased with traffic, but the size of the distressed regions remained fairly constant. Higher volumes also led to more areas of damage, but progression was gradual. Deterioration became widespread only under very high volumes.

Empty trucks running at relatively high speeds, about 72 km/hr (45 mph), caused gradual shallow distress and dispersion of material. Full trucks running at low speeds, often in reverse, led to deep damage characterized by the rapid development of ruts with confined subsidence of loose material. The worst damage occurred when heavily loaded trucks were operated at high speed. This condition prevailed where CSOGB was subjected to two-way

hauling over substantial distances. Damage was deeper and characterized by dispersion of material, aggregate fracture, and infilling of fines.

Soft areas in underlying layers caused deterioration of the CSOGB. Each mix performed adequately where the support was good, but in areas with only fair support, all the mixes showed some major deterioration. Material over soft spots tended to break up in chunks, crack, and pump fines from the subbase. Lower-cement content mixes tended toward widespread damage, whereas the high-cement material sustained only isolated damage.

CSOGB is harsh, unworkable, and susceptible to segregation. Excessive mix water caused separation of the paste from the aggregate, resulting in areas where permeability was reduced because of the infilling of paste. Dry mixes had areas of inadequate bonding that were subject to structural deterioration.

During placement, material in the finegrader hopper was pushed by the machine at the center of the roadway and augered to each

PERFORMANCE SUMMARY CHART 1  
(Good Subbase Conditions)

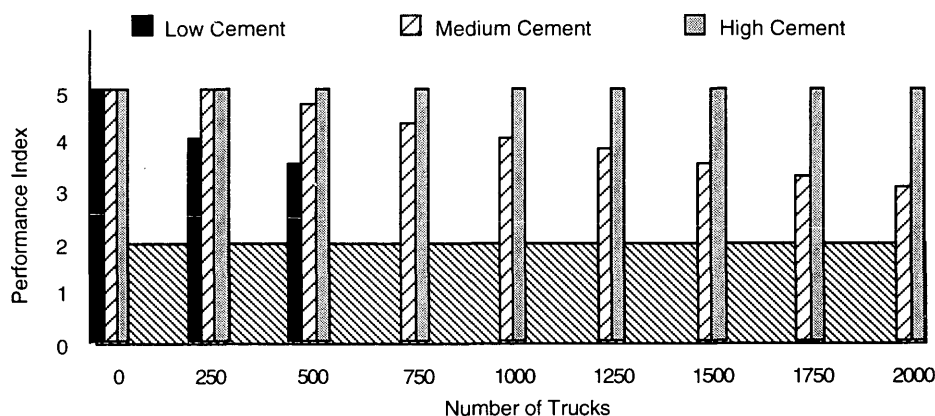


FIGURE 5 Performance over good subbase.

PERFORMANCE SUMMARY CHART 2  
(Fair Subbase Conditions)

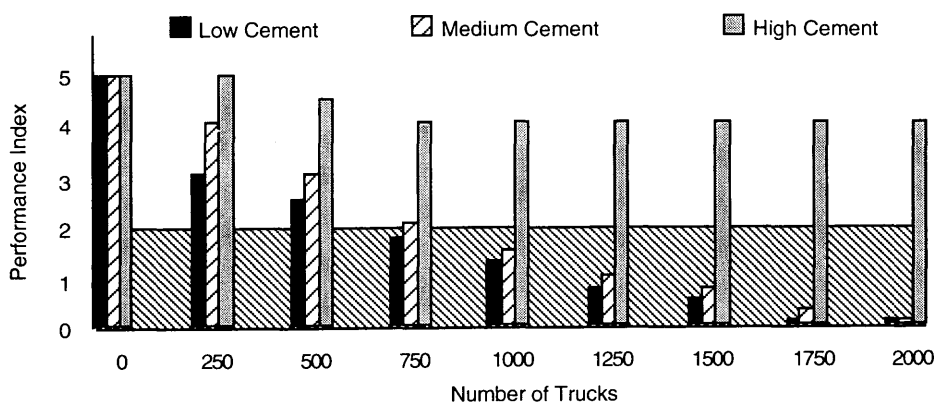


FIGURE 6 Performance over fair subbase.

side. Crescent-shaped areas of wet and dry material were formed as new material was added. These defects persisted throughout the range of water contents tried, but their severity could be limited. Performance was impaired with severe segregation, but was relatively unaffected with minimal segregation.

CSOGB does not respond as a plastic mass in a slump test and there is no other simple field test for workability. Examination of the extent of segregation of material in transit and as laid down can, however, be used to make mix-water adjustments. Visual inspection was sufficient to identify extreme segregation and a touch test was used when segregation was less pronounced. Pastes from wet and dry areas were compared for consistency. If the paste felt grainy and lacked cohesion, water was added. If the paste felt too fluid, less water was used. Using too little water proved to be more detrimental to performance.

Rough areas in the low-cement test section often developed into regions of shallow surface raveling. Roughness was less important in the higher-cement content materials, but poor compaction contributed to increased surface erosion.

## Review of Findings

The second major objective of this work was to determine how well CSOGB performs under construction traffic. Results indicate that these materials can function as a haul road without excessive damage to either their structural integrity or their ability to provide adequate drainage.

Performance improved with cement content, but even low-cement mixes demonstrated reasonable durability. Low-cement material gave good performance under one-way trucking of up to a 1.6 km (1 mi) when placed over sound sublayers. Medium-cement material also performed well under one-way trucking of up to 3.2 km (2 mi). Performance was significantly enhanced with high-cement content even under two-way trucking for hauls of up to 8 km (5 mi) although some damage occurred when support was poor. Performance of lower-cement mixes, however, showed marked deterioration when placed over less sound material.

The performance index defined in Table 4 was developed to quantify the relation between performance and cement content.

Performance is rated from 0 to 5 in terms of (a) dispersion of material, (b) depth and nature of deterioration, (c) extent of infilling or pumping of fines, (d) percentage of surface area significantly affected, and (e) extent of remedial work required.

Characterizations of performance presented in Figures 5 and 6 summarize the information collected during observation of construction activities. The cross-hatched region of each chart represents a level of damage that requires significant repair or replacement.

Predicted performance for material is shown in Figure 5. High-cement material gave excellent performance. Medium-cement material showed progressive decay but gave good performance up to passage of 2,000 trucks. Low-cement material held up well under traffic approaching 500 trucks.

Predicted performance for material with fair support is shown in Figure 6. High-cement material bridged over soft areas and gave good performance even after extensive trucking. Low- and medium-cement materials progressively deteriorated with marginal performance by the time volume reached 750 trucks.

## CONCLUSIONS AND RECOMMENDATIONS

### Physical Testing

1. Compression, split tensile, and bending tests yield meaningful strengths for CSOGB;
2. Cores can be cut and tested for in-place strength and permeability of CSOGB;
3. Four modifications should be made to standard ASTM (1) concrete testing methods: (a) larger samples should be taken, (b) specimens should be tamped rather than rodded, (c) specimens should be left in molds and covered until tested, and (d) load rates should be reduced;
4. An objective measure of workability should be developed for mix design and quality control; and
5. Relationships among cement content, w/c ratio, and strength should be explored.

## Field Performance

1. Performance of CSOGB under trucking traffic depends on cement content, trucking volume, stability of underlying layers, segregation, and surface irregularities. Primary detriments were poor underlying structural support and segregation of the paste from the aggregate;

2. Frequent access should be provided to minimize two-way trucking;

3. Cement content should be tailored to trucking and subbase conditions. Low cement should be restricted to short hauls over stable subbase; medium cement is appropriate for general use and high cement should be used in areas with poor support or heavy trucking;

4. Benefits of covering should be investigated; and

5. Long-term performance should be monitored.

## ACKNOWLEDGMENTS

The work presented in this report was funded through the Demonstration Projects Program, Office of Technology Applications, Engineering Applications Division, Federal Highway Administration. FHWA sponsored this research in the interest of information exchange and does not necessarily endorse the author's conclusions and recommendations.

## REFERENCES

1. *Annual Book of ASTM Standards*, Vol. 04.02, Concrete and Aggregates. American Society for Testing and Materials, Philadelphia, Pa., 1990.
2. *Standard Specifications for Transportation Materials and Methods of Sampling and Testing*, Part 1, Specifications. American Association of State Highway and Transportation Officials, Washington, D.C., 1986.
3. *Permeability Test for Open-Graded Base Courses*. Wisconsin Department of Transportation, Madison, Wis., 1990.

# Estimating the Design Life of a Prototype Cement-Stabilized Phosphogypsum Pavement

D. M. GERRITY, J. B. METCALF, AND R. K. SEALS

Cement-stabilized phosphogypsum (CSPG) mixtures are demonstrated to have sufficient strength at the modified Proctor compaction level to satisfy the Louisiana Department of Transportation and Development design unconfined compressive strength (UCS) criteria of 1.7 MPa at 7 days for stabilized base material. With 8–12 percent cement, at 95 percent of modified Proctor maximum dry unit weight, CSPG had greater resilient modulus and UCS values than the commonly used river silt. Life estimates for a prototype road were highly dependent on the bearing capacity of the subgrade soil. The CSPG base produced acceptable estimated design lives for secondary roads at an attractive cost compared with conventional limestone aggregate.

More than 35 million metric tons of phosphogypsum (PG), a solid by-product of phosphoric acid production, are generated annually in the United States. The combination of environmental concern associated with disposal and the increasing cost to stockpile the material has prompted a search for the commercial use of PG. To prove that PG has a use as a road pavement material, prototype pavements need to be developed and demonstrated.

A laboratory evaluation was made of a prototype road with a CSPG base, including estimates of its potential design life in equivalent standard axle loadings (ESALs) and life-cycle costs compared with conventional limestone bases. The resilient modulus studies showed that a typical CSPG mix will theoretically provide an adequate design life at a life-cycle cost less than conventional materials.

## EXPERIMENTAL PROGRAM

Conventional pavement designs have been based primarily on laboratory tests that use static loading. These tests are merely strength comparisons in which materials are judged on their total or relative strengths under failure-type loading. However, rarely do materials (in the field) receive loads that approach failure, and the performance of materials can be very different at low compared with high stress levels (1). The Louisiana Department of Transportation and Development requires a laboratory 7-day unconfined compressive strength of 1.7 MPa for Portland cement-stabilized bases (Test Method TR432-Method B).

The American Association of State Highway and Transportation Officials (AASHTO) (2) requires that the layer coefficients used in the development of the structural number of the pavement be based on the UCS or the repeated load triaxial resilient modulus test. However, a protocol for determining resilient modulus for

flexible pavement design has not been clearly established, especially in the case of stabilized materials. Values given in the Van Til nomograph of the AASHTO design guide are from a general correlation of all cement-stabilized materials.

Phosphogypsum (PG), which is about 80 percent gypsum, is characterized by the AASHTO classification system as a silty soil (A-4) with little to no plasticity or by the Unified system as a silty material (ML).

The CSPG was compared with stabilized river silt, a material commonly used in Louisiana for secondary roads. The river silt was classified by AASHTO specifications as an A-3, fine sand, and by the Unified Soil Classification System (USCS) as an SMM or silty sand. The material was nonplastic. It was stabilized with 10 percent cement to reflect common practice. The cement used in this study to stabilize the PG and river silt was a Type I portland cement.

The subgrade at the proposed trial site was classified, according to AASHTO, as an A-4 or A-6 (depending on the plasticity index). Based on the USCS, the subgrade is classified as a SC or clayey sand. Typical laboratory CBR values for the subgrade were 5 and 8 at moisture contents of 19 percent and 17 percent, respectively.

## Resilient Modulus Testing

The resilient modulus test was developed to provide a more accurate description of the behavior of soils or other paving materials under the effect of dynamic stresses similar to those generated by a moving wheel. A standard triaxial cell was modified to fit a bottom-loading Instron testing machine and to house two linear variable displacement transducers (LVDT) for the longitudinal measurement of displacement. The LVDTs were internally mounted and measured the displacement relative to the specimen end caps. The signals from the two LVDTs were averaged. A triangular loading function was used to allow changes in loading and rest periods. The raw displacement and load data were imported into a spreadsheet and converted to load and strain data. The protocol for the resilient modulus testing is presented as follows.

The triaxial resilient modulus test was conducted in load control using the Instron 8500 material-testing system equipped with a 10 Kilonewton load cell. A standard geotechnical triaxial cell was used to run these experiments. Confining pressures ranged from 5 to 15 psi. The samples used were 5.08-cm-diameter cylinders, 10.16 cm tall. All specimens were tested as cured for 7- and 28-day periods. The strain was calculated from displacements measured by 2 DC LVDTs attached at the ends of the sample. The

LVDTs had a full scale of 0.05 in. and a signal output of 10 volts. The LVDTs were calibrated independently and then each signal was channeled through a signal averager. The signal from the averager was then connected to the Strain 1 channel port on the Instron machine, which allowed viewing of the changing strain as a percent of full scale. The experimental data was collected using Instron software or BINSWARE that was installed on a 486 personal computer. The resilient modulus was calculated by dividing the change in deviator stress by the change in strain during the cyclic loading.

The following criteria and procedures were selected from the protocol listed in Barksdale et al. (9) for asphaltic concrete at low temperatures: The cyclic load for testing and preconditioning shall be 30 percent of the unconfined compressive strength of the specimen. Preliminary unconfined compression strength tests were run on the design mixtures to give approximate total strengths of the specimens. Seating loads shall be no greater than 3 percent of the total strength of the specimen. The loading pattern and preconditioning shall have a load duration of 0.1 sec and a rest period of .9 sec. The period of preconditioning shall be attained at a determined number of cycles in which 10 successive readings of deformation agree within 10 percent. The number of load pulses to be applied for determining resilient modulus shall be at a minimum of 30 load pulses. Continued beyond 30 until the range in deformation values of 5 successive deformation values is less than 10 percent of the average. Then the resilient modulus is the average of the resilient modulus values measured individually from 5 load cycles after deformations are stable.

The following procedure was used:

1. Measure height, diameter, and weight of the cured sample; place on porous stones; place LVDT assembly and loading cap onto specimen.
2. Place on Instron actuator platform and connect air.
3. Zero LVDTs using hand-held voltmeter.
4. Apply seating load to the triaxial assembly; ensure that the LVDTs are still reading within 5 percent of the null point of the LVDTs.
5. Set function generator of the Instron to provide a triangular loading having a 0.1 sec duration and a 0.9 sec rest period.
6. Within the first 2 min of the dynamic loading, increase confining pressure to the maximum desired pressure.
7. Allow the loading to continue until it reaches stability and record the maximum and minimum load and displacement voltages at the end of this preconditioning period. Run 30 cycles while recording the load and change in displacement with the PC. The resilient modulus will be calculated using the average value of the resilient modulus of the last 5 cycles.
8. Change function generator to a single ramp loading of 1.27 mm/min. Set up data acquisition file for recording the data at every 500 ms.

A series of tests was conducted to establish the relationship among UCS and moisture, density, cement content, and curing period, which together with research from the Institute for Recyclable Materials (3,4) lead to two conclusions: (a) the addition of cement to PG changes the compacted unit weight and optimum moisture content for a given compactive effort and (b) increases in strength and resilient modulus resulted from increases in cement. Therefore, the mixes tested in the study (5) were selected on the basis of the information already mentioned.

**TABLE 1** Change in Resilient Modulus With Load Duration for Specimens Cured for 7 Days

Material	Loading Duration	Average Resilient Modulus (MPa)	Standard Deviation (MPa)
12% PC, PG 95% Modified	0.1 seconds	993	55
12% PC, PG 95% Modified	0.5 seconds	938	35
12% PC, PG Standard	0.1 seconds	286	23
12% PC, PG Standard	0.5 seconds	259	16

\* Each result is the average of 3 samples.

PC = Portland cement

PG = Phosphogypsum

RS = River silt

Sensitivity of the resilient modulus value of CSPG to load duration was analyzed by altering the loading interval from 0.1 to 0.5 sec. Shown in Table 1 is the change in resilient modulus of CSPG specimens prepared at 95 percent modified and standard Proctor dry unit weight, 15 percent moisture, and a curing period of 7 days. The AASHTO-specified load duration of 0.1 sec was used for the test program. Illustrated in Figure 1 is a typical stress-strain curve for a CSPG mixture tested to failure in unconfined compression. Presented in Figure 2 is the compressive stress/strain curve for repeated load when the seating load is 270 KPa. Shown in Figure 3 is the change in resilient and plastic strain and in Figure 4 the change in modulus with the number of cycles. Based on the information presented in Figures 3 and 4, each specimen

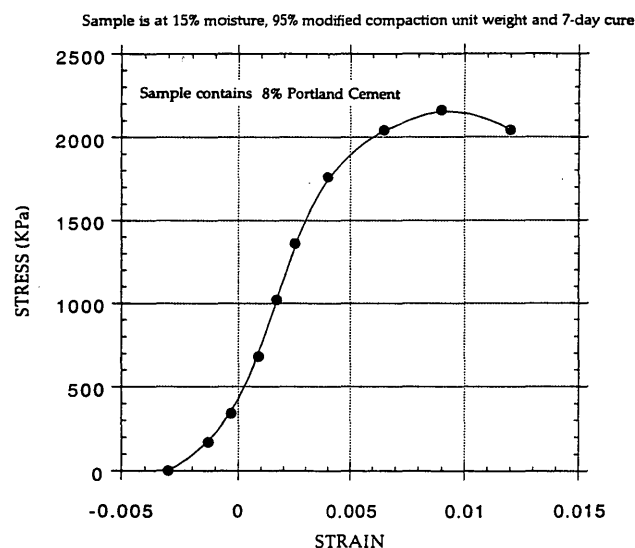


**FIGURE 1** Stress-strain curve for CSPG tested to failure in compression.

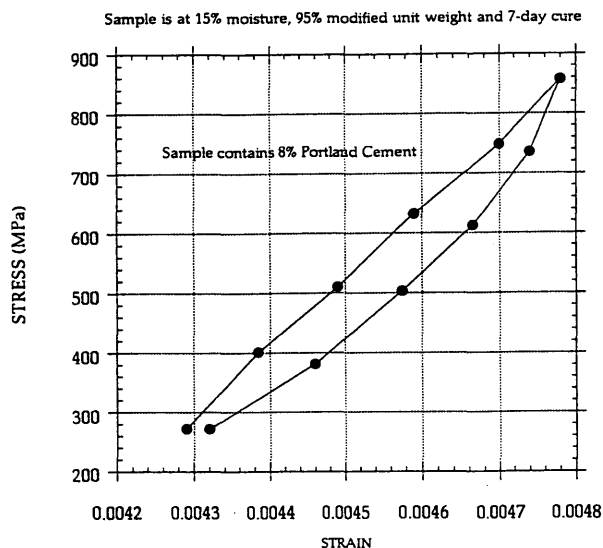


FIGURE 2 Stress-strain curve for CSPG tested in compression under repeated load.

was preconditioned with 500 cycles, at the given confining pressure (34.5 KPa), before recording stress and strain data.

### Unconfined Compressive Strength Test

On completion of resilient modulus testing, the specimens were loaded to failure at the ASTM D1633 constant loading rate of 1.3 mm/min. Presented in Table 2 are the average UCS and resilient modulus results for PG and river silt specimens stabilized with Type I portland cement. Twenty-eight-day strength and re-

silient modulus values for the river silt could not be determined because of damage that occurred to the samples during the curing process. Three samples were molded for each mix and tested for resilient modulus at a repeated load of 30 percent of the UCS. The samples were then tested for UCS.

### DESIGN LIFE EVALUATION

The elastic layer program ELSYM5 (6) was used to estimate the stress and strain magnitudes, within certain pavement geometries, for selected moduli. The range of (compressive) stresses (190 to 760 kPa) used in the laboratory measurement of resilient modulus falls within the theoretical range of magnitude of (tensile) stresses (100 to 760 kPa) calculated by ELSYM5.

### Design Lives

The design life estimates were calculated using the AASHTO DARwin program (7). Pavement geometries and structural coefficients were entered into the specified thickness design layer analysis in order to calculate a structural number for the proposed pavement. This structural number was then used to calculate a life for the pavement in ESALs given the lifetime change in present serviceability and roadbed resilient modulus.

### Selected Material Properties

Shown in Table 3 are the structural values assigned to the materials used in the pavement stress analysis and design life estimates. The Louisiana design procedures were referenced for the average resilient modulus values for asphaltic concrete, limestone, and subgrade used in the design of roads in Louisiana. The CSPG layer coefficient of 0.2 was given to the material based on the 28-day strength.

### Life Cycle Estimates

The estimated life of each of the selected pavement configurations is given in Table 4. A base thickness of 210 mm was used, which is the standard in Louisiana. By increasing the modulus of the subgrade, larger values of allowable ESALs were predicted. Two values have been presented to show the sensitivity of the roadbed soil to moisture content [20.7 MPa = California bearing ratio (CBR) of 2 at 22 percent moisture and 51.7 MPa = CBR of 5 at 19 percent]. The standard relationship  $M_r = 10.34 \text{ MPa} \times \text{CBR}$  was used to calculate these values. The higher moisture content represents the average in situ moisture content of the subgrade soil located at the proposed experimental test section during the summer of 1993, and the lower moisture content is the material compacted near optimum. Optimum moisture content for the subgrade material (American Society for Testing and Materials 1980) was 17 percent. Both subgrade modulus values represent conservative representations of life-cycle estimates.

### Life Cycle Costs

To demonstrate the effective use of CSPG, the life expectancies of two bases were compared. Design 1 used a CSPG base con-

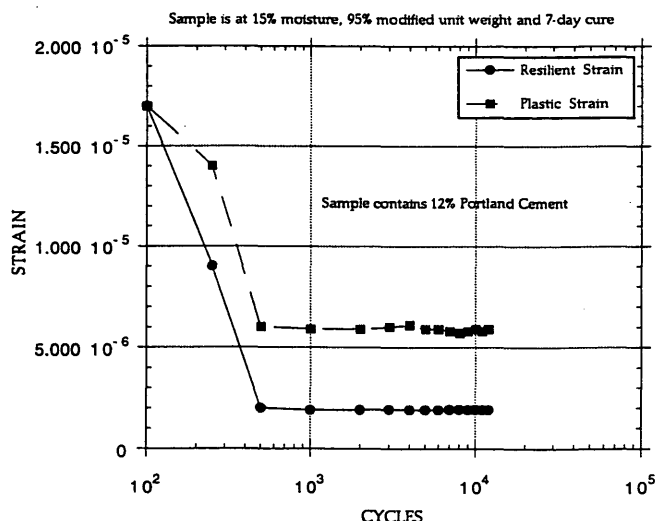


FIGURE 3 Changes in resilient and plastic strain with number of cycles.



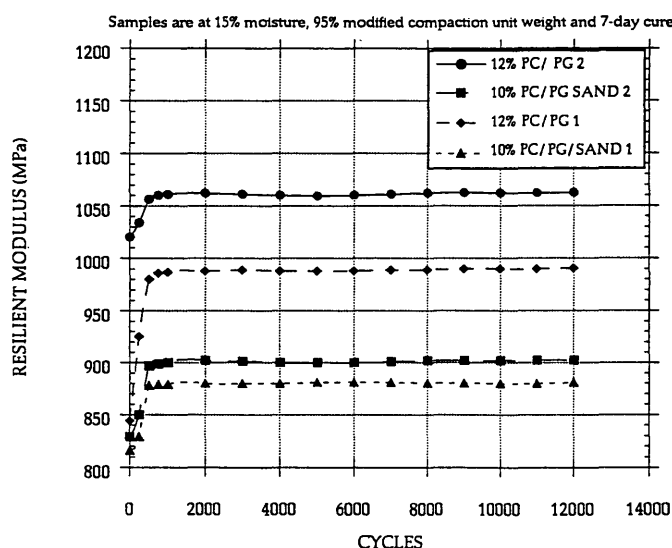


FIGURE 4 Changes in resilient modulus with number of cycles.

taining 12 percent cement. This layer was assigned an AASHTO layer coefficient of 0.2 based on its average 28-day unconfined compressive strength (3 MPa), resilient modulus (1655 MPa), and relative stiffness compared with the materials used in Louisiana. Twenty-eight day strengths were used for design because it was assumed that by the time normal traffic loadings were induced on the pavement, the CSPG would be closer to 28-day strength than 7-day strength. The second design employed a conventional limestone base with a resilient modulus of 345 MPa and a layer co-

efficient of 0.14. The two alternatives are compared in Table 5. Both designs assume a subgrade having a resilient modulus of 52 MPa.

Each analysis assumed a median year average daily traffic of 900, a projected daily ESAL value of 89 and a total 20-year ESAL value of 649,000. These data are typical for a rural secondary road in Louisiana (8). The analysis period was 20 years. Rehabilitation of the pavement consisted of a 50-mm asphaltic concrete overlay. After the first rehabilitation, this would be milled and recycled to a depth of 50 mm in order to repair cracking. The life-cycle costs are expressed in present-worth values. This analysis assumes the CSPG will have adequate durability.

TABLE 2 Average of UCS and  $M'$  Values

Material	Average UCS (KPa)	Standard Deviation (KPa)	Average Resilient Modulus (MPa)	Standard Deviation (MPa)
12% PC, PG, Standard, 7-Day	452	48	283	52
10% PC, RS, Standard, 7-Day	917	131	276	15
12% PC, PG, 95% Modified, 7-Day	2331	338	1014	62
12% PC, PG, 95% Modified, 28-Day	3082	385	1655	75
10% PC, RS, 95% Modified, 7-day	1469	210	435	61
10% PC, RS, Modified, 7-Day	1489	152	441	48

\* Each result is the average of 3 samples.

PC = Portland cement  
PG = Phosphogypsum  
RS = River Silt

## CONCLUSIONS

Examined in this paper is the correlation between resilient modulus and UCS of CSPG and river silt and estimated is the design life of a CSPG base course pavement. The results and estimates show that

TABLE 3 Estimated Structural Values of Materials Used in Pavement Analysis (2)

Material	Resilient Modulus (MPa)	Layer Coeff.	Poisson's Ratio
AC	2413	0.42	0.35
Limestone	345	0.14	0.45
Subgrade	21 - 52	- <sup>a</sup>	0.45
CSPG	1655	0.20	0.20
Lime Stabilized Heavy Clay	345	0.20	0.35
Lime Stabilized Silty Clay Subgrade	207	0.14 - 0.20	0.35

<sup>a</sup> no structural coefficient given

TABLE 4 Design Lives of Selected Pavements

Thickness	Design 1	Design 2	Design 3
AC	50	50	50
CSPG	210	210	210
Lime Stabilized Silty-Sandy Clay Subbase	150	—	—
Lime Stabilized Heavy Clay Subbase	—	150	—
Structural Number	2.77	2.95	2.35
Life in ESALs <sup>a</sup>	64,000	92,000	23,000
Life in ESALs <sup>b</sup>	545,000	813,000	195,000
	Design 4	Design 5	Design 6
AC	50	50	50
Limestone	210	210	210
Lime Stabilized Silty-Sandy Clay Subbase	150	—	—
Lime Stabilized Heavy Clay Subbase	—	15.2	—
Structural Number	2.32	2.5	1.9
Life in ESALs <sup>a</sup>	20,000	34,000	6,000
Life in ESALs <sup>b</sup>	180,000	286,000	54,000

<sup>a</sup> means the life was calculated with a subgrade resilient modulus of 20.7 MPa; <sup>b</sup> means the life was calculated with a subgrade resilient modulus of 51.7 MPa.

TABLE 5 Life-Cycle Cost for Selected Pavements

Design	Cross Section	Initial Cost, \$	Total Cost, \$
3	50mm AC, 210mm CSPG	218,000	316,000
1	50mm AC, 210mm CSPG, 150mm LSSB	286,000	308,000
4	50mm AC, 210mm LS, 150mm LSSB	229,000	322,000

LSSB = Lime Stabilized Silty-Sandy Clay Subbase.

1. Stabilized PG with 10–12 percent Type I portland cement has a resilient modulus between 275 and 1655 MPa at standard and modified Proctor unit weights. ASSHTO-specified strength criteria for cement-stabilized materials can be reached, with PG, only by using modified Proctor compaction energy.

2. Resilient modulus-UCS relationships should be determined for a given mix rather than depending on one unique relationship for all mixtures.

3. For the prototype site, with a low CBR subgrade, a pavement consisting of 50 mm of asphaltic concrete with a resilient modulus of 2400 MPa and a 210-mm CSPG base containing 12 percent cement at 1.52 t/m<sup>3</sup> and 15 percent moisture content will result in an approximate design life of 195,000 ESALs.

4. Stabilized PG can be used effectively as a road base for a secondary low-volume road providing an appropriate cement content, adequate compaction, and proper drainage are ensured.

5. Based on the analyses, the life-cycle cost of roads built with CSPG is attractive. However, an experimental test pavement must be built to determine if CSPG can withstand the environmental conditions that occur in the field.

## REFERENCES

1. Pavements Design: Principles and Practices. *Participant Notebook*, U.S. Department of Transportation, Federal Highway Administration, Washington, D.C., Sept. 1987.
2. *AASHTO Guide for Design of Pavement Structures*, 1986. American Association of State Highway and Transportation Officials, 1986.
3. Seals, R. K. *Phosphogypsum Literature Review*. Institute for Recyclable Materials, Louisiana State University, Baton Rouge, Dec. 1991.
4. Ong, S. S. Unconfined Compressive Strength of Cement-Stabilized Phosphogypsum. Institute for Recyclable Materials, Dec. 1992.
5. Gerrity, D. M. Estimating the Design Life of a Prototype Cement-Stabilized Phosphogypsum Pavement. Master's thesis, Louisiana State University, Baton Rouge, La., 1993.
6. Kopperman, S., G. Tiller, and M. Tseg. *ELSYM5 Computer Program*. Federal Highway Administration, Washington, D.C., 1985.
7. *AASHTO DARwin. Computer Program*. American Association of State Highway and Transportation Officials, Washington, D.C., 1992.
8. Temple, W. H., and W. Carpenter. *Implementation of the New AASHTO Pavement Design Procedure in Louisiana (Final Report)*. Louisiana Transportation Research Center, Louisiana State University, Baton Rouge, 1990.
9. Barksdale, R. D., G. J. Rix, S. Itiani, P. N. Khosla, R. Kim, P. C. Lambe, and M. S. Rahman. *Laboratory Determination of Resilient Modulus for Flexible Pavement Design*. Prepared for the National Cooperative Highway Research Program Interim Report 1, TRB, National Research Council, Washington, D.C., Dec. 1990.

# Selection of Design Strengths of Untreated Soil Subgrades and Subgrades Treated with Cement and Hydrated Lime

TOMMY C. HOPKINS, DAVID Q. HUNSUCKER, AND TONY BECKHAM

Selection of design strengths of soil subgrades and subgrades treated with cement or hydrated lime is a problem in pavement design analysis and construction. Different types of soils may exist in a highway corridor and different strengths may exist after the soils are compacted to form the pavement subgrade. The selected subgrade strength will largely affect the pavement thickness obtained from the design analysis, future pavement performance, and the overall bearing capacities of the subgrade during construction and the pavement structure after construction. In developing the proposed selection scheme, a newly developed mathematical model, based on limit equilibrium, is used. Relationships among undrained shear strength [or California bearing ratio (CBR)] and tire contact stresses are developed for factors of safety 1.0 and 1.5. The minimum subgrade strength required to sustain anticipated construction tire contact stresses during construction is determined. A criterion is proposed for determining when subgrade stabilization is needed and methods of selecting the design subgrade strength are examined. A least-cost analysis appears to be an appropriate approach as shown by analysis of a case study involving pavement failures. Two case studies show that soaked laboratory strengths appear to be fairly representative of long-term field subgrade strengths. Hence, using soaked laboratory strengths and least-cost analysis appears to be a reasonable means for selecting the design strength of subgrades for pavement analysis. To avoid failures of chemically stabilized layers, relationships among thicknesses of chemically treated layers and the CBR values of the untreated subgrade for a factor safety of 1.5 are presented.

A variety of soils are frequently present along any highway corridor before construction and different bearing strengths exist when the different types of soils are used to construct pavement subgrades. To avoid bearing capacity failures during construction, a certain minimum subgrade strength must exist to sustain construction traffic. Hence, the design strength selected for pavement analysis should consider the issue of pavement construction. The method of selecting the design strength is complicated when different subgrade strengths exist along the route. When the design analysis is based on a selected laboratory strength, the question arises about whether the laboratory strength is representative of the long-term field strengths after paving.

When the actual subgrade strength is smaller than the minimum strength required to sustain construction traffic, it may be necessary to stabilize the subgrade soils with chemical admixtures such as cement or hydrated lime. When chemical stabilization is used, strengths of the treated and untreated layers must be selected for the design analysis. If the improved strength created by chemical stabilization is ignored, then the pavement thickness obtained from the design analysis may be too conservative. Consequently,

the issue that arises is whether the stabilized layer should be treated merely as a working platform, with no allowance made in the pavement design analysis for the net strength gain obtained from stabilization, or whether the stabilized layer should be considered an integral part of the pavement structure with the total or a portion of the net strength gain considered in the analysis. To examine and analyze the different issues posed, a pavement bearing capacity model (1,2) is used, formulated on the basis of limit equilibrium. The selection scheme makes use of an approach described by Yoder (3).

## BEARING CAPACITY MODEL

The mathematical bearing capacity model used herein is based on limit equilibrium and may be used to calculate the factor of safety against failure. The problems to be analyzed are visualized in Figures 1 and 2. Theoretical considerations and mathematical derivations of limit equilibrium equations for analyzing the ultimate bearing capacity of a layered structure have been presented elsewhere (1). Each material layer—subgrade, base, and asphaltic layers—in the pavement structure is described in the model using shear strength parameters: the angle of internal friction,  $\phi$ , cohesion,  $c$ , and unit weights. Problems involving total stress and effective stress analyses may be solved.

The assumed theoretical failure mass consists of three zones: active and passive wedges connected by a central wedge (Figure 1). The shear surface assumed in the bearing capacity analysis of a homogeneous layer of material consists of a lower boundary,  $abcd$ . This surface consists of two straight lines,  $ab$  and  $cd$ . The portion of the shear surface shown as line  $ab$  is inclined at an entry angle,  $\alpha_1$ . Line  $cd$  is inclined at an exit angle,  $\alpha_2$ . The shear surface,  $bc$ , is determined from the properties of a logarithmic spiral. The shear surface for a layered system is visualized in Figure 2.

The approach is a generalized method of slices and is an adaptation of a slope stability method (2). Vertical, horizontal, and moment equilibrium equations are considered for each slice. In the solution of these equations, the factor of safety appears on both sides of the final equation. Iteration and numerical techniques are used to solve for the factor of safety (1). To facilitate the use of the approach, all algorithms were programmed for the mainframe computer (IBM 3090) at the University of Kentucky.

Shear strength of an asphaltic layer varies with temperature and temperature within the asphaltic layer varies with depth. Hence, the shear strength varies with depth. To account for this variation in the model analysis, unconsolidated-undrained triaxial compres-

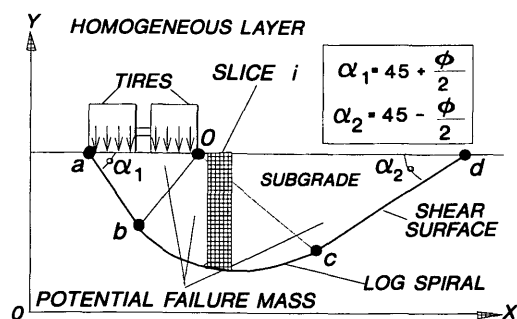


FIGURE 1 Bearing capacity analysis of a homogeneous layer.

sion tests were performed on asphaltic core specimens, which were assumed to be representative of typical flexible pavements, at temperatures ranging from 25 to 60 degrees C. As shown in Figures 3 and 4,  $\phi$  increases and  $c$  decreases as the temperature increases. In the analyses of problems involving asphaltic layers, the total thickness of asphaltic pavement is subdivided into finite layers, and a temperature-depth model (4) is used to estimate the temperature at the midpoint of each finite layer. Different surface temperatures and average air temperatures may be used in the analysis. On the basis of an estimated temperature and the correlations in Figures 3 and 4, the shear strength parameters,  $\phi$  and  $c$ , may be determined for each finite layer. Total stress parameters,  $\phi$  and  $c$ , of crushed stone (limestone) bases were assumed to be 43 degrees and 0, respectively (1).

### MINIMUM SUBGRADE STRENGTH

To avoid bearing capacity failures under construction traffic, the subgrade must possess some minimum strength. As the tire contact ground stress increases, the required minimum strength increases. This situation (Figure 1) was analyzed using the bearing capacity model previously described. Dual-wheel tires, a range of tire contact stresses (uniformly distributed), and undrained shear strengths,  $S_u$ , of the soil subgrade were assumed. The relation-

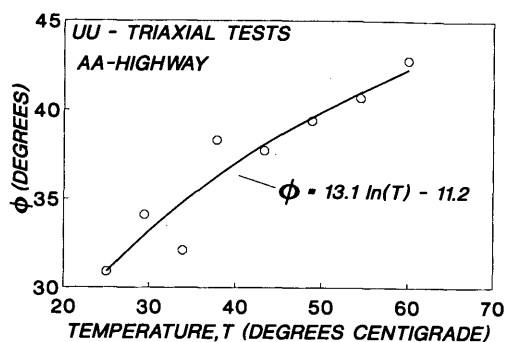


FIGURE 3 Influence of temperature on shear strength parameter  $\phi$ .

ships (Figure 5) of undrained shear strength and tire contact ground stresses corresponding to factors of safety of 1.0 (incipient failure) and 1.5 (assumed stable condition) were developed. For a selected tire contact stress and undrained shear strength, the factor of safety was computed. If the anticipated tire contact stress of construction traffic is known, then the required strengths to maintain an incipient failure condition or an assumed stable condition may be determined. For example, if the tire contact stress is 552 kPa, then the undrained shear strength for an incipient failure is 94 kPa and about 144 kPa for an assumed stable condition.

Relationships among bearing ratios (ASTM D 1883) and tire contact stresses may be developed using a relationship between bearing ratio and undrained shear strength developed by Hopkins (1,5), or

$$\text{CBR} = 0.0649 S_u^{1.014} \text{ (kPa)} \quad (1)$$

or a tire contact stress,  $T_c$ , of 552 kPa; the required bearing ratio for incipient failure is about 6.5 and about 10 for an assumed stable condition.

Minimum dynamic modulus of elasticity required to maintain incipient failure and a stable condition may be determined using

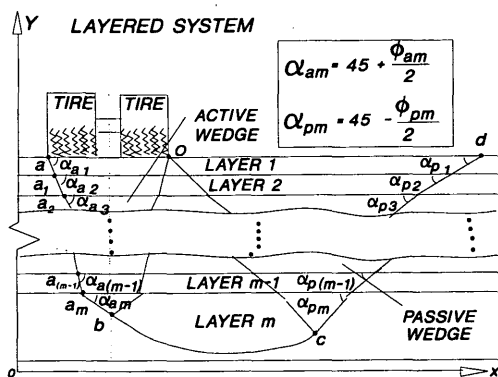


FIGURE 2 Bearing capacity analysis of a layered system.

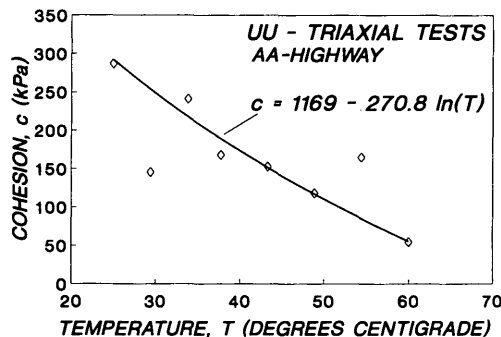


FIGURE 4 Influence of temperature on shear strength parameter  $c$ .

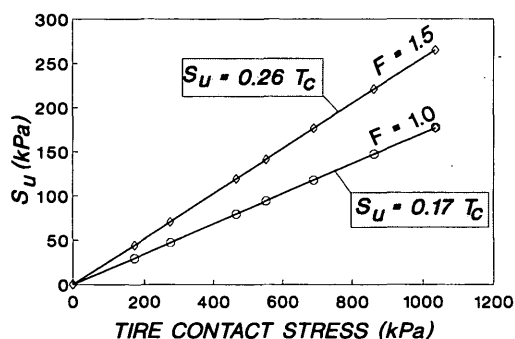


FIGURE 5 Undrained shear strength,  $S_u$ , as a function of tire contact ground stress,  $T_c$ .

the relationship developed by Heukelom and Foster (6). Re-analysis of those data yields the following expression:

$$E_s = 17,914 \text{CBR}^{0.874} \text{ (kPa)}. \quad (2)$$

Inserting the CBR values of 6.5 and 10, which correspond to factors of safety of 1 and 1.5, respectively, into Equation 2, the dynamic modulus of elasticity required to maintain an incipient failure state is 91,979 KPa. For an assumed stable condition, the required modulus is 134,031 kPa.

### SELECTION OF UNTREATED SUBGRADE DESIGN STRENGTH

Different philosophies exist concerning the method of selecting the subgrade design bearing ratio (or other types of strength parameters). Some of the approaches include using

- Lowest value,
- Average value,
- Statistical methods of estimating upper and lower values about the average value, or
- Value based on a least-cost analysis (3).

When the lowest bearing ratio of a data set is selected, the pavement may be overdesigned. If the average value is selected, approximately one half of the pavement may be overdesigned, whereas one half may be underdesigned (3). A statistical approach involving upper and lower limits for a selected confidence interval has also been proposed.

Another approach, based on a least-cost design, has been proposed by Yoder (3), who presented a series of curves that relate percentile test values to soil variability (measured by the coefficient of variance of the test data set), traffic (equivalent axle load), and unit cost of the pavement. Unit cost of maintaining a highway is expressed in terms of a cost ratio, or unit maintenance cost divided by the unit initial construction cost. When detailed information is lacking, Yoder suggests using the bearing ratio at the 80th to 90th percentile test value.

To test and compare the results of the different approaches, an analysis of soaked laboratory CBR values of two adjacent sections (12.2 km) of a highway route located in Kentucky was performed.

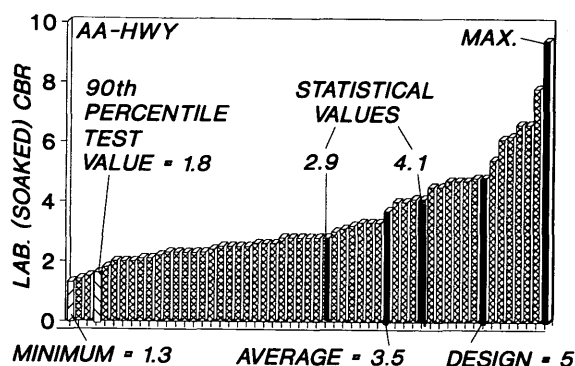


FIGURE 6 Soaked laboratory CBR values of corridor soils.

The planned pavement structure consisted of 26.7 cm of asphaltic pavement and 10.2 cm of dense-graded aggregate. The design CBR and equivalent single-axle load (ESAL) were 5 and 4 million, respectively. During construction, the partially completed flexible pavements failed at numerous locations along the two highway sections.

Soaked laboratory CBR values of corridor soil samples obtained before construction are shown in Figure 6. The lowest CBR value is 1.3 and the average is 3.5. Lower- and upper-bound CBR values for a 95 percent confidence interval are 2.9 and 4.1, respectively. Percentile test value (3) as a function of the soaked laboratory CBR is shown in Figure 7. Cost ratio for the two highway routes was not available. Therefore, the CBR at the 90th to 80th percentile test value may be considered. At the 95th, 90th, and 80th percentile test values, the CBR values are 1.4, 1.8, and 2.1, respectively.

To compare the different CBR selection approaches, factors of safety of the design pavement section were computed using the bearing capacity model already described. Surface and air temperatures at the time of the failures were 60 and 26.7 degrees C, respectively. A temperature-depth model (1,4) was used to estimate the temperatures at the midpoint of each 2.54-cm asphaltic layer. Using these estimated temperatures,  $\phi$  and  $c$  values for each

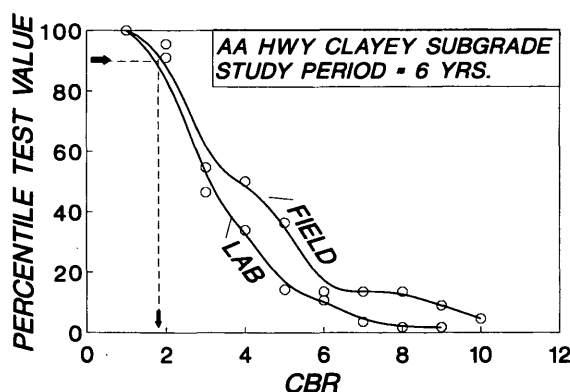


FIGURE 7 Field and laboratory percentile test values as a function of CBR: AA Route.

finite layer were estimated from the curves shown in Figures 3 and 4. CBR values were converted to undrained shear strengths using the relationship given by Equation 1. A uniformly distributed tire-contact stress of 552 kPa (dual wheels) was assumed in the analysis.

Factors of safety, based on different CBR design assumptions, are compared in Figure 8. When the average CBR is assumed to be the correct value, a factor of safety of 1.33 is obtained. If the assumption that the CBR (equal to 5) used in the original design is correct, then a factor of safety of about 1.59 is obtained. If CBR values obtained from statistical theory are used, then factors of safety of 1.22 and 1.43 are obtained. In each of these three cases, the factor of safety is much greater than 1. However, because the pavements failed, the factor of safety should be near 1. On the basis of CBR values equal to 1.4, 1.8, and 2.1, factors of safety of 0.91, 1.00, and 1.07 are obtained, respectively. The CBR value of 1.8 (90th percentile test value), yields a factor of safety of 1 and represents an appropriate design choice.

The problem of selecting a design CBR value may be illustrated in another manner using model analysis to determine the required thickness for a given design factor of safety. On the basis of an analyses (1) of 237 asphaltic pavement sections of the American Association of State Highway Officials' (AASHTO) Road Test (7), an approximate relationship (serviceability index = 2.5) between factor of safety and (weighted) ESAL was developed, or

$$F = (0.095) \ln(\text{ESAL}) - 0.005 \quad (3)$$

Inserting the design ESAL of 4 million into Equation 3, the design factor of safety is 1.44. The total pavement thickness corresponding to a selected subgrade CBR and design factor of safety was obtained from the bearing capacity model by iteration. Thickness of the pavement is varied until the factor of safety is equal to the selected design factor of safety obtained from Equation 3. Thickness of the DGA (10.2 cm) was held constant so that the various thicknesses (based on different assumed CBR design values) could be compared to the thickness of the pavement sections after overlays were constructed.

Thicknesses obtained from the analyses, based on different assumed design values of CBR and corresponding to a factor of safety of 1.44, are shown in Figure 9. If the lowest CBR value (1.3) is assumed, then a total thickness of 53.1 cm is required. This thickness is 16.3 cm larger than the planned thickness. If the

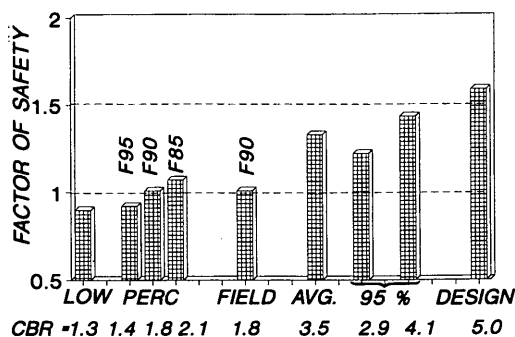


FIGURE 8 Factors of safety for different CBR design values.

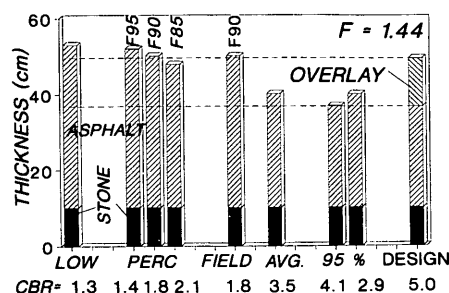


FIGURE 9 Flexible pavement thicknesses obtained for different CBR design values.

average CBR value (3.5) is used, then a thickness of 40.1 cm is obtained, which is only 3.3 cm larger than the original planned thickness. A CBR of 3.5 corresponds to a percentile test value of only about 40 (Figure 7). Accordingly, numerous portions (spot-to-spot) of the pavement would require future maintenance. Required thicknesses obtained from the upper- and lower-bound values of CBR are only 0.25 cm to 2 cm greater, respectively, than the original design section. If the CBR of 1.8 is assumed, then a thickness of 50 cm is obtained—a thickness that is 13.2 cm greater than the original planned section. As shown in Figure 6, CBR values less than 1.8 occur at only about 10 percent of the sampling sites.

Approximately one half of the total length of the highway sections were repaired using an overlay thickness of about 12.7 cm. Total thickness of the pavement at those locations was about 49.5 cm—a value that is nearly identical to the thickness (50 cm) obtained when the 90th percentile CBR value is used. The method proposed by Yoder appears to be a reasonable approach to the problem of selecting a design subgrade strength as strongly indicated by this case history analyses. Using the 1981 Kentucky design curves (8) and a CBR of 1.8, a thickness of 47 cm is obtained. Proper selection of a subgrade design CBR is vital to avoid construction failures and to ensure good pavement performance.

## EFFECT OF MOISTURE ON SOIL SUBGRADES

Subgrades built with clayey soils and compacted according to standard compaction specifications generally possess large bearing strengths immediately after compaction. However, there is no assurance that the subgrade soils will retain their original strength. Bearing strength of completed subgrades depends on long-term density and moisture. Clayey soils tend to absorb water and increase in volume. As volume increases, the density decreases and the shear strength available to resist failure decreases. Differences in bearing strength of compacted soils in soaked and unsoaked states may readily be illustrated by analyzing the results of 727 laboratory CBR tests (1). Each specimen was penetrated before and after soaking. Before soaking and immediately after compaction, bearing ratios of 95 percent of the specimens were greater than 6. After soaking, the bearing ratio of only 54 percent of the specimens exceeded 6.

Field observations show that bearing strength of clayey subgrades may decrease significantly after construction (1,9). Field CBR tests were performed on a clayey subgrade at a highway construction site in Kentucky immediately after compaction. Values of CBR ranged from about 20 to 40. A second series of field CBR tests was performed after exposure of the subgrade to one winter season. Values ranged from about 1 to 4—a dramatic decrease in bearing strength. Hence, as noted by Yoder and Witczak (10), pavement design analysis should be based on the characteristics of the completed subgrade. In areas where water infiltrates the subgrade from surface and subsurface sources, the design should be based on the strength of the soaked condition of the completed subgrade.

Many projects are scheduled years in advance and it may not be convenient, or the opportunity may not be available, to perform field tests on a subgrade in a soaked condition before the design analysis. Hence, the design analysis should be based on the soaked strengths of laboratory tests. When the design is based on laboratory tests, a question arises concerning the similarity of field and laboratory strengths.

### COMPARISON OF FIELD AND LABORATORY SUBGRADE STRENGTHS

To determine the similarity of laboratory and long-term field strengths, two highway routes were selected where numerous laboratory (soaked condition) bearing ratios had been performed on the corridor soils. Field-bearing ratio tests were performed through core holes on top of the untreated subgrades over a period of 6 years. Testing did not begin until the pavement had been placed and at least one winter and spring season had passed. Because it was not certain where particular corridor soils would be placed in the subgrades of each route, curves of percentile test value as a function of laboratory and field CBR values were developed and compared. Soil classification of these residual soils were A-6 and A-7, or, according to the Unified Soil Classification System, CL (clay) and CH (inorganic clay). A comparison of percentile test values as a function of laboratory and field CBR values is presented in Figure 7. Average values of laboratory and field CBR were 3.5 (56 tests) and 4.1 (22 tests), respectively. At the 90th and 80th percentile test values, the laboratory strength is about 90 percent of the field CBR. Between 80 and about 10 percent, the laboratory CBR was about 90 to 70 percent of the field CBR.

Comparison of laboratory and field CBR values of the second highway route is shown in Figure 10. Soil classifications ranged from A-4 to A-7 and ML-CL (inorganic silt-clay) to CL (clay). Between percentile test values of 90 and 10, the field value is some 100 to 75 percent of the laboratory CBR. On the basis of these comparisons, soaked laboratory CBR values provide a reasonable representation of the field CBR values of the completed subgrade after sufficient time has elapsed for soaking conditions to develop. Therefore, design strength of the untreated subgrade may be based on the soaked laboratory CBR test.

### DESIGN STRENGTHS OF CHEMICALLY STABILIZED SUBGRADES

Selection of a design strength of a subgrade treated with cement or hydrated lime will be controlled by the time allowed for curing.

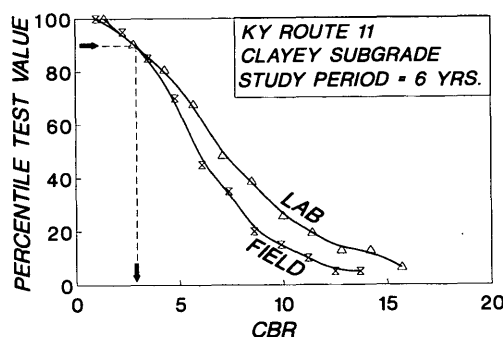


FIGURE 10 Field and laboratory percentile test values as a function of CBR: KY-11.

At the end of the curing period, sufficient strength must exist to withstand construction traffic loadings. If the subgrade strength at the end of a selected curing period can be estimated with confidence, then that strength may be used in the pavement design analysis. In Kentucky, treated subgrades are allowed to cure for 7 days and substantial strength gains occur during the curing period. Optimum percentages, as determined by testing (1), of cement or hydrated lime are used in treating the subgrades.

General guidelines for selecting design strengths of hydrated lime- and cement-treated subgrades were developed on the basis of 7-day strengths. Several highway routes were selected and core specimens of the hydrated lime- or cement-treated subgrades were obtained at about the end of the 7-day curing period. Numerous soils, ranging from A-4 to A-7, were used in constructing the subgrades of those routes. Unconfined compression tests were performed on the core specimens. Bag samples of the untreated soil subgrades were obtained at several locations along each route of the completed subgrade before treatment. Soil specimens were remolded to optimum moisture content and 95 percent of maximum dry density (AASHTO T 99). Optimum percentages of chemical admixture were used in remolding the specimens. Unconfined compression tests were performed after aging the sealed specimens for 7 days.

Field and laboratory unconfined compressive strengths of the cement- and hydrated lime-treated specimens, as a function of percentile test values, are compared in Figures 11 and 12.

Unconfined compressive strengths of the field, hydrated lime-treated specimens were about 85 to 90 percent of the unconfined compressive strengths of the laboratory specimens for percentile test values ranging from 100 to about 10. Unconfined compressive strengths of the field, cement-soil core specimens ranged from about 75 to 50 percent of laboratory unconfined compressive strengths for percentile test values ranging from 100 to 3, respectively. Assuming that the 90th percentile test value is a reasonable working value, unconfined compressive strengths of about 333 kPa and 707 kPa ( $S_u = 167$  and  $354$  kPa, respectively) appear to be reasonable values to assume in the design of hydrated lime- and cement-treated soil subgrades, respectively. Corresponding bearing ratios, estimated from Equation 1, are about 11.6 and 24.9, respectively. Estimated values of dynamic modulus of elasticity (Equation 2) are about 152,590 and 297,489 kPa, respectively.

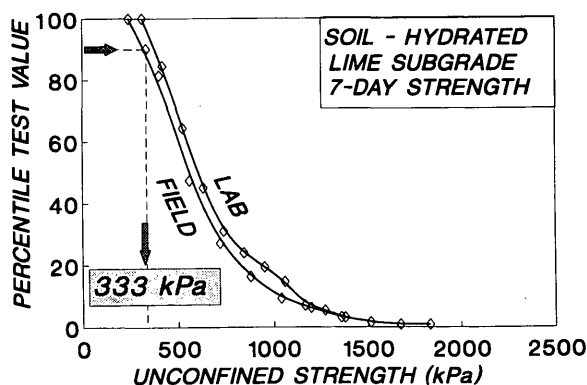


FIGURE 11 Field and laboratory percentile test values as a function of CBR: soil-hydrated lime subgrades.

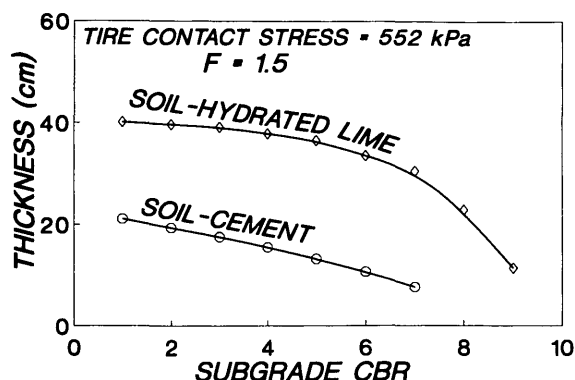


FIGURE 13 Thickness of treated subgrades as a function of untreated subgrade CBR values.

### APPROXIMATE REQUIRED THICKNESS OF TREATED SUBGRADES

By using 7-day strengths, some portion of the strength gain of the chemically treated subgrade may be considered in the pavement design analysis. Bearing capacity of the treated layer is a function of thickness of the treated layer and bearing strength of the underlying untreated layer. To estimate thickness required to maintain an assumed stable condition ( $F = 1.5$ ), bearing capacity analyses were performed. In the analysis of this two-layered problem, a tire contact stress of 552 kPa was used. The unconfined compressive strength at the 90th percentile test value (Figures 11 and 12) was assumed for the treated layer. Bearing ratio of the untreated layer ranged from 1 to 9 (or  $S_u$  - values ranging from 15 kPa to 130 kPa). Required thickness, (Figure 13), of hydrated lime-treated subgrades ranged from about 40 cm to 11 cm for CBR values of the untreated layer ranging from 1 to 9. For cement-treated subgrades and CBR values ranging from 1 to 7, required thickness ranged from about 21 cm to 7.6 cm.

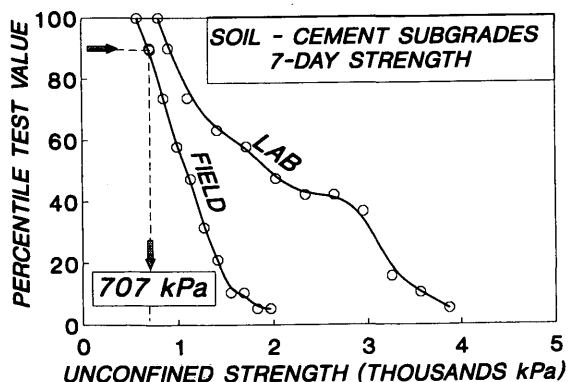


FIGURE 12 Field and laboratory percentile test values as a function of CBR: soil-cement subgrades.

### SIGNIFICANCE OF TREATED SUBGRADES TO PAVEMENT STRUCTURE

Use of hydrated lime or cement increases the shear strength of a soil subgrade and improves the overall bearing capacity of a flexible pavement. This may be demonstrated by a design example. Assume that a flexible pavement is to be designed for an ESAL value of 18 million and subgrade soils are the same as those used at the 1960 AASHO Road Test (7). Percentile test values as a function of field CBR values [Table 2 of the 1960 AASHO Road Test (7)] were determined. At the 90th percentile test value, bearing ratios, corresponding to spring and summer, are 2.5 and 3.0, respectively. Average CBR values are 3.6 and 5.3, respectively. The design consists of one-third asphaltic concrete and two-thirds crushed stone. Layer coefficients,  $a_1$  and  $a_2$ , are 0.44 and 0.14, respectively; terminal serviceability index is 2.5; and tire unit contact stress is 466 kPa. The soil support value is 3.

The structural number, SN, is 5.6. Total pavement thickness is 59.2 cm—19.8 cm of asphaltic concrete and 39.4 cm of crushed stone base. Using the CBR of the untreated subgrade (2.5 or  $S_u = 36.7$  kPa), model analysis yields a factor of safety of 1.29. From Equation 3, the estimated ESAL is only 800,000—much lower than the design ESAL of 18 million. If the average CBR (3.6) is used, then a factor of safety of 1.55 is obtained. The estimated ESAL equals 16 million, which is near the design ESAL of 18 million. However, the percentile test value is only about 40. Hence, much maintenance may be required if the average CBR is used.

Because the CBR values at the 90th and 40th percentile test values are below a CBR of 6.5, stabilization of the soil subgrade should be considered. Moreover, difficulties may be encountered during placement of the first lift of crushed stone base if treatment is not performed. Bearing capacity analysis of the untreated soil subgrade (CBR equal 2.5) yields a factor of safety of only 0.46. Using the average CBR, the factor of safety is only 0.65. If the subgrade soils remained free of water during construction, then the CBR strength may be greater than 6.5 and construction difficulties would not be encountered during paving. The designer cannot rely on this unlikely condition and subgrade stabilization should be performed.

In the design analysis, both hydrated lime- and cement-treated subgrade layers were considered. For the hydrated lime-treated



subgrade, an undrained shear strength at the 90th percentile test value was used. A strength of 36.7 kPa (CBR = 2.5) was used for the underlying untreated layer. For an assumed thickness of 30.5 cm, a factor of safety of about 1.36 was obtained. This factor of safety should be sufficient to avoid bearing capacity failures and deep rutting during construction. A factor of safety of 1.35 is obtained when a 12.7-cm soil-cement layer is analyzed.

Analyses were performed to determine the factor of safety of the full 59.2 cm of pavement resting on the 30.5-cm layer of hydrated lime-treated subgrade or the 12.7-cm layer of cement-treated subgrade. In both cases, undrained shear strengths of the treated and untreated layers at the 90th percentile test value were used. When the lime-treated layer is included in the design, a factor of safety of 1.85 is obtained. Hence, the factor of safety increases from 1.29 (no treatment) to 1.85, or about 31 percent. Predicted values of ESAL (Equation 3) are greater than 18 million. Similarly, when a 12.7-cm layer of cement-treated subgrade is used, a factor of safety of 1.85 is obtained. Based on Equation 3, a design factor of safety of 1.57 is required. Accordingly, thickness of the asphaltic layers could be reduced from 19.8 cm to 12.7 cm and the crushed stone thickness could be reduced from 39.4 cm to 25.4 cm when a 30.5-cm layer of hydrated lime-treated subgrade or 12.7-cm layer of soil-cement are used. In both cases, the factor of safety is about 1.57—the required value that satisfies Equation 3.

#### LAYER COEFFICIENTS OF HYDRATED LIME AND CEMENT SOILS

The coefficient,  $a_3$ , may be estimated for the hydrated lime-treated subgrade and the soil-cement layer for the example previously described.

Structural number, SN, is defined as

$$SN = a_1 d_1 + a_2 d_2 + a_3 d_3, \quad (4)$$

where  $a_1$ ,  $a_2$ ,  $a_3$  equals layer coefficients representative of surface, base, and subbase (in this case, the treated layer), respectively, and  $d_1$ ,  $d_2$ ,  $d_3$  equals actual thickness of surface, base, and subbase courses, respectively.

Because  $a_1$  and  $a_2$  are equal to 0.44 and 0.14, respectively, the structural number is 5.6, the thickness of the asphalt is 12.7 cm (or  $d_1 = 5$  in.), the crushed stone thickness is 25.4 cm, and the hydrated-lime layer is 30.5 cm (or  $d_3 = 12$  in.),  $a_3$  equals 0.17. Similarly,  $a_3$  equals 0.34 when the 12.7-cm layer of soil-cement is considered.

#### SUMMARY AND CONCLUSIONS

Guidelines for selection of design strengths of untreated soil subgrades and subgrades treated with cement or hydrated lime were proposed. Theoretical bearing capacity analysis shows that a minimum subgrade strength must exist to avoid bearing capacity failures during construction. To maintain an incipient failure state ( $F = 1.0$ ) and an assumed stable state ( $F = 1.5$ ), the undrained shear strength should be 94 kPa and 144 kPa, respectively. These values correspond to CBR values of about 6.5 and 10, respec-

tively. Corresponding values of dynamic modulus of elasticity are 92 mPa and 134 mPa. Based on a case history involving the failure of a partially completed pavement, the method proposed by Yoder (3) is a reasonable approach for selecting design strengths on the basis of percentile test values.

It was proposed that if the minimum strength for a selected percentile test value is less than the minimum strength required to avoid bearing capacity failures during construction, then chemical or mechanical stabilization should be considered. For example, if the tire contact stress of construction equipment is 552 kPa and the CBR is 2.5 at a selected percentile test value, then subgrade stabilization should be performed because a CBR of 2.5 is less than a CBR of 6.5. However, to avoid bearing-capacity problems during construction, the subgrade CBR should be greater than about 6.5.

Field CBR values of untreated clayey subgrades obtained at two highway sites during a period of about 6 years were compared with soaked laboratory CBR values of corridor soils. Soaked laboratory CBR strengths appeared to represent reasonably well the long-term field CBR strengths of the clayey subgrades of the two routes. Use of soaked laboratory CBR strength provides a reasonable approach for selecting design CBR strengths of clayey subgrades.

Strengths of subgrade core specimens mixed with hydrated lime were about 85 to 90 percent of laboratory remolded strengths. Strengths of soil-cement cores were about 75 to 50 percent of laboratory strengths for percentile test values ranging from 100 to 10. Seven-day unconfined compressive strengths of 333 kPa and 707 kPa indicate reasonable values to assume in the design of hydrated lime- and cement-treated soil subgrades, respectively. Corresponding CBR values are 11.6 and 25. Dynamic modulus of elasticity is 152 mPa and 298 mPa, respectively. Bearing capacity model analysis of an example problem showed that treated subgrades, based on those values, increased the overall bearing capacity of flexible pavements substantially.

#### ACKNOWLEDGMENTS

This work was a task of a research study funded by the Federal Highway Administration and the Kentucky Transportation Cabinet.

#### REFERENCES

1. Hopkins, T. C. *Bearing Capacity Analysis of Pavements*. Research Report KTC-91-8, College of Engineering, University of Kentucky Transportation Center, Lexington, June 1991.
2. Hopkins, T. C. *A Generalized Slope Stability Computer Program: User's Guide for HOPK-I*. Research Report UKTRP-86-2, College of Engineering, University of Kentucky Transportation Center, Jan. 1986.
3. Yoder, E. J. Selection of Soil Strength Values of the Design of Flexible Pavements. In *Highway Research Record 276*, HRB, National Research Council, Washington, D.C., 1969.
4. Southgate, H. F., and R. C. Deen. Temperature Distribution Within Asphalt Pavements and Its Relationship to Pavement Deflection. In *Highway Research Record 291*, HRB, National Research Council, Washington, D.C., 1969.
5. Thompson, M. R. Admixture Stabilization of Subgrades. In *Proc., Nineteenth Annual Ohio River Soils Seminar (OVRSS)*, Lexington, Kentucky, Oct. 1988.

6. Heukelom, W., and C. R. Foster. Dynamic Testing of Pavements. *ASCE Journal of the Structural Division*, SM1, 86, Feb. 1960.
7. HRB *Special Report 73: The AASHO Road Test*, HRB, National Research Council, Washington, D.C., May 1962.
8. Havens, J. H., R. C. Deen, and H. F. Southgate. *Development of a Thickness Design Guide for Bituminous Concrete Pavement Structures*. Research Report UKTRP-81-17, University of Kentucky Transportation Center, Lexington, Aug. 1981.
9. Hopkins, T. C., D. Hunsucker, and G. W. Sharpe. Highway Field Trials of Chemically Stabilized Soil Subgrades. In *Proc., Nineteenth Annual Ohio River Valley Soils Seminar (ORVSS)*, Lexington, Ky., Oct. 1988.
10. Yoder, E. J., and M. W. Witczak. *Principles of Pavement Design*. 2nd ed., John Wiley and Sons, New York, N.Y., 1975.

# Long-Term Performance of Flexible Pavements Located on Cement-Treated Soils

TOMMY C. HOPKINS, DAVID Q. HUNSUCKER, AND TONY BECKHAM

Long-term performance of flexible pavements located on cement-treated soils and the longevity of soil-cement subgrades are examined at sections of four highway routes. Ages of the soil-cement subgrades range from 6 to 30 years. Field and laboratory studies were conducted at each section. Generally, the soil-cement subgrades were non-plastic and were classified as SM, or sandy silt, according to the Unified Soil Classification System, although the classification of the untreated soil subgrades located below the treated layers ranged from CL (clay) to GC (clayey gravel). Plasticity index of the untreated soils ranged from non-plastic to 44 percent. Generally, the untreated soils were moderately plastic. In situ bearing ratios of the soil-cement subgrades were generally very large. Based on a percentile test curve, the in situ bearing ratios of the cement-treated subgrades at the 90th and 50th percent test values were about 24 and 90, respectively. Based on overlay histories of the routes, flexible pavements located on the soil-cement subgrades have performed well. In the older sections, overlays had been constructed every 11 to 14 years. Use of cement to construct stabilized subgrades represents a good design alternative when compared with other stabilizing methods and other design alternatives.

Although cement has been used in past years as a chemical admixture to improve bearing strengths of highway soil subgrades, there is little published information concerning the long-term bearing strengths of cement-treated soils and the long-term performances of flexible pavements located on the cement-treated soils. Roberts (1) reported that in 1938 the Oklahoma Highway Department investigated the use of cement-modified subgrades by constructing 7 mi of test sections along US-62. Plasticity index of the clayey subgrade soil was reduced from 39 to 13 percent at the time of construction. Plasticity indices of the cement-treated subgrade after 45 years of service ranged from non-plastic to 13 percent. Roberts indicated that the pavements placed on the treated subgrades performed well during the 45 years of service. McGhee (2) reported on the use of cement-treated subgrades in Virginia and the long-term performance of pavements located on the treated subgrades. A major conclusion was that pavements constructed on cement-treated subgrades were much more resistant to rutting and other distortions when compared with most pavements 10 or more years old. No long-term strength data are shown in the reports by Roberts or McGhee. Laboratory tests performed on remolded mixtures of soils and cement generally exhibit large shear strengths in excess of 700 kPa (3).

To determine the long-term strengths and field durability of cement-treated subgrades and to examine the long-term performance of pavements constructed on cement-treated subgrades, four highway routes that have been in service for a number of years

were selected. Two of the routes have been in service for some 30 years. Two sections of the third route have been in service for 9 and 14 years, respectively. Two sections of the fourth route have been in service for about 6 years. The findings of geotechnical field and laboratory studies performed at the four highway routes are summarized in this paper and the general performance of flexible pavements located on the soil-cement subgrades is described.

## TESTING PROCEDURES

Geotechnical field studies consisted of performing in situ bearing ratio tests on the top of the soil-cement subgrades and the top of the untreated soil subgrade located below the treated layer. These tests were performed through cored boreholes. Samples of the cement-treated subgrades and the untreated subgrades were obtained during the field testing for laboratory testing. Procedures of ASTM D 4429-84 were followed in performing the in situ bearing ratio tests. The reactive force necessary to push the penetrating rod was developed by jacking against the frame of a drill rig. Load and deflection measurements were obtained from a calibrated load ring and deflection dial. Efforts to obtain thin-walled tube samples were unsuccessful because of the hardness of the cement-treated subgrades. Core specimens of the pavement and cement-treated subgrades were obtained at each site. Diameter of the cores was 15 cm. Measurements and visual inspections of the core specimens were used to determine the actual in situ thickness of the flexible pavements and the number and thickness of overlays. Pavement performance was generally evaluated using overlay history (when available) and visual inspections.

Geotechnical laboratory tests were performed on the retrieved samples to determine the index properties of the cement-treated and untreated soils. Index tests included liquid limit (ASTM D 4318-84) and plastic limit (ASTM D 4318-84), particle-size analysis (ASTM D 422-63), specific gravity (ASTM D 854-83), and moisture content (ASTM D 2216-80). The materials were classified according to the Unified Soil Classification System (ASTM D 2487-85) and the American Association of State Highway and Transportation Officials' Classification System.

## CASE STUDIES

### KY-15

KY-15, located between Campton and Jackson, Kentucky, is about 32 km in length. The flexible pavement of this stretch of highway

has been in service for approximately 30 years. The original design section consisted of 19.1 cm of flexible pavement, 15.2 cm of dense-graded limestone aggregate, and 15.2 cm of a soil-(portland) cement subgrade. Approximately 10 percent of cement (by dry unit weight) was mixed with the in situ soil subgrades. Details of the mixing operation were not available.

Index properties of the cement-treated and untreated subgrade soils at various locations are summarized in Table 1. At six locations, the untreated soils were classified as CL (clay) and A-4 to A-6. At other locations, the soils were classified as GC-GM (clayey gravel-silty gravel), and SC (clayey sand). Plasticity index of the untreated soils generally ranged from 6 to 16, although one specimen was nonplastic. Classification of the cement-treated soils was SM (sandy silt) and GM (silty gravel) (after 30 years) and either A-1, A-2, or A-4. All specimens of the treated layer were nonplastic. Hence there were noticeable differences in the index properties of the treated and untreated soils.

In situ bearing ratios of the cement-treated layer and underlying soil subgrade are compared in Figure 1. Except for the bearing ratio of 9.2 at Milepost 0.6, the bearing ratios of the cement-treated subgrades ranged from 54 to values greater than 100. In situ bearing ratios of the untreated soils ranged from 3.3 to 14.2. After 30 years, the in situ bearing ratios of the soil-cement were generally some 4 to 33 times greater than the untreated subgrade soils.

Total pavement thickness ranged from 47.6 cm to 63.5 cm, as shown in Figure 2. At 7 of 10 locations where the soil-cement subgrade was constructed, overlay thickness ranged from 3.2 to 6.4 cm. At 3 of the 10 locations, the overlay thickness ranged from 12.1 to 19.1 cm. Those three locations exist on a side-hill fill and apparently the fill settled over the 30-year period. It is conjectured that the large overlay thickness observed at those three locations was the result of adding leveling courses or patching

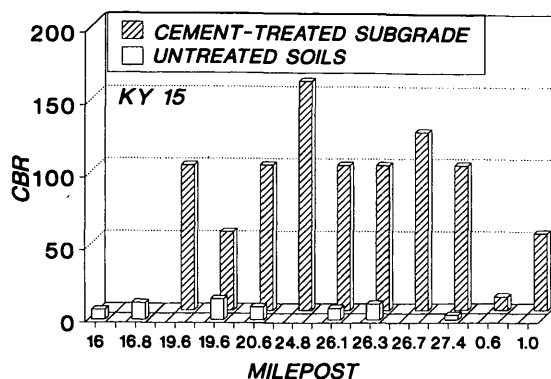


FIGURE 1 In situ bearing ratios of treated/untreated soils of KY-15.

when the overlays were constructed. At two locations (Mileposts 16 and 16.8), total pavement thickness ranged from 57.2 to 76.2 cm. Overlay thicknesses were 10.2 and 14 cm, respectively. At Milepost 16 the pavement was constructed on an untreated subgrade, whereas at Milepost 16.8 the pavement was placed on a subgrade built with a select rock material.

The time interval between overlay construction generally ranged from 11 to 15 years for the flexible pavements and averaged 12.2 years. On the basis of visual inspections made in 1990, only nominal rutting was observed. Hairline cracks were observed in the surface of the pavement. However, these did not affect the riding quality of the pavements. Annual daily traffic (ADT) of KY 15, as reported in 1989, was 5,000 vehicles per day (VPD). About 13 percent (650 VPD) of the ADT consisted of trucks, whereas 4 percent (200 VPD) of the ADT value consisted of coal trucks. Estimated equivalent single axle loads (ESAL)—converted from ADT values observed each year at different locations from 1986 to 1992—ranged from about 0.8 to 4.0 million and averaged about 2 million per year.

TABLE 1 Index Properties of Soil-Cement Layer and Untreated Soils of KY-11

Soil-Cement Layer								
Location (MP)	LL PL PI	Percent Passing			Classification		CBR	
		No. 4	No. 10	No. 200	AASHTO	Unified		
0.6	non-plastic	87.2	77.5	44.3	A-4 (0)	SM	9.2	
19.6	non-plastic	77.8	60.7	23.0	A-1-B (0)	SM	53.9	
24.8	non-plastic	72.8	63.7	26.1	A-2-4 (0)	SM	>100	
26.7	non-plastic	55.6	45.6	21.3	A-1-B (0)	GM	>100	
19.6	non-plastic	73.9	58.1	25.1	A-1-B (0)	SM	>100	
20.6	non-plastic	72.4	57.5	19.9	A-1-B (0)	SM	>100	
Untreated Soils								
0.6	26 20 6	56.2	53.5	32.0	A-2-4 (0)	GC-GM	9.2	
*16.0	28 20 8	86.4	84.1	52.0	A-4 (0)	CL	6.8	
*16.8	non-plastic	58.0	57.8	28.4	A-2-4 (0)	GM	11.5	
19.6	26 17 9	91.9	86.0	62.1	A-4 (3)	CL	14.3	
26.7	26 19 7	47.8	44.7	27.4	A-2-4	GC-GM	15.1	
19.6	34 21 13	86.9	72.2	53.3	A-6 (4)	CL	14.2	
20.6	29 19 10	96.0	84.2	59.5	A-4 (3)	CL	8.9	
26.1	35 21 14	89.2	77.5	55.5	A-6 (5)	CL	8.0	
26.3	25 16 9	96.7	93.7	36.3	A-4 (0)	SC	10.9	
0.0	38 22 16	98.1	91.8	71.6	A-6 (10)	CL	3.3	

\*No soil cement -- sandstone subgrade \*Sections reconstructed (untreated sections)

## KY-79

KY-79 was relocated and reconstructed in 1959-1960 when a dam was constructed to create Rough River Lake. Reconstruction be-

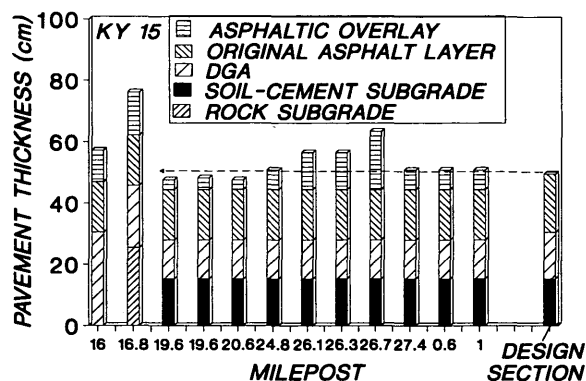


FIGURE 2 Thickness of the pavement at several locations of KY-15.

gan at the intersection of KY-110 (Milepost 18.1) in Grayson County and extended to the edge of the dam at Milepost 19.7. Reconstruction resumed at the Breckinridge county line (Milepost 0.0) and extended north to the intersection with KY-105 (Milepost 1.9) in Breckinridge County. Total length of reconstruction was 3.2 km, not including the length of roadway that traverses the dam (0.17 km). This flexible pavement and the cement-treated subgrade have been in service some 30 years.

The subgrade was constructed with a soil-cement-aggregate mixture designed by the U.S. Army Corps of Engineers. Proportions of the materials that were blended and construction specifications were not available. The thickness of the flexible pavement and stabilized subgrade, obtained from core measurements, is shown in Figure 3.

Total thickness of the pavements, as determined in 1991 and including the thickness of the treated layer, ranged from 25.4 cm to 35.6 cm. Thickness of the treated layers (Locations 2 through 7) ranged from 16.5 to 22.9 cm. Thickness of the flexible pavement, including overlays, ranged from 7 cm to 19.1 cm. A soil-cement layer was not used at Location 1 and 8 as shown in Figure 3. Locations 1 and 8 in Figure 3 are just beyond the limits of stabilization and are included for comparative purposes.

Index properties of the untreated and treated soils are shown in Table 2. The untreated soils were classified as CL, SM, and GC, and A-6, A-2-4, and A-2-7 at sampling locations. Plasticity indices of the untreated soils ranged from nonplastic to 44. Specimens of the cement-aggregate-soil subgrade obtained from three sampling sites were classified as SM and A-2-4 and A-1-B. The treated material was non-plastic. The untreated soils located below the treated layer of the section of roadway in Grayson County were non-plastic. Untreated soils below the treated layer of the section in Breckinridge County were generally plastic. The plasticity index ranged from 13 to 44 percent. In situ bearing ratios of the treated and untreated layers are shown in Table 3 and compared in Figure 4. In situ bearing ratios of the treated materials ranged from 62 to values in excess of 100. In situ bearing ratios of the untreated subgrade ranged from 2 to 7.1. The bearing ratios of the cement-treated materials were some 7 to 50 times the bearing ratios of the untreated soils. After about 30 years, the bearing strength of the cement-aggregate-soil layer was substantially greater than the bearing strength of the underlying untreated subgrade.

ADT, as measured in 1990, was 1,950 vehicles/day. About 140 vehicles/day, or about 7.2 percent of the total value of ADT, were

**TABLE 2 Index Properties of Untreated Soils and Cement-Aggregate-Soil Subgrade of KY-79**

Soil Cement-Aggregate						
Grayson Co. South						
Location (MP)	LL PL PI	Percent Passing			Classification	
		No. 4	No. 10	No. 200	AASHTO	Unified
18.2 (2)	non-plastic	84.7	81.9	16.1	A-2-4 (0)	SM
18.9 (3)						
19.5 (4)						
Breckinridge Co. North						
0.6	non-plastic	73.9	56.4	22.2	A-1-B (0)	SM
1.4						
1.8	non-plastic				A-1-B (0)	SM
Untreated						
Grayson Co. South						
18.2 (2)	non-plastic	98.8	94.0	29.2	A-2-4 (0)	SM
18.9 (3)						
19.5 (4)						
Breckinridge Co. North						
0.6	72 28 44	40.0	31.1	24.8	A-2-7 (0)	GC
1.4						
1.8	36 23 13	82.9	71.0	59.3	A-6 (6)	CL

classified as trucks. Values of ESAL, as observed in Grayson County at Milepost 18.1 to Milepost 1.9 in Breckinridge County, were 140,000 in 1989.

Overlays were constructed on the section in Breckinridge County in 1979 and 1989. Time intervals between overlay construction were about 10 years and 19 years, respectively. One overlay was constructed on the section in Grayson County in 1979, or about 19 years after construction. Reportedly an overlay was scheduled for 1991 or 1992, or about 14 years after the first overlay. Hence the time interval between overlays ranged from about 10 to 19 years and averaged about 15 years. As shown in Figure 3, the thickness of the asphaltic overlays added to the Breckinridge section in a 31-year period was substantially larger

**TABLE 3 Index Properties of Treated and Untreated Subgrades of US-23**

US 23 Boyd Co. 1991							
Soil Cement (10%)							
Location (MP)	LL PL PI	Percent Passing			Classification		CBR
		No. 4	No. 10	No. 200	AASHTO	Unified	
4.05	non-plastic	76.4	66.0	30.9	A-2-4 (0)	SM	>100
4.5	37 31 6	74.2	56.9	24.2	A-1-B (0)	SM	>100
4.95	non-plastic	75.7	62.5	18.4	A-1-B (0)	SM	>100
7.5							123
7.55							88.4
7.65							>100
Untreated							
4.05	24 15 9	80.0	68.0	36.4	A-4 (0)	SC	13.6
4.5	35 18 17	82.9	62.7	42.7	A-6 (2)	SC	5.9
4.95							8.1
7.5							2.5
7.55							13.5
7.65	27 16 11	93.4	84.2	45.7			3.7
Rock Subgrade Section (Untreated)							
8.25							13.2
8.65	30 17 13	75.8	59.9	40.6	A-6 (2)	SC	15.0
8.95	26 17 9	57.6	43.9	24.5	A-2-4 (0)	GC	31.0
8.98							33.6
9.00							190.9
9.00	27 18 9	62.8	59.1	44.5	A-4 (1)	GC	40.0

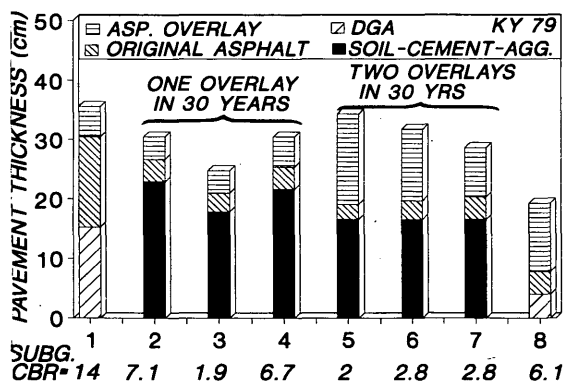


**FIGURE 3 Pavement thickness of KY-79.**

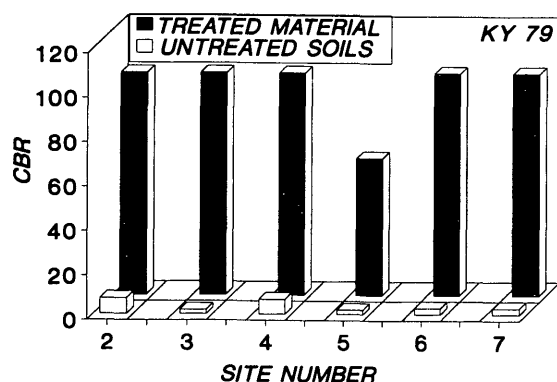


FIGURE 4 In situ bearing ratios of soil-cement-aggregate layer and untreated soils.

than the thickness added to the Grayson section. In the former case, the overlay thickness ranged from 3.8 to 5.1 cm, whereas in the latter case the overlay thickness ranged from 8.3 to 15.2 cm. As shown in Figure 4, bearing ratios of the untreated soils located below the cement-treated materials of the Breckinridge section ranged from 2 to 2.8. Bearing ratios of the untreated soils of the Grayson section ranged from about 2 to 7. Generally, the bearing ratios of the untreated soils of the Grayson section were greater than those of the Breckinridge section.

## US-23

US-23 in Boyd County, Kentucky, was reconstructed in the late 1970s. Two sections containing cement-treated soil subgrades were included in the reconstruction. The first section, extending from Station 837+00 to 916+50 (2.4 km), was reconstructed in 1977–1978 and has been in service about 14 years. The original design cross section consisted of 28.6 cm of flexible pavement, 31.8 cm of dense graded (limestone) aggregate, and 15.2 cm of soil-cement. Total thickness of the pavement is 60.3 cm. When the soil-cement layer is included, the thickness is 75.53 cm. Observed thickness obtained from core specimens in 1990 is compared with the original design thickness in Figure 5. The second section, which extends from Station 916+50 to 1040+75 (3.9 km), was completed in 1984 and has been in service about 9 years. The design cross section consisted of 35.6 cm of asphaltic pavement and 15.2 cm of soil-cement. As shown in Figure 5, the actual thickness of flexible pavement at three locations ranged from about 27.9 cm to 28.6 cm. Thickness of the soil-cement layer ranges from 15.2 to 20.3 cm. This section contained no drainage layer. The top 15.2 cm of the soil subgrades of Sections 1 and 2 were mixed with 10 percent portland cement. The third section extends from Station 1040+75 to 1151+36 and the design cross section consisted of 31.1 cm of asphaltic pavement resting on a rock subgrade. This section was included for comparative purposes. It was completed in 1985 and has been in service for about 8 years. Actual thickness of flexible pavement at three locations was 29.8, 26.7, and 26.7 cm.

Index properties of the cement-treated subgrades and untreated soil subgrades of Sections 1 and 2 are shown in the top portion of Table 3. The untreated materials were classified as SC and A-4 and A-6. The cement-treated subgrades were classified as SM

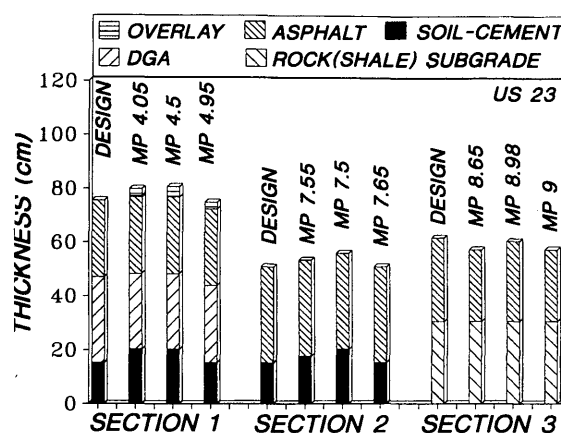


FIGURE 5 Pavement thickness of US-23 at different locations.

and A-1-B and A-2-4. Plasticity index of the soil-cement materials ranged from non-plastic to 6 percent. Plasticity index of the untreated soils ranged from 9 to 17 percent. The rock subgrade materials were classified as SC or GC and ranged from A-2 to A-6. Plasticity indices ranged from 9 to 13.

In situ bearing ratios (Figure 6) of the soil-cement subgrades were exceedingly large and ranged from 88 to values in excess of 100. In situ bearing ratios of the untreated soils of Sections 1 and 2 ranged from 2.5 to 13.6. In situ bearing ratios of the rock subgrade of Section 3 ranged from 13.2 to 191. Excluding the latter value, the bearing ratios generally ranged from 13.2 to 40. Bearing ratios of the soil-cement subgrades are several times greater than the untreated subgrades located below the treated layers and the rock subgrades of Section 3.

Based on core measurements, one overlay has been constructed on the pavement of Section 1 during its service period of about 14 years. Overlay thickness range from about 2.54 to 4.11 cm, as shown in Figure 4. No overlays have been constructed on Sections 2 and 3 during their service periods of about 9 and 8 years, respectively. ADT on the three sections, as obtained in 1989, is 8,890 VPD. About 3,645 VPD, or 41 percent, of the total ADT, or 2,578 VPD/day, were classified as coal trucks. Based on con-

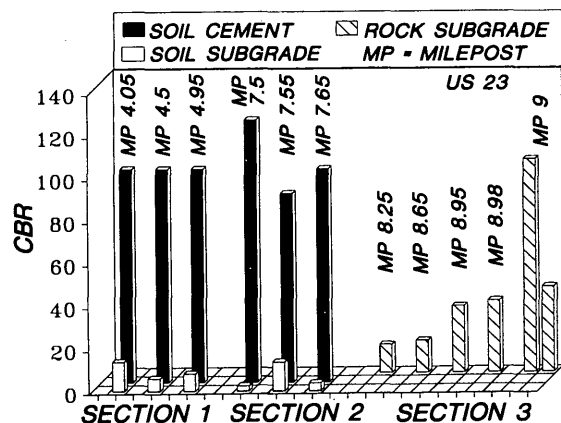


FIGURE 6 In situ bearing ratios of treated and untreated materials of sections of US-23.

verted values of ADT and percentage of trucks, the estimated ESAL value is 16.2 million for 1989, as observed between Mileposts 4 and 9. Between 1985 and 1991, the average ESAL was 7.2 million, as observed at seven different locations between milepost 0.1 and 13.2. Although these sections carry a large volume of truck traffic, the three sections have performed reasonably well.

### KY-11

Portions of KY-11 were realigned and reconstructed in 1986-1987. The route is located about 11.7 km north of Beattyville, Kentucky. Total length of the reconstructed route is 9.6 km. The reconstructed route starts at Station 260+00 and ends at Station 576+50. Originally the pavement was to consist of 19.1 cm of asphaltic pavement and 43.2 cm of dense-graded limestone aggregate. A second option consisted of stabilizing the top 30.5 cm of subgrade with portland cement for the entire route. However, the final plan, which was implemented by a change order, consisted of dividing the entire length of the roadway subgrade into sections and treating each subgrade section with different chemical admixtures. Chemical admixtures used in the different subgrade sections consisted of hydrated lime, multicone kiln dust (byproduct), a byproduct obtained from an atmospheric fluidized

bed combustion process, and portland cement (Type IP). Two sections of the subgrade were treated with cement. The first section extends from Station 317+00 to 348+00 (0.94 km) and the second section extends from Station 429+00 to 522+00 (2.82 km). The subgrade soils of the first section were mixed with 10 percent cement and the soils of the second section were mixed with 7 percent cement. The pavements of the two sections consisted of 15.2 cm of asphaltic concrete and 12.7 cm of dense-graded limestone aggregate. To provide some basis for comparison, a section of the subgrade of reconstructed Route 11 was not treated. This section of the roadway extends from Station 522+00 to Station 532+00 (0.3 km) and consisted 27.9 cm of asphaltic concrete and of 12.7 cm of crushed stone.

Geology of the route consisted of interbedded layers of shales, sandstones, siltstones, and coal. The residual soils along the corridor are derivatives of those materials. Liquid and plasticity index of 25 corridor samples obtained before construction at approximately 152.4-m intervals along the route (Station 264 to 484) generally were classified as CL (clay) and ML-CL (silt-clay).

At the 90th percentile test value of the 25 corridor samples, the liquid limit and plasticity index were 30 and 8, respectively, whereas the liquid limit and plasticity index were 34 and 12 percent at the 50th percentile test value, respectively. Residual soils used to construct the subgrade were stockpiled at three locations

**TABLE 4 Index Properties of Treated and Untreated Soils of KY-11**

CEMENT-TREATED SOIL							
1991	LL PL PI	Percent Passing			Classification		CBR
		No. 4	No. 10	No. 200	AASHTO	Unified	
319+20*	non-plastic	87.4	68.4	21.3	A-1-B (0)	SM	248
433+75**	37 28 9	87.2	71.4	41.0	A-4 (1)	SM	133
463+00							
1989							
321+50*	36 20 10	100.0	96.9	52.7	A-4 (3)	CL	21.2
333+90*	36 29 7	96.3	90.9	51.5	A-4 (2)	ML	
334+12*	44 37 7	97.3	92.6	37.1	A-5 (0)	SM	21.7
480+00**	non-plastic	97.1	95.9	48.6	A-4 (0)	SM	18.8
480+10**							10.5
433+15*8							5.8
MP 14**							18.8
273+00***							
354+00***							
574+00***							
UNTREATED SOIL							
319+20*	28 22 16	82.6	68.7	52.8	A-6 (5)	CL	9.0
433.75**							
463+00	42 23 19	95.4	83.4	72.8	A-7-6 (13)	CL	8.0
1989							
321+50*							
333+90*							
334+12*							
480+00**							
480+10**							
433+15**							
MP 14**							
273+00***	39 25 14	100	91.2	74.0	A-6 (10)	CL	
354+00***	43 28 15	100	92.4	73.0	A-7-6 (11)	CL	
574+00***	36 24 12	100	89.7	70.0	A-6 (8)	CL	

\*10%

\*\*7%

\*\*\* Stockpiles 1, 2, and 3

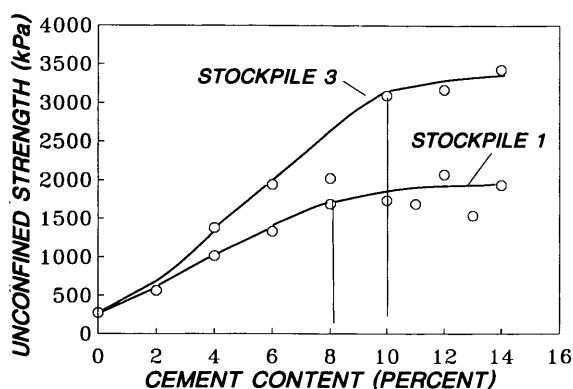


FIGURE 7 Optimum percentage of cement.

(Stations 233+00, 354+00, and 574+00), as shown in Table 4, along the route. Samples obtained from these stockpiles were classified as CL. Plasticity index ranged from 12 to 15 percent.

Optimum percentage of cement was determined following procedures described by Hopkins et al. (4) and Hopkins and Beckham (5). In this approach, different percentages of cement were mixed with the soil and compacted to a known volume, dry unit weight, and moisture content. After aging the specimens in sealed containers for 7 days, unconfined triaxial compression tests are performed. The optimum percentage of cement is the point at which no increase occurs in the unconfined compressive strength as the percentage of cement increases. Two soil-cement series of unconfined compressive tests were performed on soils from stockpiles located at Stations 273+00 and 574+00. Because the maximum dry density and optimum moisture content of treated and untreated soils were essentially the same, all unconfined compressive specimens were molded to maximum dry density and optimum moisture content obtained from standard (ASTM D 698, Method A) compaction on untreated soils. Unconfined compressive strengths are shown in Figure 7 as a function of the percentage of cement. The optimum percentage of cement occurs at about 8 to 10.

In situ bearing ratios of the soil-cement layers, the soil subgrades located below the treated layers, and the soil subgrade of

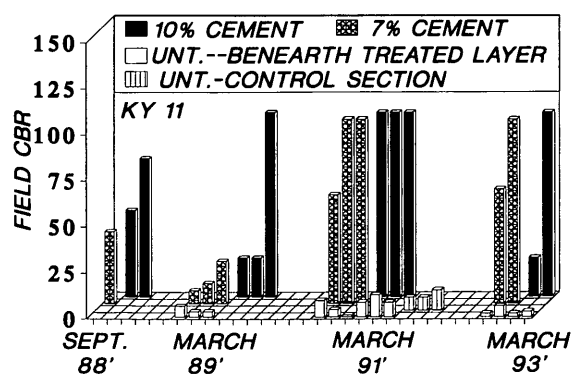


FIGURE 8 In situ bearing ratios of soil-cement layers and untreated soil subgrades of KY-11.

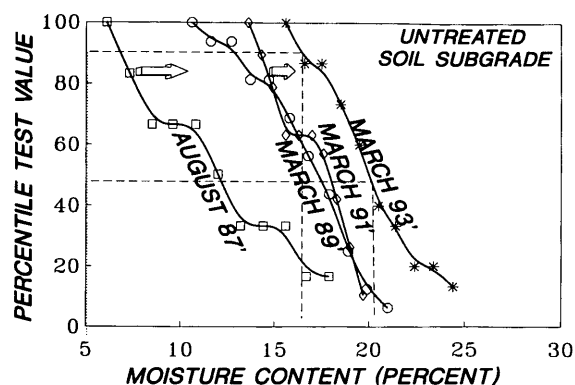


FIGURE 9 Moisture content of KY-11 untreated soil subgrades during a 5.5-year period.

the untreated section were obtained over a period of about 6 years. The field-bearing ratios obtained for the two cement sections are shown in Figure 8. The lowest bearing ratio of the cement subgrades observed during the 6-year period was 7. Excluding that value, bearing ratios ranged from 11 to values in excess of 100 and averaged about 62. In situ bearing ratios observed during the 6-year period of the soil subgrade located below the cement-treated layers and the subgrade of the control section are shown in Figure 8. Bearing ratios ranged from 2 to 14 and averaged 5.7. Because the soils throughout the length of the reconstruction were essentially the same, the change in subgrade moisture content was measured during the study period. As shown in Figure 9, the moisture content of the untreated subgrade increased with increasing time. At the 90th and 50th percentile test values, the moisture contents increased from about 6.5 and 12 percent at the time of construction in 1987 to about 16.5 and 20 percent, respectively. With an increase in moisture content, there was a decrease in the bearing ratios, as shown in Figure 10. Whereas in situ bearing ratios of the soil subgrades during construction ranged from about 20 to 40, the in situ bearing ratios determined in March of 1993 ranged from 1 to 6. Percentile test values as a function of laboratory California bearing ratio (CBR) values of corridor soils and field CBR values of the untreated subgrade soils observed during the study period are shown in Figure 11.

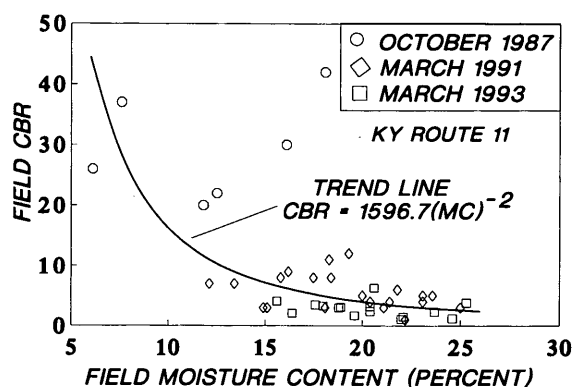


FIGURE 10 Relationship among in situ bearing ratios and field moisture contents measured at different times.



At the 90th percentile test value, the field and laboratory CBR is about 3. The field and laboratory CBR values at the 50th percentile test value are 6 and 7, respectively.

Rutting measurements of the pavement obtained in 1993 for all experimental sections are compared in Figure 12. Depth of rutting of pavements located on the cement-treated subgrades ranged from 0.00 to 0.15 cm after 6 years and was less than pavement rutting depths of the other experimental sections. Depth of rutting of the pavement in the control section ranged from 0.33 to 0.48 cm.

ADT of KY-11, as measured in 1990, was 2,200 VPD. About 13 percent of the ADT value was classified as trucks. Three percent of the trucks were classified as coal trucks. Estimated values of ESAL observed in 1988 and 1989 were 434,000 and 365,000, respectively.

## SUMMARY AND CONCLUSIONS

Long-term in situ bearing ratios of cement-treated soil subgrades of four highway routes were measured. Ages of the routes and cement-treated subgrades ranged from 6 to 30 years. Thickness of the treated subgrades varied from 15.2 to 30.5 cm. Cement content used to treat the subgrades was 10 percent, although in one section of one route a cement content of 7 percent was used. Pavement thickness, which excludes the thickness of the cement-treated layers but includes thickness of overlays of the various sections of three of the four routes, ranged from 25.4 to 48.3 cm. Thickness of the fourth route was about 58.4 cm. Subgrade soils were classified as CL or ML-CL. Plasticity index of those soils was low to moderate. All specimens obtained from the various cement-treated layers during the study period were generally classified as SM, or silty sand.

Bearing strengths of the cement-treated subgrades were generally very large. The relationship among percentile test value and in situ bearing ratios of all treated layers of all sections is shown in Figure 13. At the 90th and 50th percentile test values, the bearing ratios are 24 and 90, respectively. These values compare well

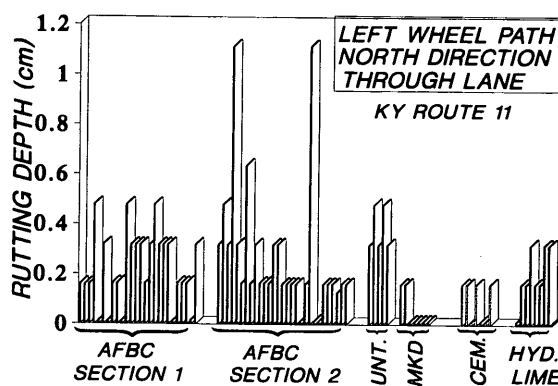


FIGURE 12 Rutting measurements obtained 5.5 years after construction.

with bearing ratios of crushed stone. The strength of the cement-treated subgrades of the four routes was long lasting. Based on these data, the large bearing strengths of cement-treated soils could be expected to prevail throughout a 20-year design life that is typically assumed in flexible pavement design. Moreover, at two sections of one route, rutting depths of pavements placed on cement-treated subgrades were nominal after 6 years. On the basis of visual inspections of the other three routes, rutting was nominal.

Typically, flexible pavements constructed on the cement-treated subgrades had required an overlay about once every 11- to 14-year period. However, the overlays were generally thin; that is, less than about 6.4 cm. ADT of all routes included in the study ranged from about 2,130 to 8,000 VPD. Truck traffic ranged from about 800 to 3,200 vehicles/day.

Findings of this study demonstrate that the use of cement-treated subgrades is a valuable technique for stabilizing low-bearing soil subgrades and is a good design alternative when compared with other stabilizing methods and design alternatives.

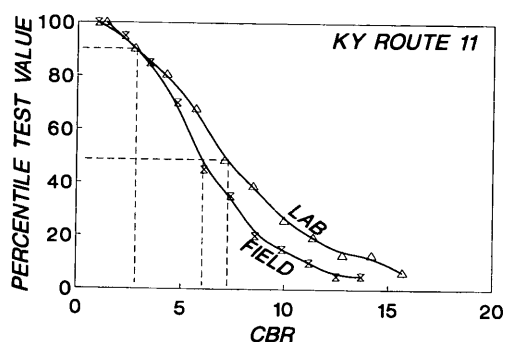


FIGURE 11 Comparison of laboratory California bearing ratio values of corridor soils and in situ bearing ratio values of KY-11 untreated subgrade soils.

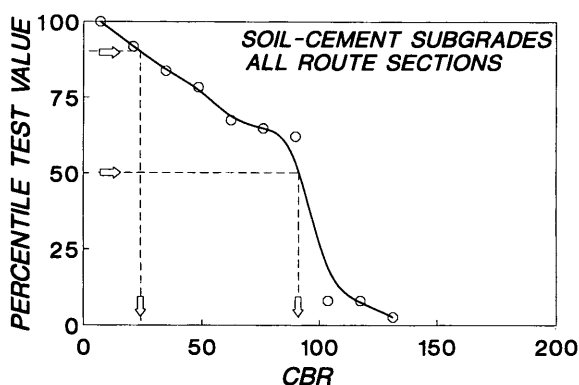


FIGURE 13 Percentile test value as a function of in situ California bearing ratio of soil-cement subgrades.

## ACKNOWLEDGMENTS

The research reported herein was funded by the Federal Highway Administration and the Kentucky Transportation Cabinet through the University of Kentucky Research Foundation.

## REFERENCES

1. Roberts, J. D. Performance of Cement-Modified Soils: A Follow-Up Report. In *Transportation Research Record 1089*, TRB, National Research Council, Washington, D.C., 1986.
2. McGhee, K. H. *Performance Design and Performance Studies* (Final Report on Phase A), Charlottesville Research Council, Charlottesville, Va., April 1972.
3. Terrell, R. L., J. A. Epps, E. J. Berenberg, J. K. Mitchell, and M. R. Marshall. *Soil Stabilization in Pavement Structures*, (A User's Manual, Vol. 2, Mixture Design Considerations), Federal Highway Administration, U.S. Department of Transportation, Oct. 1979.
4. Hopkins, T. C., D. Q. Hunsucker, and G. W. Sharpe. Highway Field Trials of Chemically Stabilized Soil Subgrades. In *Proc., 19th Ohio River Valley Soils Seminar*, Lexington, Ky., Oct. 1988.
5. Hopkins, T. C., and T. L. Beckham. Proposed Procedure for Compacting Laboratory Specimens for Physical Properties Testing. In *Proc., 10th Annual International Pittsburgh Coal Conference*, Pittsburgh, Pa., Sept. 1993.

# Drained Shear Strength of Lime-Clay Mixes

C. D. F. ROGERS AND S. J. LEE

Lime-stabilized clay is being used for novel applications such as slope stabilization and appropriate proof tests are required. The testing of lime-stabilized clay is described in the context of different site applications and recommendations are made. Two British clays of different mineralogies have been tested in unconfined compression and in quick-undrained and slow-drained triaxial tests to examine the difference in both strength and stiffness. The results clearly demonstrate that lime-stabilized clay is a remarkably frictional material. Significant differences were found between the drained and undrained triaxial tests, whereas stiffnesses were approximately similar. In particular the frictional component of strength is shown to be more dominant in drained tests. Unconfined compression tests, which are unable to take account of frictional behavior, are shown to be of value only as index tests to establish whether lime treatment is feasible. The detailed results show that the clays can be treated with relatively low lime contents for use as bulk fill in drained applications. Atterberg Limits are reported for lime-clay mixes between 0 and 56 days after compaction and implications for reaction progress are discussed. The authors conclude that failure envelopes obtained for simulated site conditions should be used for design purposes and that other aspects, such as strain compatibility, should be considered.

Lime has been used extensively to improve the properties of clay soils worldwide, the first records of the process dating back to Roman times. The lime reacts with water contained within the clay, thereby releasing calcium cations ( $\text{Ca}^{2+}$ ) and hydroxyl anions ( $\text{OH}^-$ ) into solution. The calcium-saturated solution surrounding the clay mineral particles results in cation substitution and particle flocculation and agglomeration, thereby modifying the clay. Under conditions of a high pH, slower, longer-term stabilization reactions occur, resulting in gel formation and subsequent crystallization. Modification of the clay changes its nature, from essentially cohesive to cohesionless, and stabilization results in a brittle, cemented material being progressively formed. The rate and extent of property change vary with many factors, including temperature, water content, lime content, and, most important, clay mineralogy. All of this is well known to the engineering community, and yet problems still appear to occur in the interpretation of data from the testing of lime-clay mixes. The latter problem is addressed in this paper.

It is clear from experience of the technique that the properties of a lime-stabilized clay are very different from those of the original clay. For example, there are changes (improvements) in plasticity, strength, stiffness, and volume stability. It is therefore natural that engineers should adopt lime stabilization for ground improvement in preference to the direct and indirect environmental costs of importing crushed rock or other granular fill. The most widespread application must be for road subgrade stabilization,

although increasing use is being made of lime stabilization for bulk fill operations, embankments, and cutting slope repair and as a bearing stratum for lightly loaded foundations. This is in addition to the more novel techniques such as lime slurry pressure injection, lime columns and lime piles for ground improvement (1).

Recent experience in the United Kingdom (UK) has included many successful applications of the technique together with a few, highly publicized failures. One of these, at Saxmundham in Suffolk, concerned a case in which compaction took place to the dry of optimum water content. Thus, although the dry density was within specification because of the considerably flattened compaction curve, the void content was relatively high. The compacted material was left during the winter, water penetrated via the voids, and freezing ruined the coherence of the stratum. This occurred as a result of a fundamental misunderstanding of the material characteristics and, perhaps, a reluctance to add water at compaction to a clay material. The point here is that the material is no longer a clay when mixed with lime and if the same engineer were to be asked to add water to a granular material to reach the optimum water content, no such reluctance would exist. The authors believe that the same symptoms are prevalent in the approach to lime-clay testing.

The most notable UK failure occurred on the M40 Birmingham-to-Oxford motorway, but this is believed to have concerned sulphate concentrations in the natural soil. The study of clay mineralogy, clay chemistry, and the lime-clay reaction processes is not yet fully complete and lies without the scope of this paper. Guidelines have been adopted in the UK to avoid such problems in the future. Perhaps the most important change, however, is that lime stabilization is being considered from the start of the planning and design process, that is at the site investigation stage, instead of being introduced as an alternative at the tender stage only. This is both encouraging and important, and yet is potentially only of full value if appropriate laboratory testing is carried out as part of the investigation.

It has often been stated that lime-stabilized clay can achieve considerable strength (2). However, it is often the case that these very high strengths are not required in practice and engineers are not designing lime-clay mixes to create the properties that they require for the particular purpose. For example, clay modification alone is being increasingly specified. It is apparent, however, that the testing of lime-clay mixes has not progressed in the same way and standard tests, producing little more than index values, are still being specified. Lime-clay testing should run parallel to the design process and attempts to recreate applied inherent stress conditions and site loadings should be made. Presented in this paper are data from three standard tests to illustrate the need for attention to this point.

## TESTING OF LIME-STABILIZED CLAY

Designers necessarily assume material properties for their designs and specify minimum properties for materials to be used on site. Testing of those materials, whether in the laboratory or in situ, is carried out for proof of purpose. Testing should necessarily simulate site conditions, whether of stress or strain, if proof of purpose is to be achieved with efficiency. It should only be necessary to fall back on index values if it proves impossible or impractical to simulate site conditions.

A good example is the case of a lime-stabilized clay road foundation. The foundation has several purposes, which include the need to

1. Provide a suitably stiff platform on which to compact the overlying layers;
2. Act as a haul road during the construction operation (i.e., to carry construction traffic); and
3. Support the stresses transmitted by the overlying layers when the pavement is in use.

The second purpose involves direct trafficking by—albeit relatively few passes of—heavy vehicles. The prime functions of the material itself are to resist permanent deformation (rutting) and to spread the load sufficiently well so that the underlying subgrade does not become overstressed. For this the material must be both sufficiently strong (most important) and stiff, respectively. For the third purpose the same requisite characteristics apply, although resilient stiffness under repeated load applications has most importance. It is apparent, therefore, that the test required here is the repeated load triaxial test: pace, the hollow cylinder test with principal stress rotation. The sample should be confined to match the ambient stress conditions and should be subjected to both relatively few (say 50 to 100) applications of a high deviator stress and a large number (millions) of applications of a relatively low deviator stress. The rate of application, in terms of frequency and duration, of these stress pulses should similarly be representative of site conditions within reasonable limits of practicality. Instead an index test is used, in the form of the California Bearing Ratio (CBR), and correlations are attempted among the requisite parameters and the CBR. The inaccuracy and inefficiency of this approach is amply illustrated by Brown et al (3).

For the bulk fill applications, such as slope repair and bearing strata for light foundations, the loading regime is altogether different. In these cases the load application is typically extremely slow and very slow shearing tests should be conducted.

At this point, therefore, it would be useful to examine what is meant by strength. Traditional soil mechanics defines the Mohr-Coulomb envelope as the boundary in shear stress-normal (total or effective) stress space above which the soil will fail in shear. In the case of testing under effective stress, no pore water pressures are reflected in the data, the samples under test being tested very slowly in a fully drained manner. The resulting effective stress envelope, defined by effective cohesion ( $C'$ ) and effective angle of internal friction ( $\phi'$ ), would thus apply to the bulk fill applications previously mentioned. A second particular type of test, the quick undrained triaxial test, is used for saturated clays to produce a total stress plot in which porewater pressures are permitted to influence the results. Interpretation of undrained tests is based on the assumption that a saturated clay has a small, often negligible, undrained angle of internal friction ( $\phi_u$ ) and thus a

mean horizontal line can be drawn parallel with the axis of normal stress to create an intercept on the shear stress axis of undrained cohesion ( $C_u$ ). A third variation is the unconfined compression strength (UCS) test, which uses the arguments behind the quick undrained triaxial test to dispense with confining pressure altogether, the mean maximum shear stress in the test representing  $C_u$ .

Strength measurement for lime-stabilized clay is often quoted in terms of UCS or  $C_u$ , and yet a lime-stabilized clay in practice is generally not saturated and does not behave like a clay. These results must surely, therefore, represent index values of strength under a certain set of arbitrary conditions. If the strength characteristics of a lime-clay mix vary with the rate of testing, as will be demonstrated hereafter, then the rate chosen for testing should match that in practice. In addition a lime-clay mix, which is widely known to have a particulate nature and will be shown to have a significant frictional component of strength, will necessarily be subject to some degree of confinement because of its placement and compaction in addition to site confinement. Thus the argument for selecting UCS for design is invalid, and indeed can result in an overestimation of strength at relatively low confining stresses, most notably in the fully drained (long-term) case. Thus considerable care should be exercised in the interpretation of data from such tests.

## RESEARCH PROGRAM

### Research Philosophy

The three test techniques already described were applied to two British clays of different characters and mineralogies. Lower Lias clay, which outcrops in the midlands of England, is an illitic silty clay having a liquid limit (LL) of 59 percent and a plastic limit (PL) of 29 percent. The second clay is a refined kaolinite, known as English china clay, derived from the weathering of granite in the south-west of England and has an LL of 60 percent and a PL of 33 percent.

The primary aim of these tests was to consider the behavior of the lime-clay mixes around the lime fixation point, with the aim of assessing their performance in a drained, bulk-fill, possibly slope-stabilization application. Accordingly a relatively high water content was chosen for the initial clay so that, when mixed with lime, the water content would remain slightly above the optimum water content at compaction. Immediate strength gain was not considered important although the development of strength with time was. A further aspect of the results that was of interest was the change in stiffness and brittleness of the material, because differential stiffness in a slope has implications for progressive failure mechanisms. In addition, it has been reported that the strain at failure of the stabilization products (calcium silicate hydrate and calcium aluminate hydrate, CSH and CAH respectively) is approximately 1 to 2 percent (2,4).

### Experimental Procedure

Both the lower Lias and English china clay were air dried and mixed with water to achieve a liquidity index of 0.1. This was found from previous research (4) to be the best method for correlation among different soils, instead of using arbitrary moisture

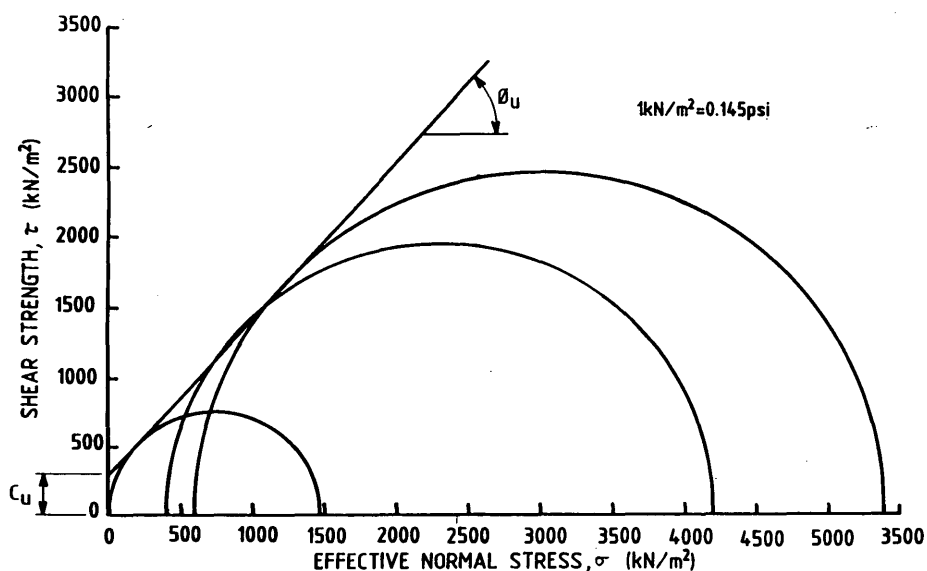


FIGURE 1 Mohr-Coulomb plot for an undrained test on china clay with 5 percent Quicklime at 28 days.

contents that could lead to misinterpretation. Three lime contents were used for the tests: the Eades and Grim value (5), and 2 percent above and 2 percent below this value for each clay. Once again this facilitated a true comparison among the clays. The lime-clay batches were mixed in a large pan mixer for 12 min, a time that was found from preliminary trials to ensure intimate mixing. The lime-clay mixes were then stored for 48 hr in heavy-duty polythene bags at  $21 \pm 2^\circ\text{C}$  to allow for mellowing, for example completion of the modification reaction. This was characterized by changes in Atterberg Limits (measured at 0 and 8 hours, and 1, 2, 7, 28, and 56 days) followed by stability at a reduced plasticity. Once mellowed the modified material was compacted into 100-mm (4-in.)-diameter tubes of 500-mm (20-in.) length in accordance with the British Standard heavy-duty compaction test (6). Thirty-eight-mm-diam specimens 76 mm in length were sampled immediately after compaction to avoid damage to the rapidly strengthening samples.

Four sets of 27 samples were prepared (one set of each clay type for drained and undrained testing), again sealed individually, further sealed in groups of three, and stored at  $21 \pm 2^\circ\text{C}$ . The samples were tested in standard triaxial test machines in accordance with British Standards Institution Report BS1377: Part 8 (7) at 7, 28, and 56 days. The undrained tests used a shearing rate of 1.000 mm/min (0.0400 in./min) and the drained tests 0.009 mm/min (0.00035 in./min). At each stage of testing three undrained and three drained specimens were tested at confining pressures of 0, 400 and 600 kN/m<sup>2</sup> (0, 58, and 87 psi), one undrained sample thus being tested under unconfined compressive stress conditions. In addition, untreated clay samples were dried, mixed with water, and stored in the same manner, and were tested at cell pressures of 0, 100, and 200 kN/m<sup>2</sup> (0, 14.5, and 29 psi) after 28 days. Additional samples were prepared for each clay and lime content for replicate testing to both confirm experimental data trends and the veracity of unexpected results. The large confining stress range for the lime-treated clay was chosen to facilitate the production of accurate best-fit lines on the Mohr-Coulomb plots

(see Figure 1 for a treated clay in comparison with Figure 2 for an untreated clay). From the test data drained and undrained shear strength parameters were obtained, secant moduli calculated, failure strains recorded, and unconfined compressive strength values calculated.

## EXPERIMENTAL RESULTS

### General Observations

The test program proved successful and although some (expected) scatter of the data occurred, the trends in the results followed expected patterns (2,4) and were reasonably well defined. Supplementary data, such as Atterberg Limits, not reported in detail herein, confirmed that the clays were modified as expected. Good compaction of the lime-clay samples was achieved after mellowing, as evidenced by the measured densities (which were consistent with the water content measurements of the specimens given in Table 1), the shear strength results and the appearance of the samples. The Atterberg Limits for the china clay LL = 60 percent, PL = 33 percent showed a rise in LL and PL of 11 to 12 percent and 4 to 8 percent, respectively, after 48 hr. The LL reduced and PL increased thereafter causing a reduction in Plasticity Index (PI) by 5 percent to +4 percent in relation to the PI of the untreated clay for 1 percent lime, and by 9 percent to -4 percent and 18 percent to -13 percent for 3 percent and 5 percent lime, respectively. A similar trend was noticed for Lias Clay (LL = 59 percent, PL = 29 percent) with LL rising by 0 to 13 percent and PL by 12 to 14 percent after modification. The PI reduced by 11 percent to -12 percent, 5 percent to -17 percent, and 10 percent to -23 percent for 4 percent, 6 percent, and 8 percent lime respectively. The approximate equivalence of 5 percent lime addition to china clay and 4 percent to Lias clay was demonstrated.

The Eades and Grim test (5) demonstrated that the nearly pure kaolinite required 3 percent lime for fixation, whereas the Lias

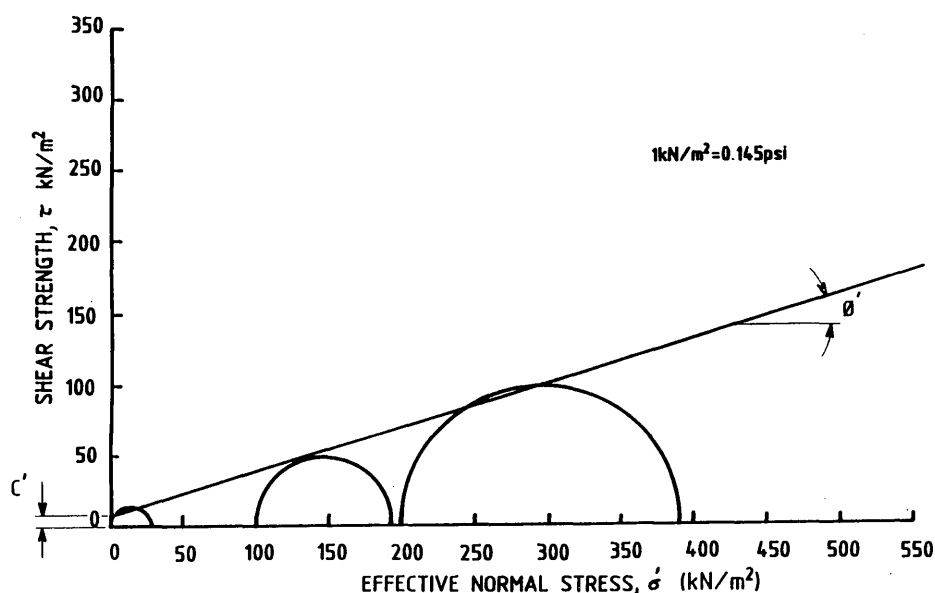


FIGURE 2 Mohr-Coulomb plot for a drained test on untreated china clay at 28 days.

clay required 6 percent lime. However, the undrained and drained shear strengths, shown in Table 2 and discussed in subsequent sections, show that the higher lime contents used for the Lias clay resulted in considerably higher strength gains. There are several factors that influence the magnitude and rate of strength gain, the most important being clay mineralogy, and these undoubtedly account for the observations. Nevertheless, it is important to note that the strengths achieved when mixing lime with clay at the fixation point are likely to be considerably different because some engineers unfamiliar with the process have been misled in this respect.

A further general point to note is that the lime-clay mix is particulate before compaction and that cementation occurs within the flocculated, agglomerated structure. Although cementation tends to produce a coherent structure, the use of 38-mm-diameter samples, out of practicality, will almost certainly result in some variation in strength measurements, depending on the location of the shear plane in relation to the flocs. This will, in part, explain some of the scatter noticed in the data.

### Undrained Shear Strength

Lime stabilisation improves both the (apparent) cohesive ( $C_u$ ) and frictional ( $\phi_u$ ) components of the undrained shear strength, as shown in Table 2. Only small amounts of lime are required to radically improve the strength, whereas increasing lime content and time tend to improve the parameters further. It should be noted that the strength derives from a combination of  $C_u$  and  $\phi_u$ , and thus the two values should be considered together. The impossibility of precise determination of  $C_u$  and  $\phi_u$ , especially when high strengths have been reached, should not be forgotten in subsequent interpretation. Indeed it is clear from the Mohr-Coulomb plots that even the relatively high confining pressures used in this study were inadequate for accurate determination of  $C_u$  and  $\phi_u$  and that values of 0, 2000, and 4000 kPa (or, say, 0, 300, and 600 psi) or more should be used for the high lime contents. From inspection of the Mohr-Coulomb plots (e.g., Figure 1) it is noticed that the angle of friction ( $\phi$ ) will be more reliable than the cohesion intercept ( $C$  perhaps better representing "cementation")

TABLE 1 Moisture Contents of Lime-Clay Mixes After Compaction (%)

Soil Type	Lime Content (%)	Time (days)						
		0	0.33	1	2	7	28	56
China Clay	0						33	
	1	37	37	37	36	39	39	39
	3	37	37	37	38	38	37	36
	5	40	38	39	38	35	35	35
Lower Lias Clay	0						32	
	4	32	32	32	32	31	31	31
	6	24	23	25	26	26	29	29
	8	26	26	26	26	26	28	28

than "cohesion") because slight changes in  $\phi$  will cause radical changes in  $C$ .

The results show that in general  $C_u$  increases with lime content,  $C_u$  increasing typically twofold for the 4 percent increase in lime content from below to above the Eades and Grim value.  $C_u$  also increases with time, the difference between 7 and 56 days being typically threefold for lower Lias clay and somewhat less on average for china clay. Any variations from this trend can be explained by imprecision in data interpretation. The changes within 7 days are attributed primarily to modification and compaction, whereas at 56 days the changes reflect also the development of the pozzolanic (stabilization) reactions.  $\phi_u$  has also increased substantially above that for untreated clay in the first 7 days for both clays. In the case of English china clay,  $\phi_u$  has reached a value of a good quality granular material after 7 days even with a lime content of only 1 percent. This trend, confirmed by other recent UK work, is attributed to the fact that the clay has been modified. The trend of increasing  $\phi_u$  with time and lime content (Figure 3) is perfect for the china clay with the exception of 5 percent lime at 56 days, when cementation ( $C_u$ ) increased dramatically. The conclusion here would appear to be that  $\phi_u$  increases as stabilization proceeds (i.e., the Mohr-Coulomb envelope rotates with time, and rises with lime content). Once the stabilization reactions are largely complete, however, this trend appears to break down as very large  $C_u$  values are accompanied by lower (though still high in absolute terms)  $\phi_u$ . These findings have been confirmed by other work at Loughborough, but warrant further work to examine their universality (especially between clay minerals).

For lower Lias clay with its significantly higher lime contents,  $\phi_u$  is high, even for a granular material, after 7 days implying exaggerated dilational behaviour. At 28 days  $\phi_u$  falls in all cases, although  $C_u$  rises sharply and at 56 days  $\phi_u$  starts to rise again, although such fine distinctions cannot be concentrated on for the reasons already mentioned. Taking the results together, it can be concluded that  $\phi_u$  rises as the stabilization reactions progress, but when significant cementation is complete, a moderate reduction in  $\phi_u$  is accompanied by high (greater than 1000 kPa or 145 psi)  $C_u$ . Thus only the 5 percent, 56-day English china clay sample

has reached that point, whereas only the Lias clay samples at 4 percent and 6 percent lime at 7 days have not reached that point. These conclusions have also been reached by Lees et al. (8) in their work on kaolinite and montmorillonite.

### Drained Shear Strength

Similar increases in  $C'$  and  $\phi'$  occurred in drained tests (Table 2), with the largely consistent trends already explained. With one exception,  $\phi'$  is higher in the drained condition than in the undrained condition for both treated and untreated soil. For untreated soil this occurs because the drained test measures essentially only frictional behavior. That the same observation is true of treated soil implies that pore water, or fluid, pressure generation occurs in the undrained tests on these materials. Drained shear test data should thus be used for slope or bearing applications.

### Unconfined Compressive Strength

With only a few exceptions, UCS increases with time and lime content (Table 2). The UCS for china clay at 5 percent lime content and 56 days, and for all lime-treated samples of lower Lias clay, is high (>2200 kPa or 139 psi), whereas otherwise is less than 1010 kPa (146 psi), adding evidence to the conclusion that only in these samples have the stabilization reactions been substantially completed. Noting that UCS should be halved for comparison with  $C_u$ , and by extension with  $C'$ , it is apparent that overestimation of  $C_u$  is only significant when significant stabilization has occurred (say  $UCS > 2000 \text{ kN/m}^2$  or 290 psi), whereas considerable overestimation of  $C'$  occurs in all cases.

Therefore, using UCS in the design process would underestimate the strength at high confining pressures, because the frictional component of strength is de facto ignored in any interpretation using UCS, providing a large factor of safety. This would be uneconomic—hence poor engineering—but not dangerous. However, at low confining pressures, UCS would overestimate the

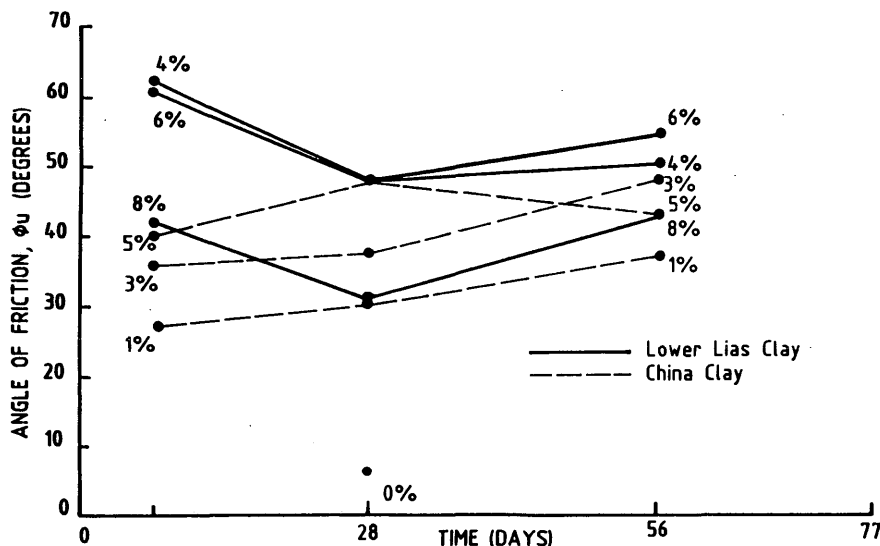


FIGURE 3 Undrained angle of friction versus time for lower Lias clay and china clay.

strength and this could be unsafe. When the loading is not applied rapidly, these problems are exacerbated and unsafe designs could easily result.

### Elastic Modulus

Lime stabilization causes considerable improvement in the elastic modulus, changing a soft, plastic material into a stiff, brittle material. This change occurs with both time and lime content (Table 3, Figure 4), and is approximately the same, although with some scatter, for the drained and undrained tests. Comparison with untreated soil leads to the conclusion that lime stabilization is very effective when used to improve, for example, subgrade properties, albeit that repeated load triaxial tests at appropriate stress levels and application rates should be conducted.

The elastic modulus was much higher with lower Lias than English china clay and certainly far higher than could be attributed to any variation in the properties of the remolded clays, as evidenced by the data for the untreated clay. This suggests that either

the pozzolanic reaction was more advanced in the lower Lias clay, or that the flocs and their bonds were stiffer. Data presented earlier confirm the former explanation. A typical set of curves, in this case for the undrained tests on lower Lias clay with 4 percent quicklime addition, illustrated the increase in both strength and stiffness with time for the unconfined compression test data (Figure 5). It is clear that the failure strains have reduced from approximately 4 percent to 2 percent between 7 and 28 days. It is equally evident that the brittle behavior of a stabilized soil (i.e., one in which stabilization reactions are substantially complete), characterized by failure strains of 1 to 2 percent and a rapid fall off in strength post peak, is exhibited by the two later curves. A further point, once more typically found from the experimental data, is that when high confining pressures are applied, the stiffness remains approximately constant (evidenced by the gradient of the stress strain curve ignoring zero drift), and yet the strain at failure increases from approximately 2 percent to 4 to 6 percent or more (again ignoring zero drift). This was consistently evident throughout the test program and thus accounts, at least in part, for the increase in strength at higher confining stresses (i.e., frictional

TABLE 2 Strength of Lime-Clay Mixes

Soil Type	Lime Content %	7 days	28 days	56 days
Undrained Shear Strength $C_u, \phi_u$ (kN/m <sup>2</sup> , degrees)				
China Clay	0	-	45,6°	-
	1	230,27°	170,30°	270,37°
	3	120,36°	360,38°	410,46°
	5	475,40°	300,48°	1000,42°
Lower Lias Clay	0	-	41,7°	-
	4	720,62°	1860,48°	2450,50°
	6	600,61°	1800,48°	2300,54°
	8	1670,43°	3130,31°	5100,42°
Drained Strength $C', \phi'$ (kN/m <sup>2</sup> degrees)				
China Clay	0	-	7,16°	-
	1	125,48°	140,51°	200,50°
	3	125,52°	120,64°	240,60°
	5	275,60°	300,61°	310,63°
Lower Lias Clay	0	-	7,18°	-
	4	1025,43°	950,55°	1500,58°
	6	1175,56°	1225,57°	1400,62°
	8	1450,43°	1800,55°	3500,48°
Unconfined Compressive Strength (kN/m <sup>2</sup> )				
China Clay	0	-	82	-
	1	317	269	526
	3	225	750	957
	5	1009	725	2245
Lower Lias Clay	0	-	83	-
	4	3132	4853	6601
	6	2330	5050	7449
	8	3803	5613	6584



TABLE 3 Secant Elastic Modulus (N/mm<sup>2</sup>)

Soil Type	Lime Content %	Time (days)					
		Drained			Undrained		
		7	28	56	7	28	56
China Clay	0	-	1.45	-	-	1.51	-
	1	67	123	52	78	50	182
	3	95	82	106	46	68	225
	5	204	214	248	80	223	251
Lower Lias Clay	0	-	3.18	-	-	1.48	-
	4	300	339	612	266	455	624
	6	276	332	549	330	521	627
	8	422	566	794	356	566	720

1 N/mm<sup>2</sup> = 145 psi

behavior as denoted by  $\phi_u$  or  $\phi'$ ) because of the need for significant dilation of the sample before shearing being possible. This finding has considerable relevance for geotechnical design because strain compatibility between stabilized and untreated soils will need to be designed.

One final point is that a great improvement is seen in the English china clay with 1 percent lime. This must be caused by flocculation and agglomeration (i.e., modification) as very little, if any, of the lime contributes to pozzolanic reaction (9). These and earlier observations demonstrate that a substantial amount of the strength and stiffness improvements associated with lime are caused by modification alone.

### Failure Strains

Many authors have stated that the ultimate strain of crystalline CSH and CAH lies between 1 and 2 percent (2,4,9), and nearing these failure strains indicates completion of the pozzolanic reac-

tion within a stabilized soil. The smallest recorded average failure strains in the tests, shown in Table 4, are approximately 3 percent, apparently indicating that, although substantial cementing has occurred, further reaction is necessary before cementation is complete. However, when consideration is given to the detailed results illustrated in Figure 5, presented in Table 4, and discussed in the previous section, it is clear that full (or at least substantial) stabilization has occurred in many of the samples. The data for no confinement in the undrained tests indicate that all of the Lias clay samples excepting the two lower lime contents at 7 days fail at or below 3 percent axial strain. Similarly the china clay samples with 3 and 5 percent lime contents at 56 days have low undrained failure strains. This trend would be completely defined if it were not for the low failure strains for the china clay with 1 percent lime at 28 and 56 days, the reasons for which are not clear. The higher average strains thus clearly result from larger strains at higher normal effective stresses, and this is clearly borne out by the results in Table 4. These effects are exaggerated in the case of drained shear testing (Table 4), in which the failure strains are

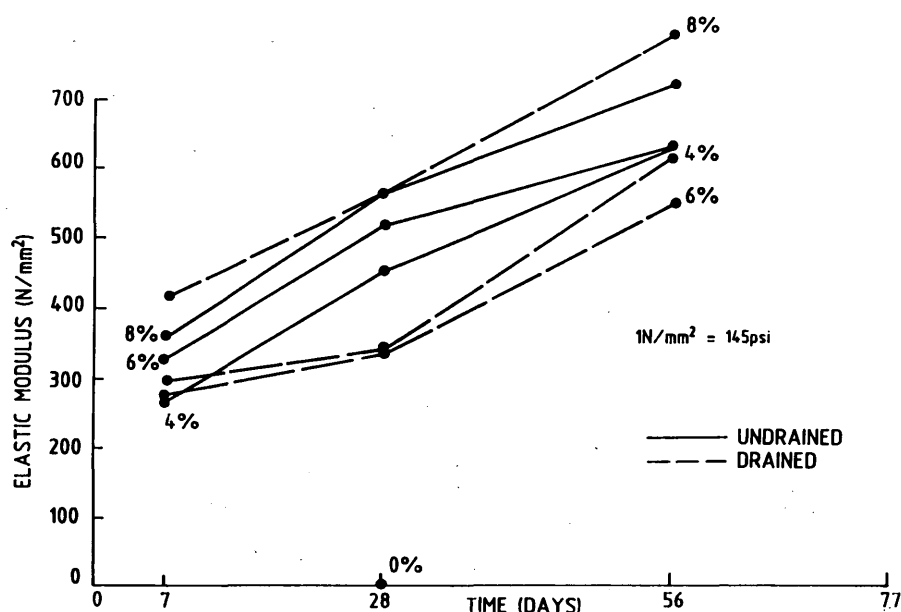


FIGURE 4 Secant elastic modulus versus time for lower Lias clay.

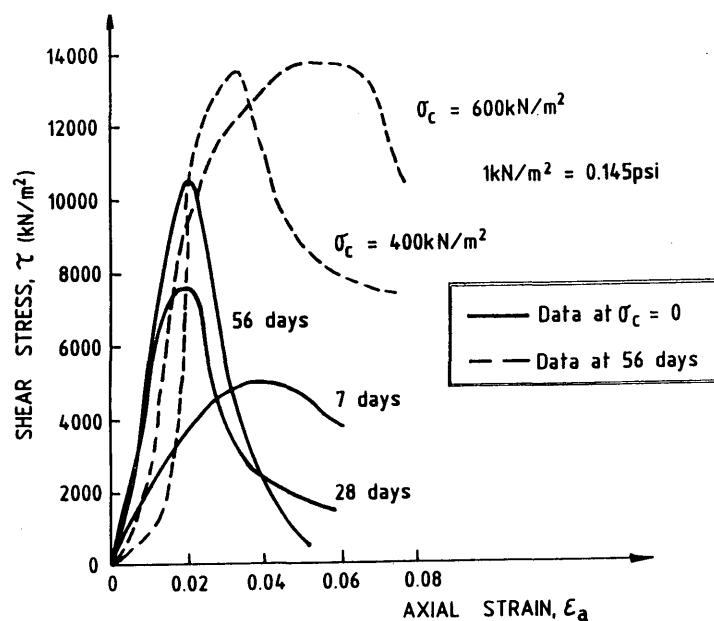


FIGURE 5 Graph of shear stress against axial strain for undrained triaxial tests on lower Lias clay with 4 percent lime.

TABLE 4 Strains at Failure

Soil Type	Lime Content %	Time (days)											
		$\sigma_c = 0$	7 days				$\sigma_c = 0$	28 days				56 days	
			400	600	av			400	600	av		$\sigma_c = 0$	av
Strains at Failure in Undrained Tests													
China Clay	0*					0.110	0.133	0.158	0.134				
	1	0.190	0.200	0.200	0.197	0.020	0.038	0.054	0.037			0.013	0.031
	3	0.073	0.079	0.093	0.082	0.042	0.104	0.092	0.079			0.016	0.053
	5	0.039	0.072	0.099	0.070	0.040	0.032	0.027	0.033			0.020	0.040
Lower Lias Clay	0*					0.142	0.185	0.132	0.153				
	4	0.040	0.071	0.080	0.064	0.018	0.054	0.045	0.039			0.020	0.036
	6	0.038	0.053	0.062	0.051	0.030	0.045	0.040	0.038			0.027	0.046
	8	0.020	0.040	0.058	0.039	0.020	0.038	0.027	0.028			0.025	0.045
Strains at Failure in Drained Tests													
China Clay	0*					0.050	0.110	0.080	0.080				
	1	0.078	0.078	0.150	0.102	0.014	0.080	0.026	0.040			0.027	0.124
	3	0.150	0.150	0.070	0.123	0.020	0.126	0.156	0.101			0.020	0.076
	5	0.103	0.076	0.088	0.089	0.012	0.096	0.080	0.063			0.013	-
Lower Lias Clay	0*					0.030	0.105	0.130	0.088				
	4	0.036	0.049	0.033	0.039	0.033	0.060	0.023	0.039			0.025	0.045
	6	0.042	0.043	0.053	0.046	0.026	0.065	0.094	0.062			0.020	0.050
	8	0.053	0.025	0.033	0.037	0.020	0.033	0.065	0.039			0.032	0.041

\* Confining pressures for zero lime contents were 0, 100, 200 kN/m<sup>2</sup>  
1 kN/m<sup>2</sup> = 0.145 psi

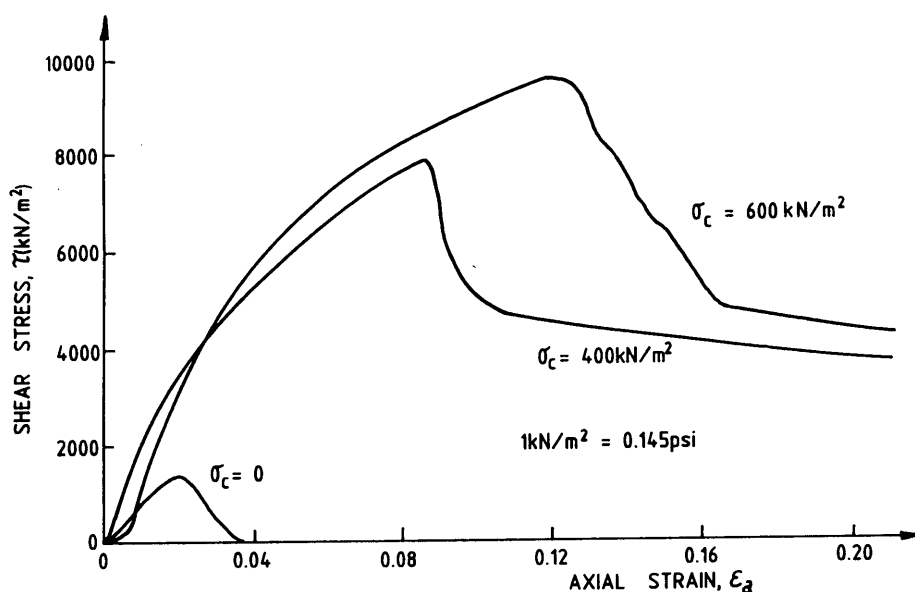


FIGURE 6 Graph of shear stress against axial strain for drained triaxial tests on English china clay with 3 percent lime at 56 days.

typically larger than those of undrained testing. A graphic illustration of the trend for higher strengths and failure strains with higher normal stresses is given in Figure 6, in which the different shear stress-strain behavior of china clay is also demonstrated. These data are crucial for good geotechnical design in certain practical cases, and particularly where slow, or relatively slow, loading is applied.

## CONCLUSIONS

From the data presented herein, which are consistent with recent UK thinking on the subject, it is clear that lime improves substantially both the "cohesive" and "frictional" components of shear strength, and only small lime contents (1 to 3 percent) are required for considerable strength and stiffness increases. The "frictional" behaviour of lime-stabilized clay, both immediately on modification and during progressive stabilization, has been clearly demonstrated and must be accounted for in design. "Frictional" behavior can only be accurately determined using high confinement pressures in laboratory testing.

As more applications of lime-stabilized clay are being introduced, greater consideration of proof testing is required. Distinct differences have been demonstrated between drained and undrained behavior, and thus magnitude, rate, frequency, and duration of applied loading should simulate those prevalent in practice if accurate results are to be obtained. In this respect, the quick undrained triaxial test can be considered arbitrary only and thus indicative of relatively rapid loading. The unconfined compressive strength test, which is unable to account for frictional behavior, has been shown to be variously overly conservative and unsafe for design. This test should only be used as an index test to demonstrate whether a clay can be modified and stabilized. The Atterberg Limits also provide a good indication of the progress of

lime-clay reactions and can be considered to be valuable index tests.

The two clays tested have been shown to be suitable for drained applications such as slope stabilization, even at lime contents below the Eades and Grim values. The strength and stiffness of the treated materials are sufficiently high after 7 days for operations to continue at an economic rate and the data show that the parameters, particularly  $\phi$ , will increase significantly with time. However at sufficiently high lime contents for full stabilization to occur, very high (cementation) strengths (typically greater than 1000 kN/m<sup>2</sup>, or 145 psi) will be obtained and the value of  $\phi'$  will become less important. The failure strains conformed to the expected pattern in the unconfined case, but at high cell pressures higher failure strains were observed and these were considered to explain, at least in part, the "frictional" component of strength because of the need for sample dilation. Further work on lower Lias Clay to examine the performance at lower lime contents is warranted.

## REFERENCES

1. Rogers, C. D. F., and C. J. Bruce. Slope Stabilization Using Lime. In *Proc., International Conference on Slope Stability Engineering*, Isle of Wight, United Kingdom, Institution of Civil Engineers, London, April 1991.
2. *State of the Art Report 5, Lime Stabilization*, TRB, National Research Council, Washington, D.C., 1990.
3. Brown, S. F., M. P. O'Reilly, and S. C. Loach. The Relationship Between California Bearing Ratio and Elastic Stiffness for Compacted Clays. *Ground Engineering*, Vol. 23, No. 8, Oct. 1990, pp. 27-31.
4. Rogers, C. D. F., and C. J. Bruce. The Strength of Lime-Stabilized British Clays. In *Proc., British Aggregates Construction Materials Industries Lime Stabilization '90 Conference*, Sutton Coldfield, United Kingdom, 1990, pp. 57-72.

5. Eades, J. L., and R. E. Grim. A Quick Test to Determine Lime Requirements for Lime Stabilization. In *Highway Research Record 139*, HRB, National Research Council, Washington, D.C., 1966, pp. 61–72.
6. *British Standard Methods of Test for Soils for Civil Engineering Purposes, Part 4, Compaction-Related Tests*. British Standards Institution, BS1377: Part 4: 1990, Her Majesty's Stationery Office, London.
7. *British Standard Methods of Test for Soils for Civil Engineering Purposes, Part 8, Shear Strength Tests (Effective Stress)*. British Standards Institution, BS1377: Part 8: 1990, Her Majesty's Stationery Office, London.
8. Lees, G., M. O. Abdelkader, and S. Hamdani. Effects of Clay Fraction on the Mechanical Properties of Lime-Soil Mixtures. *Journal of the Institution of Highway Engineers*, Nov. 1992, pp. 3–7.
9. Thompson, M. R. Shear Strength and Elastic Properties of Lime-Soil Mixtures. In *Highway Research Record 139*, HRB, National Research Council, Washington, D.C., 1966, pp. 1–14.

# Deep-Slope Stabilization Using Lime Piles

C. D. F. ROGERS AND S. GLENDINNING

Lime piles have been successfully used in practice in several countries worldwide but their mechanism of operation has not been adequately explained. The literature on the subject has been briefly reviewed and a list of suggested stabilizing processes has been compiled. Programs of experimental work to investigate each process are described and the results are presented. Lime piles, which usually consist of columns of quicklime placed in pre-formed holes in clay soils, draw in water during hydration and expand. No lateral consolidation of the surrounding clay occurs, however, because of the stoichiometry of the hydration reaction. The water loss in the surrounding clay causes an increase in undrained shear strength. The associated pore water pressure reduction, or suction, caused by the hydration reaction is shown to be significant in the short term to increase the stability of the slope and in the long term by overconsolidation of the shear plane. Migration of calcium and hydroxyl ions from the piles has been shown to be limited to less than 30 mm (1.2 in.), as might be expected from considerations of clay liners. The pile itself is shown to have significant strength. The laboratory work has been supported by the initial findings of a program of field trials.

The problem of failing slopes has been addressed by engineers over millennia and, with the need for reduced land-take in the United Kingdom (UK), is increasing. Slopes were formed for the waterways, then the railways, and more recently have been formed for the ever-increasing miles of motorways. Failed slopes are a current problem in each of these transportation networks, but have recently been quantified in terms of UK motorways by Perry (1), who surveyed 570 km (354 mi) of motorway slopes covering all of the principal geologies. Although the study focused on both cutting and embankment slopes, only the latter will be considered here. The conclusions of this work make recommendations for side slopes to be adopted in new embankment construction in different materials and provide criteria to facilitate recognition of slopes that are at risk of failure. The survey revealed significant incidence of shallow slope failure (a total of more than 17 km or 10.5 mi of embankment slope and 5.5 km or 3.5 mi of cutting slope) and it was estimated that at least three times as many failures will occur in the future in the area surveyed as have occurred over the past 25 years.

It was reported that remedial works in the case of failed embankment slopes almost invariably took the form of excavation, sometimes in benches, to below the failure surface and replacement of the excavated material with compacted granular, free-draining material such as gravel, crushed rock or brick rubble. Topsoil is sometimes placed over the repaired area to permit vegetation to become re-established. This remedial process will typically require closure of part of the transport route, even if only the hard shoulder on a motorway for example, and requires excavation plant and significant equipment movements to both dispose of excavated material and deliver the granular fill. It is apparent that remedial methods that require small plant and minimal

associated traffic would be of advantage. Lime piles provide one such solution.

The technique of using lime to improve the engineering properties of clay soils is reasonably well established if not yet fully understood. It is well known that lime reacts chemically with some of the constituents of clay to first modify and then stabilize the clay (2). Modification takes place within approximately 24 to 72 hr of mixing lime and clay together and causes flocculation and agglomeration of clay particles, changing the cohesive nature of the material. The clay becomes friable and granular in nature, and its strength and stiffness are improved (Rogers and Lee, in a paper in this Record). Stabilization occurs more slowly and concerns the long-term strength development brought about by the development of cementitious compounds from the reaction of lime with the siliceous clay components.

Lime has been widely used in road construction by intimate mixing with clay subgrades to improve workability, shear strength, and bearing capacity through the reactions already described, and is now being used for many applications. The use of lime as a deep stabilizing technique is a more recent development. In Sweden, China, Japan, and Singapore, lime, in the form of intimately mixed lime-clay columns created in situ, has been used to prepare soft ground for foundations. The stabilization reactions that subsequently occur produce columns of material of greater strength, and arguably increased permeability, than the surrounding untreated clay. The technique does, however, require large plant to carry out. Lime slurry pressure injection has been established as a stabilizing technique in the United States. As the name suggests, lime in the form of a slurry is injected into the ground using specialist, although relatively small, equipment. It has been used to treat expansive clay soils, silts, and other soft ground and to stabilize failed embankment slopes, although the problem of increased pore water pressures induced by this technique could be seen as a drawback with this latter application.

The final technique, and the subject of this paper, is lime piles, which are holes in the ground filled with lime. Ingles and Metcalf (3) show one method of construction as illustrated in Figure 1, in which a hollow tube is pushed into the soil to the required depth of pile and quicklime is forced into the tube under pressure as it is withdrawn. The pressure forces open the end of the tube allowing the lime to fill the cavity below. After each meter is filled, the end of the tube is closed and used to compact the lime. In stiff or strong clay soils holes are formed using a powered auger and the lime is fed in and compacted once the auger has been withdrawn. It is believed that lime piles are potentially a simple solution, being both cheap and easy to install using small plant, even in the most remote places. As a result a major research program is being carried out at Loughborough University of Technology in the UK (4) to investigate how lime piles work and how they can be designed and installed. The aim of this paper is to outline their potential and to provide supporting experimental data.

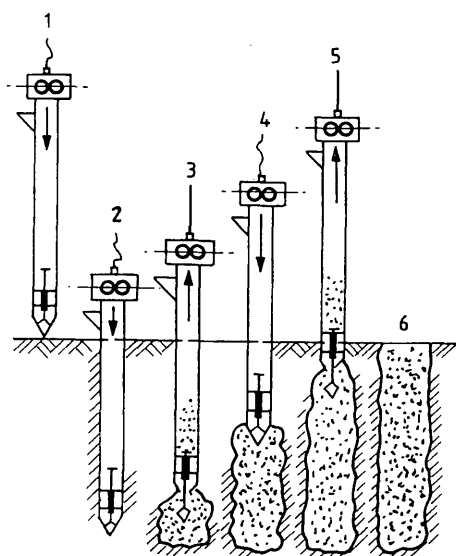


FIGURE 1 Procedure for construction of lime piles in soft clay soils (4).

## LITERATURE ON LIME PILES

The use of lime piles has been documented in many countries although no consensus on their mode of operation has been reached. Two distinct themes emerge concerning the mechanism of stabilization and authors largely discuss one independent of the other. The first of these is the idea of lime pile expansion and surrounding clay dehydration. Quicklime has a great affinity for water and thus draws in water from the surrounding soil to be consumed by the (expansive) reaction. The piles then expand and are said to cause lateral consolidation of the surrounding clay, although because the reaction is highly exothermic and large volumes of quicklime are used, it is likely that significant quantities of water are removed in the form of steam. In general, the authors who propose this mechanism are using the lime piles to improve the bearing capacity and settlement characteristics of soft ground. The most notable exponents of this technique are the Japanese (5), who describe the use of quicklime piles of diameters up to 1 m (39 in.) placed at spacings less than 1.5 m (5 ft) in clays of very high water content (up to 400 percent). The changes produced appear to be proportional to the initial water content of the soil. Wang (6), describes similar work being carried out in China. Laboratory studies have been described by Chui and Chin (7), at the National Taiwan University, using clay (Taipei silt) compacted into boxes in which small quicklime piles are formed. They also believed that initial moisture content was the key to the success of the process, but mention the possibility of chemical reaction between the lime and the surrounding soil.

The suggested principle of direct clay stabilization by lime is that calcium ions from the piles migrate outward into the surrounding soil and react beneficially in the manner described earlier. Several U.S. authors describe the use of 150-mm (6-in.)-diameter lime piles in slope stabilization, with the review by Luttenegger and Dickson (8) being indicative of the ideas being expressed. In general, quicklime is used and water added after placement. Montmorillonitic soils are favored for this treatment. Although several case studies are described and the idea of sta-

bilization through lime-clay reaction presented, few scientific data are given. Water flow was believed to promote calcium ion migration.

Considerable attention has been given to the use of lime piles in India, both in the field and in the laboratory. Model tests similar to those described by Chui and Chin (7) have been carried out to investigate such variables as clay type, pile shape, and pile spacing. Presentation of results is, however, rather poor. This means that although the results are interesting, quantitative information cannot be retrieved.

The use of lime piles for improvement of slope stability has been documented in Austria (9) and Thailand (10). Both papers pursue lime migration as the major stabilization mechanism.

A summary of possible stabilizing mechanisms taken from the literature follows:

1. Lateral Consolidation: Quicklime draws in water from the surrounding ground and reacts to form slaked lime, which has a lower density than quicklime and hence expansion occurs. The diameter of the pile can increase by 30 to 70 percent. This expansion is said to cause lateral consolidation of the ground surrounding the pile.

2. Water Content Reduction: The slaking reaction "uses up" some water from the soil surrounding the piles and produces a significant amount of heat. These two processes in combination cause a significant water content reduction.

3. Clay-Lime Reaction: Lime migrates from the piles to a considerable distance. This lime then reacts with, and stabilizes, the ground in a manner described earlier.

4. Reduction in Pore Water Pressure: The slaking reaction in the piles causes a net flow of water toward the pile. This suction reduces pore water pressures in the ground.

## RESEARCH AIMS AND PHILOSOPHY

On the basis of the various suggested principles of operation, an experimental program was devised to study the various stabilization processes independently of one another, where possible. Experiments were designed and initial results were analyzed in order to further develop tests, thus using an iterative approach. In this way it was considered that the mechanisms of operation of lime piles could be determined and quantified.

The technique is to be tested in two full-scale field trials toward the end of the project and a second aim of the laboratory investigations is to provide sufficient data to facilitate design. The field trials should not only provide supportive data on pile performance but allow experimentation with installation techniques. A small-scale field trial on one of the sites has already provided useful data. Following the fieldwork, recommendations will be made concerning site investigation and testing programs necessary for design. A design guide, based on a parallel theoretical study, will be produced, and installation methods and equipment will be recommended, so that the technique may be used in practice with confidence. The first link in the chain is described in this paper.

## LABORATORY INVESTIGATION

### Migration

It appeared from the literature that the most significant stabilizing process would be the transportation of calcium ions from the pile

into the surrounding soil and the subsequent lime clay cementitious reaction. Pile models were created in an 0.4 by 0.4 by 0.4 m (16 in.) rigid box filled with a predominantly illitic lower Lias clay, similar to that of previous researchers (11,12). To facilitate compaction into the box, achieve homogeneity, and create minimal voids, the clays were first mixed to a high moisture content ( $w = 40$  percent; liquidity index = 0.5). Compaction was effected by a small manual "sheepsfoot compactor," designed specifically for this purpose, in approximately 50-mm (2-in.) layers. After placement of the first layer, two manometer tubes were positioned on opposing faces of the box. The ends of the tubes were wrapped in geotextile and placed in a sand reservoir to prevent ingress of clay particles. Once filled, the box was covered in polythene and a static stress of 40 kPa (6 psi) was applied to the surface. The system was then allowed to equilibrate, as dictated by the pore water pressure readings, over a 3-week period. A central pile was then created using a 50-mm (2-in.) -diameter hand auger for excavation and quicklime was compacted using a tamping rod into the resulting hole. The surface stress was then reapplied. Samples were taken using the same hand auger at various distances from the pile over the next 8 weeks and tested for free calcium ions.

No real evidence for migration of lime was found at the positions tested. An acid base indicator (phenolphthalein) was painted onto the clay surface after progressive excavation in order to locate the distance of migration (a lime solution is highly alkaline because of hydroxyl ions). However, no evidence of ion migration further than approximately 20 mm (0.8 in.) from the pile was recorded at any depth. It was believed likely that the successes of the previous authors in testing for lime in a similar experiment were attributable to the scatter of lime on the surface of the clay, because edge contamination is inevitable when forming the pile, and possibly the fluctuating free calcium ion concentration in natural clay, which was the parameter measured. These problems combined to cause the apparently larger migration distances reported by Rogers and Bruce (12).

A further set of experiments examined the effects of moisture content and clay type on the rate and distance of ion migration. Perspex tubes, 32 mm (1.3 in.) in diameter, were filled with clays mixed with the acid-base indicator at different moisture contents. A 6-mm (0.24-in.) -diameter quicklime pile was placed at the center of each tube and the time taken for the ions to reach the edge of the tube (13 mm or 0.51 in.), evidenced by the change of color of the indicator, was recorded. This was achieved by the integration the acid base indicator into the clay, which changed color as the alkaline lime passed through it.

It was concluded in this study that 20 to 30 mm (0.8 to 1.2 in.) migration was all that could be expected in the conditions provided. Higher moisture contents increased the rate of migration, and clay mineralogy also influenced the rate. The latter point could be attributed to increased porosity. It was also noted that migration would occur preferentially along paths of least resistance (i.e., a slip plane that typically has a higher moisture content) as long as moisture continuity was provided. Similar conclusions were reached by Fohs and Kinter (13), investigating lime migration into small blocks of clay.

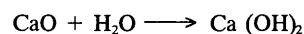
The question of the effect of a flow of water on migration still remains, particularly when associated with a slip plane. The successful migration of lime slurry under a hydraulic head in a fissured shale (10) is understandable. However, the migration recorded by the American authors [e.g., Lutenecker and Dickson (8)] reporting on lime piles in the field was difficult to explain,

especially as no indication is given of what physical signs were used to detect the lime. One explanation considered was that of water flow through the ground. Because of the low permeability of clay, water flow over a significant distance would have also to be accompanied by zones or features of higher permeability, while retaining sufficient clay content for the clay-lime reaction to occur. A reasonable explanation could therefore be that preferential migration occurred due to the increased permeability created by the shear zone of the slip itself. Although attempts to achieve ion migration by this means have been made, in both specifically designed box experiments and an adapted permeability apparatus, they have proved unsuccessful. Other possible influences on ion migration such as vapor, suction, and osmotic pressures are recognized. However, such a detailed study lies beyond the scope of this investigation. These influences will be considered within a study of chemical movement in the ground, which is on the point of commencement.

Despite the possibility of increased migration produced by a water flow, it now seems unlikely that this forms the major stabilization process and so additional processes to explain the undoubted success of the technique had to be considered carefully.

## Expansion

It is possible to calculate the volume of a pile after hydration simply using the equation for slaking

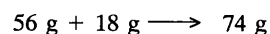
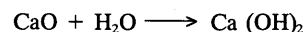


and the relative densities of quicklime and slaked lime.

As mentioned previously (12), the additional volume of the slaked lime in relation to the quicklime is less than the volume of water required by the reaction. This phenomenon was illustrated by radial cracks in the clay surrounding the piles formed in model tests in the laboratory (described later) caused by the slaking reaction. These penetrated a considerable distance down the length of the pile and could only indicate a reduction in volume in the lime-clay system as a whole because no steam was given off and the system was sealed.

## Dehydration

Again, from the stoichiometry of the slaking reaction it is possible to calculate the expected moisture content of the soil after treatment with quicklime. From the equation below the molar masses of the reactants and products are



Given piles of known dimensions and spacing and assuming a density for compacted quicklime, it is relatively straightforward to calculate the volume of water consumed in the entire reaction. This is readily converted into a change in moisture content by assuming an area of treatment and a clay density.

This calculation was carried out for a soil of 30 percent moisture content with 3-m (10-ft) -deep piles of 0.1 m (4 in.) diameter at 1-m (39-in.) spacing. Assuming that all of the material in the

piles reacts, this would give a final moisture content of 29 percent (i.e., very little change).

However, the topic remained troublingly evident in much of the literature, and thus it was considered that an investigation was necessary. A set of tests was carried out on samples of English china clay, which is almost wholly kaolinitic, at different moisture contents and on one lower Lias (predominantly illitic mixed mineralogy) clay sample. Sample of 100-mm (4-in.) diameter were created by compaction at a known moisture content and piles were created using a 12-mm (0.47-in.) rod driven to create a central hole into which quicklime was poured. This was compacted using a smaller rod. The samples were sealed in plastic. After various curing periods, 38-mm (1.5-in.) samples were cut from the clay surrounding the pile and subjected to undrained triaxial compression tests. Moisture contents were also found.

After a curing time of 8 weeks the moisture contents were compared with both the original values and with the calculated value after the water loss caused by slaking. The measured values were significantly lower than those calculated. This was initially attributed to inadequate sealing of the samples, although a subsequent explanation can be postulated. The pile itself will absorb water both during slaking and subsequently into the pore spaces between the particulate slaked lime, and the amount of water that can be absorbed will increase as the pile expands. A very simple calculation of the water required by the pile to come into equilibrium with the original clay moisture content produces values almost identical to those measured.

The significance of this moisture loss was also investigated. Strength improvements associated with these levels of drying were calculated using the formulae of Skempton and Northey (14) and compared with the measured strengths from undrained triaxial tests carried out on the samples. The method of calculation is based on the fact that clays at both the liquid and plastic limit fail at the critical state. Experiments carried out by the authors showed that the undrained shear strength at the plastic limit was 100 times that at liquid limit. As shown in Table 1 the measured and calculated values compare favorably.

In practice, this formula may be used to calculate the improved strength of a clay caused by drying, because little additional drying will occur because of evaporation as the top of the piles were sealed with a clay plug. The extent of the affected area remains a problem. In practice, a very small zone surrounding the pile may become very dry, leaving the rest of the clay at the same original

water content. This seems particularly likely when cracks form. Careful sampling during excavation of the field trials should provide evidence on this subject.

### Pile Strength

Clay-lime pile models were set up in order to study several different factors, pile strength being one of them. A 1.0-m by 1.0-m by 0.5-m (39-in. by 39-in. by 20-in.) deep steel box was fabricated with the facility of a "water-bag" arrangement within its lid to supply an even, maintainable pressure to its contents (Figure 2). The box was divided internally into four equal compartments so that different clay and pile types could be studied simultaneously. The box was filled with an almost wholly kaolinitic English china clay at a moisture content of 48 percent (equivalent to a liquidity index of 0.5) in layers using hand compaction, as in the previous model. The clay was allowed to consolidate under a normal load of one bar (14.5 psi). Manometers and thermocouples were placed in the positions shown during the compaction process. Piles were formed, as before, with diameters of 100 and 150 mm (4 and 6 in.) at two different degrees of lime compaction, a plastic sheet being spread over the clay surface to prevent lime scatter. The 100-mm (4-in.) -diameter piles were compacted in four layers using 10 blows of a 2.5-kg (5.5-lb) compaction hammer, 20 blows being applied to the layers for the 150-mm (6-in.) -diameter pile. A 40-mm (2-in.) -thick clay "cap" was placed on the top of each pile. After the piles were formed the normal stress was reapplied and the system left intact while pore water pressure changes and temperature fluctuations were monitored. Measurements were taken until a state of equilibrium had been established (i.e., cessation of changes in the readings).

Ultimately the individual piles were excavated and 38-mm (1.5-in.) samples tested to destruction to obtain a value for pile strength. The strength of piles was found to be between 300 kPa (44 psi) and 500 kPa (73 psi).

### Pore Water Pressure Changes

The box study previously described considered the changes in pore water pressure both close to, and somewhat removed from, the edge of the pile. These distances are different for the two pile diameters and are illustrated in Figure 2. Two readings were taken close to the piles but only one, at the base, was taken near the edge of the box. The reductions in pore water pressure, or suctions, measured for the 150-mm (6-in.) -diameter uncompacted pile were 8.2 and 10.7 kPa (1.19 and 1.55 psi) close to the pile and 2.5 kPa (0.36 psi) at the edge. The data for the 100-mm (4-in.) -diameter uncompacted pile were 16.2, 12.6, and 3.6 kPa (2.35, 1.83, and 0.52 psi) and for the 100-mm (4-in.) -diameter compacted pile were 13.0, 11.0, and 5.1 kPa (1.89, 1.60, and 0.74 psi), respectively.

Allowing for experimental error, no particular trend relating pore water pressure change to either pile size or degree of compaction has emerged from these or subsequent data, although the pile sizes chosen may be insufficiently dissimilar to discern a difference. It is, however, apparent that the magnitude of the reduction is lower at the edge of the box when compared with that close to the pile in clays of relatively high water content.

To create a better idea of the rate of change across the box, some additional data were retrieved from the original small-box

**TABLE 1 Strength Changes Related to Moisture Content Change**

CLAY TYPE	MOISTURE CONTENT (%)		Cu (kPa)		
	INITIAL	FINAL	INITIAL	FINAL	CALC
LOWER LIAS	42	40	25.5	36.5	36.9
ENGLISH CHINA CLAY	35	33	85	124	126.8
	45	43	26	34	37.9
	55	51	18	27	28.4

Note: 1 kPa = 0.15 lbf



tests. The manometer had been placed 50 mm (2 in.) from the base of the box and 100 mm (4 in.) away from the 50-mm (2-in.) -diameter pile. This was placed in lower Lias clay of the same liquidity index as the china clay previously mentioned. After a similar time period to the readings already mentioned, a reduction of 8.5 kPa (1.23 psi) was reached. If this is compared with the data from the 100-mm (4-in.) -diameter compacted pile at the base of the box, the reduction appears approximately linear with distance away from the pile.

A feature that has been noted in all tests is the formation of radial cracks around the pile. In the large model tests, cracks were

observed to develop within 3 days of pile placement, although without subsequent enlargement. The most pronounced cracks were recorded for the 150-mm (6-in.) -diameter compacted pile, in which four 3- to 5-mm (0.12- to 0.2-in.) -wide cracks developed at 90 degrees to one another and extended from the pile to the edge of the box. The size and extent of cracking appeared to be directly related to pile size and degree of compaction, with no cracks being observed in the 100-mm (4-in.) -diameter uncompacted pile. This is likely to be related to the amount of water required by the lime to react and the pressure on the clay from the expanding pile. It may also be a function of the effect of

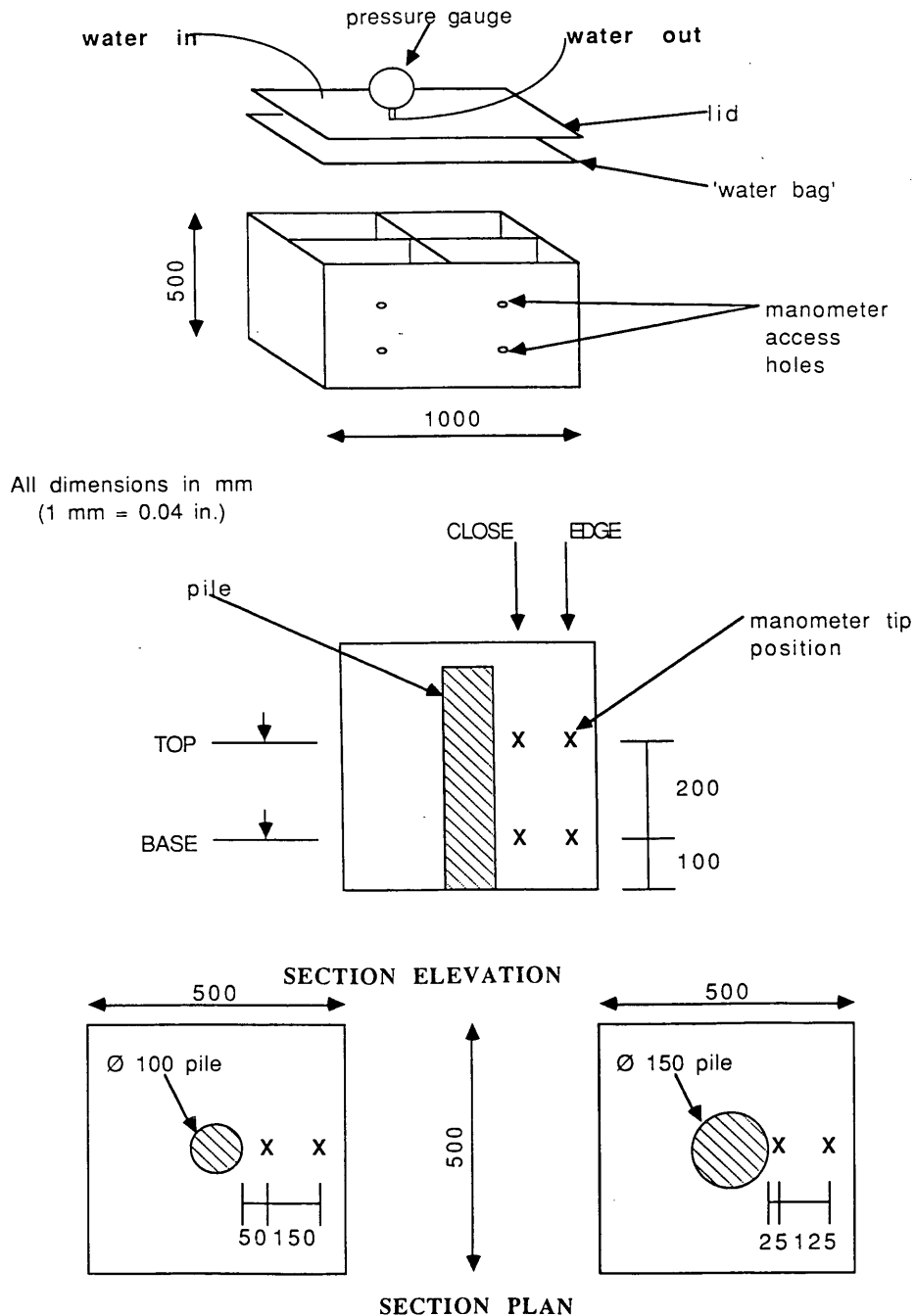


FIGURE 2 Laboratory setup of pile models.

temperature rise, because the recorded temperatures follow a similar pattern to that of the formation of the cracks (i.e., greatest for the largest well compacted pile). The formation of cracks may be quite significant when considering the radius of influence of the reduction in pore water pressure and of moisture content reduction. Careful observations will be made of the development of cracks and their influence in the field trial.

### Overconsolidation of the Shear Plane

The idea of pore water pressure reduction as a benefit to a failing slope was first raised by Rogers and Bruce (12), although its effects were then only considered to be of temporary benefit before the longer-term reactions took place. Its consequences were thus only considered over the time in which it was present and at best the effect could last until pore water pressures naturally resumed initial values over a number of years. In the longer term the effect on any shear failures present within a slope could be more crucial, however, if the reduction in pore water pressure is considered as an increase in effective stress. Such an increase in stress would lead to consolidation of the remolded zone associated with a shear failure and raise the shear strength in this area above residual. This rise in shear strength may be sufficient to prevent further failure when combined with small additional physical or chemical improvements from the processes previously mentioned.

This phenomena was studied in English china clay in the direct shear box. The residual strength parameters for the clay were determined using normal effective stresses of 150, 300, and 400 kPa (22, 44, and 58 psi). Shear strengths of 39, 69, and 80 kPa (5.66, 10.01, and 11.61 psi) were derived, respectively, thus giving a residual friction angle ( $\phi_r'$ ) value of  $11^\circ$ . This is in agreement with published data.

Both normally consolidated and overconsolidated (ranging from slightly to highly) samples were tested for comparative purposes, the latter being typical of cutting slopes studied by Perry (1). The shear surface was formed by rapid winding of the box, initial tests proving that five passes were sufficient to reach the residual state. The sample was then allowed to reconsolidate for 24 hr before being sheared under fully drained conditions at a rate of 0.036 mm/min. (0.0014 in./min.) until a consistent shear stress was achieved. The box was then stopped and allowed to rest overnight. The normal effective stress was then increased by 20 kPa (3 psi) to simulate pore water pressure reduction and the sample was again left overnight. [It should be noted that this value is greater than the suctions measured in the laboratory, but that these refer to relatively wet clays, and an initial field trial produced suctions of approximately 20 kPa (3 psi) 700 mm (28 in.) away from 63-mm (2.5-in.) -diameter piles constructed on a grid in a clay near to its plastic limit]. The 20-kPa (3-psi) increment was then removed and the sample allowed to swell, again overnight, before shearing was resumed. Stress changes were noted at every juncture.

Stoppage alone caused a small but rapid immediate reduction in shear stress in all cases after half an hour, followed by a much slower relaxation recorded after leaving the sample overnight. If shearing was resumed after half an hour, the stress rapidly resumed its initial value, whereas if the sample was left overnight, a small rapid increase in stress over and above that of the original value was generally observed before steady state resumed. The results for a sample overconsolidated to 300 kPa (44 psi) and allowed to swell back to 15 kPa (2 psi), giving an overconsoli-

dation ratio of 20, are presented in Figure 3 and illustrate this trend. It was considered that the small initial reduction in stress could be attributed to pore water pressure dissipation, the pore water pressure being rapidly rebuilt on shearing. The rate of loading was chosen, however, following preliminary testing, to ensure fully drained conditions. The longer-term reduction could be made up of several components, including relaxation of the machine itself and consolidation of the shear plane or shear zone. Most significantly under low normal stresses, the shear surface will be uneven with the platy kaolin crystals tumbling over one another (termed turbulent shearing) rather than being fully aligned (as in sliding shear). It is believed that cessation of shearing could promote a degree of "knitting" of the shear zone, which requires an increase in stress to disrupt when shearing is resumed (the shear surfaces could not be separated when taken out of the box).

The effects of overconsolidation are similar to those previously described for cessation of shear, although they are more pronounced. One important difference shown in Figure 3, however, is that the baseline shear stress rises after overconsolidation and requires considerable further shearing before it falls to the original value. Predictably the effects of overconsolidation were most pronounced in the sample sheared at the lowest normal effective stress, having the most disrupted shear plane, with little or no effect being observed for a normally consolidated sample tested at a high normal effective stress. Such a sample was found to have a smooth easily separable shear surface.

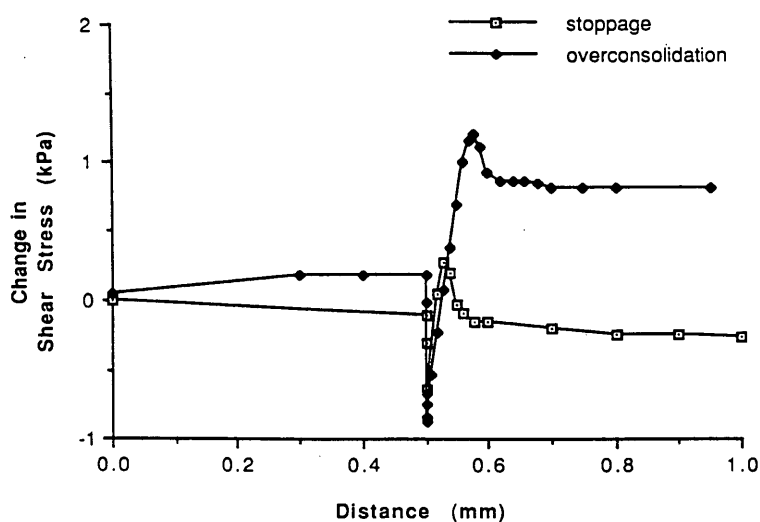
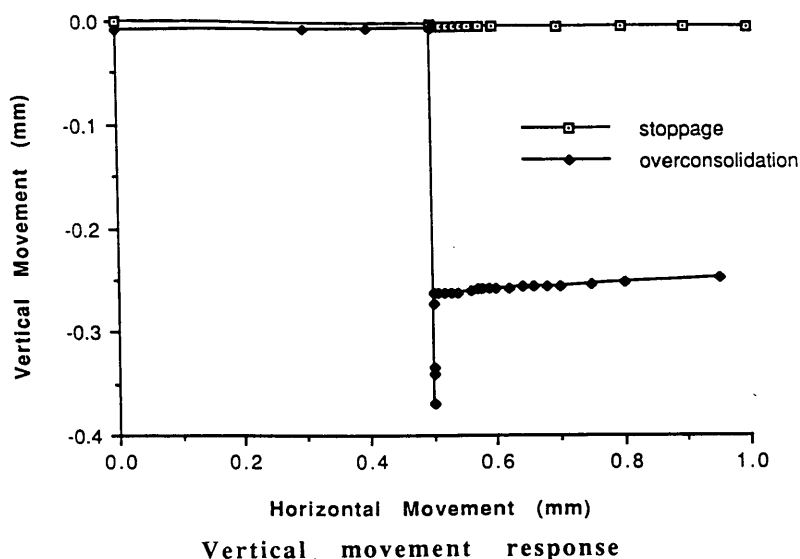
Measurement of vertical movements (Figure 3) show small compressions associated with consolidation for stoppage and much larger compressions (although still small in absolute terms), followed by a small dilation once shearing is resumed for overconsolidation of the shear plane.

A summary of the results obtained to date is given in Table 2, in which the improvements have been quantified in terms of increases in shear strength and equivalent increases in  $\phi_r'$ . The dashed entries for the normally consolidated samples indicate that no clear, significant increase in strength was obtained and the result has been assumed to be zero until further investigations have been conducted.

Because of complications caused by the limited travel and stress changes at the end of the travel of the shear box, ring shear tests have also been conducted. The effect of overconsolidation on a normally consolidated sample with a normal effective stress of 300 kPa (44 psi), if observed over a similar shearing distance to that of the shear boxes, is remarkably similar in shape, whereas vertical movements indicate the creation of a smoother shear surface. However, over a longer distance (10 mm or 0.4 in. as opposed to 1 mm or 0.04 in.) the pattern looks very different. A net rise in shear strength of 1.39 kPa (0.20 psi) is observed before the pre-stop value is resumed.

### CONCLUSIONS

The literature, although providing valuable information about the successful use of lime piles for several applications along with some details of laboratory experimentation, does not adequately prove the modes of operation of lime piles. A list of possible processes leading to successful stabilization was compiled, although it was mostly based on authors' speculation rather than experimental evidence. This formed the basis for the study reported herein, which examines the viability of each theory and



Note: 1 mm = 0.04 in.  
1 kPa = 0.15 lbf

FIGURE 3 Response of direct shear box.

quantifies their relative effects and their mutual influences. The stabilization processes have thus now been isolated and quantified. The second phase of the project, involving further laboratory experiments to confirm the efficacy of the processes under different conditions and, predominantly, field trials, is under way. The initial results of the field work support the findings reported herein.

An allied research project is being carried out to develop a computer model for slope stabilizing techniques, the use of which will allow lime pile treatment of failing or failed slopes to be modeled and designs to be carried out.

The processes that contribute to lime pile stabilization of slopes are as follows:

1. Reduction in pore water pressure;

2. Overconsolidation of the slip-plane, as a consequence of the reduction in pore water pressure, leading to increased strength of the clay along the slip plane;

3. Pile strength;

4. Increased strength of the clay surrounding the piles in a small annular zone because of lime-clay reaction; and

5. Dehydration of the clay, causing a rise in undrained shear strength.

#### ACKNOWLEDGMENTS

The research is supported by the Science and Engineering Research Council and four industrial partners: Geotechnics Ltd., Cementation

TABLE 2 Direct Shear Box: Strength Change Caused by Overconsolidation

Consolidation Stress (kPa)	Shearing Stress (kPa)	O C R at Shear	Rise in kPa	Rise in $\phi'$ (degrees)
150	30	5	0.54	1.03
	75	2	0.23	0.18
	150	1	-	-
300	15	20	1.01	3.85
	30	10	0.44	0.84
	300	1	-	-
400	20	20	1.00	2.86

Note: 1 kPa = 0.15 lbf

Piling and Foundations Ltd., Buxton Lime Industries, and the British Waterways Board. Their financial assistance, technical input, and enthusiasm for the project are gratefully acknowledged.

## REFERENCES

- Perry, J. A Survey of Slope Condition on Motorway Slopes in England and Wales. Research Report RR199, Transport Laboratory, Crowthorne, Berkshire, United Kingdom, 1989.
- State-of-the-Art Report—Lime Stabilization: Reactions, Properties, Design, and Construction. TRB, National Research Council, Washington D.C., 1987.
- Ingles, O. G., and J. B. Metcalf. *Soil Stabilization Principles and Practice*. Butterworths, Stoneham, Mass., 1972.
- Rogers, C. D. F., and S. Glendinning. Stabilization of Embankment Clay Fills Using Lime Piles. In *Proc., International Conference on Engineered Fills*, Newcastle-Upon-Tyne, United Kingdom, 1993, pp. 226–238.
- Kitsugi, K., and R. H. Azakami. Lime-Column Techniques for the Improvement of Clay Ground. In *Proc., Symposium on Recent Developments in Ground Improvement Techniques*, Bangkok, Thailand, 1982, pp. 105–115.
- Wang, W. T. Experimentation on Improving Soft Clay with Lime Columns. In *Proc., International Conference on Engineering Problems of Regional Soils*, 1989, pp. 477–480.
- Chui, K. H., and K. Y. Chin. The Study of Improving Bearing Capacity of Taipei Silt by Using Quicklime Piles. In *Proc., Second Asian Regional Conference on Soil Mechanics and Foundation Engineering*, Vol. 1, 1963, pp. 387–393.
- Lutenegger, A. J., and J. R. Dickson. Experiences with Drilled Lime in the Midwest U.S.A. In *Proc., 4th International Symposium on Landslides*, 1984, pp. 289–293.
- Brandl, H. Stabilization of Slippage-Prone Slopes by Lime Piles. In *Proc., 8th International Conference on Soil Mechanics and Foundation Engineering*, Moscow, USSR, Vol. 4, 1973, pp. 300–301.
- Ruekraitergsa, T., and T. Pisarn. Deep Hole Stabilization for Unstable Clay Shale Embankment. In *Proc., 7th South East Asian Geotechnical Conference*, Hong Kong, 1982, pp. 631–645.
- Ayyar, T. S. R., and K. Ramesan. A Study of Lime Columns in Expansive Clay. In *Proc., Indian Geotechnical Conference*, Visakhapatnam, India, 1989, pp. 185–189.
- Rogers, C. D. R., and C. J. Bruce. Deep Stabilization Using Lime. In *Proc., British Aggregates Construction Materials Industries Lime Stabilization 90 Conference*, Sutton Coldfield, United Kingdom, 1990.
- Fohs, D. G., and C. B. Kinter. Migration of Lime in Compacted Soil. *Public Roads*, Vol. 37, Part 1, 1972, pp. 1–8.
- Skempton, A. W., and R. D. Northey. The Sensitivity of Clays. *Geotechnique*, Vol. 3, 1953, pp. 1–8.

# Lime and Fly Ash Admixture Improvement of Tropical Hawaiian Soils

PETER G. NICHOLSON, VINAI KASHYAP, AND CLINT F. FUJII

A study was performed to evaluate the soil improvement and stabilization potential of several tropical Hawaiian soils. These improvement techniques included stabilization with locally generated high-quality fly ash, and locally available hydrated lime admixtures. Use of these admixtures has shown tremendous potential as an economical method to upgrade the geotechnical properties of several "poor to marginal" types of tropical Hawaiian soils. The study shows such improvements as increase of unconfined compressive strengths; increases in California bearing ratio (CBR) of more than 10-fold; reduction in plasticity; reduction in swell to less than 10 percent of the unstabilized values; greatly increased workability; and changes in moisture-density relationships resulting in lower maximum dry densities, higher optimum water content, and less variation of dry density from the maximum over a much wider range of water contents.

Studies on lime, fly ash, and lime-fly ash stabilization have been conducted on soils in the many regions around the world (see examples in Reference section). Currently several states in the continental United States have written specifications for these applications. Organizations such as the National Lime Association and the American Coal Ash Association have been instrumental in accumulating and disseminating the results of research and case studies in which this type of soil improvement has been applied. In addition, the Beneficial Use of Coal Ash Act implemented by the Federal Highway Administration in 1987 provides an incentive to states by increasing federal funding for projects in which significant amounts of coal ash are used.

The study of using such admixtures to upgrade and enhance the engineering properties of tropical soils of volcanic origin has been extremely limited. This has been partially because the types of equipment and technology for field mixing necessary for achieving the desired results of admixture improvements have not until recently been readily available in certain locations. Furthermore, the unique differences among these soils and those from the more temperate climates and more common geologic settings that have been much more widely studied and tested, have left local authorities with some skepticism about the improvement that may be attained for these soils. Unfortunately, this has led to a lack of good understanding about the engineering properties and characteristics of these soils that may be significantly enhanced by the use of lime and fly ash admixtures. There are currently, and will be in the future, more and more instances of desired construction in tropical regions where significant deposits of these often undesirable soils are found. The recent introduction of coal-

burning power generation to Hawaii has given an incentive to evaluate the useful benefits of an industrial byproduct while providing a very low-cost material that continues to be proven to be of great engineering benefit as a soil admixture in various other regions of the world.

Tropical volcanic soils have significant differences from the more commonly studied (and documented) soils of temperate climates as they have been generated from volcanic parent rock and have been weathered under conditions of high temperatures and humidity with well-defined alternating wet and dry seasons. Among the types of soils that are of particular interest are (a) the highly expansive, high plasticity, so-called "adobe" colluvial clays commonly found on the flanks and at the base of valleys between eroding silica poor basaltic lava flows; (b) residual volcanic soils typically found weathered in place with widely varied degree of weathering in a saprolitic structure; and (c) partially weathered lateritic soils, which are continually leached by rain water, causing a tendency for deterioration of its strength characteristics. Some of these soil types are considered to have particularly "poor" engineering characteristics, exhibiting expansive properties, high plasticity, poor workability, and low strength. An added problem often encountered with these types of soils is their tendency to retain high natural moisture contents that complicate the achievement of desired optimum construction and compaction properties. Many of the regions of the world that have these types of soil conditions are developing areas for which there will continue to be much new engineered construction.

Many of the Hawaiian soils present engineering problems that can be adequately solved by the use of certain types of lime and fly ash soil admixtures. Until recently, the only record of stabilization of these soils were a few early attempts using lime admixtures, which were very costly and of only marginal success. The mechanics of modern field mixing techniques applicable to difficult soils, together with a renewed interest in stabilization of these soils, has sparked an interest in the improvements that may be possible with locally available admixtures. A new electric cogeneration plant, now in service in Hawaii, is generating a fly ash with significant lime content, which by itself or with additional lime would provide an inexpensive source of high-quality stabilizing admixture. The use of this material for soil stabilization would be beneficial for improving soils for development and construction purposes, while at the same time using an industrial waste product that might otherwise require costly transportation and disposal in a region where waste disposal sites are in very short supply.

Presented in this paper is a study of the changes in engineering properties of a variety of these soils with the addition of lime and fly ash admixtures as exemplified through a series of laboratory tests.

P. G. Nicholson and Clint F. Fujii, Department of Civil Engineering, University of Hawaii, 2540 Dole Street, Honolulu, Hawaii, 96822. V. Kashyap, Pacific Geotechnical Engineers, Inc., 1030 Kohou Street, Suite 101, Honolulu, Hawaii 96817.

## PROBLEM IDENTIFICATION

### Tropical Hawaiian Soils

The Hawaiian soils have been formed from the weathering of volcanic rock and debris over a period of millions of years. The soils have unique characteristics because of a combination of their volcanic origin and the weathering conditions of tropical heat and humidity. Most of these soils contain a substantial amount of iron and aluminum (1). Among the soils tested in this study were a range of "poor to marginal" clayey soils from various areas of Oahu, Hawaii, that have been known to present problems in construction and possess a variety of undesirable characteristics. The generally undesirable properties include low strengths, high plasticity, poor workability, difficult compaction, and high swell potential.

### Soils Investigated

The soils tested include two highly plastic "adobe" clays from Manoa and Palolo Valleys, a plastic clay from Kapolei, a silty clay from Kailua, and a silty-clayey soil from Kaneohe consisting of moderate to highly weathered saprolite. These soils represent a range of different "troublesome" soils found in Hawaii and are similar in nature to many other tropical soils found in comparable geologic and climatic regions elsewhere in the world.

The Manoa and Palolo clays are classified as CH soils according to the unified soil classification system [Unified Soil Classification System (USCS), ASTM D-2487], and have a high percentage of high-activity smectite clays. These clays present problems of excessive expansive characteristics, which have caused much damage to structures built in and on them, as well as low shear and compressive strengths, low CBR values, and high plasticity [with plasticity index (PI) values greater than 50 and liquid limits (LLs) above 100]. These soils may also have high natural water contents with values as high as 200 to 300 percent. The high LLs and PI values exhibited by these soils also provide an indicator of further potential problems with engineering properties and workability of these soils.

The Kapolei silty clay (CH) contains considerable histosols. It has a fairly low compressive strength and CBR, poor workability, and a steep compaction curve that makes it difficult to compact to a high relative density in the field.

The Kailua silty clay (MH) may also have a high moisture content in the field. It belongs to the oxisols (soils with low activity clays), and exhibits a high plasticity, low compressive strength and CBR value, and a moderately high swell potential.

The Kaneohe soil is a silty clay that classifies as MH according to USCS with a significant percentage of halloysite. It contains low-activity clays and is characterized by "low specific surfaces, low surface charge densities, or both" (1). This soil typically has a relatively high moisture content in the field in the range of 55 to 75 percent and its compaction characteristics are subject to variability depending on the way it is handled before and during compaction (i.e., drying, remolding, and so on). The soil undergoes irreversible changes in a number of its geotechnical properties upon drying. In general this soil has a moderately low compressive strength and low CBR value.

Each of these soil types was tested with combinations of fly ash and fly ash mixed with 3 percent lime. Only the MH soils were treated with higher percentages of lime without fly ash.

## ADMIXTURE STABILIZATION REACTIONS

The addition of lime, fly ash, and lime-fly ash mixtures causes two basic sets of reactions with the soil: (a) short-term ("immediate") reactions and (b) long-term reactions. The details and theory of these reactions, along with discussion of the physical, chemical, and mineralogical processes involved, have been topics of several earlier studies [for example, Diamond and Kinter (2), Usmen and Bowders (3), and Glenn and Handy (4), and others]. The immediate effect of the introduction of lime or fly ash to the soil (including the lime already present in the fly ash) is to cause flocculation and agglomeration of the clay particles caused by ion exchange at the surfaces of the soil particles. The result of these short-term reactions is to enhance workability and provide an immediate reduction in swell, shrinkage, and plasticity.

The long-term reactions are accomplished over a period of time (many weeks, months, or even years may be required for completion of these reactions) depending on the rate of chemical breakdown and hydration of the silicates and aluminates. This results in further amelioration and binds the soil grains together by the formation of cementitious materials. For cementation to occur, there must be a sufficient source of pozzolans available. Pozzolans are a source of silica or alumina with high surface area that are available for hydration by alkali or alkali earth hydroxides to form cementitious products in the presence of moisture at ordinary temperatures. Soils that do not contain a suitable amount of pozzolans will not react with lime admixtures. Fly ash provides a source of pozzolans for those deficient soils. The extent and reaction rate is affected by "fineness" of the soil, which gives greater surface area, chemical composition of both the fly ash and the soils to be mixed with it, and the temperature, moisture content, and amount of stabilizer used (3).

### FBC Fly Ash Generated in Hawaii

Until recently, Hawaii was the only state in which fly ash was not available (5). Coal is now being imported from Indonesia by Applied Energy Services, Inc. (AES Barber's Point, Inc.) as an energy source for electric power generation from a recently constructed plant that began operation in late 1992. This plant is expected to produce roughly 80,000 yd<sup>3</sup> of ash per annum.

The fly ash is generated using recently developed advanced combustion and emissions control technologies that use a fluidized bed of limestone. This produces an ash (FBC ash) that differs substantially from the typical pulverized coal (PC) class F and C fly ashes, because (a) it contains a significant amount of calcined (CaO) and sulfated sorbent (CaSO<sub>4</sub>) from the limestone injected, and (b) the ash is derived from burning the coal at a lower temperature (1550°F for FBC as opposed to typically 2500°F for PC), and instead of being glassy like the PC ash, the FBC fly ash is composed of dehydroxylated (calcined) clays and other minerals in their oxide form.

The ash used as soil admixture in this study was actually a blend of fly ash (collected by cyclone from the upper regions of the combustion furnace) and bottom ash collected by gravity at the bottom of the furnace mixed in proportions of 75:25 (fly ash to bottom ash by dry weight), representing the approximate proportions actually generated from the coal burning process.

To a large extent the physical and the chemical properties of the fly ash and the bottom ash determine the optimum amount to

be used for enhancing the properties of the soils. These properties also give a general idea about the compounds formed upon hydration and reaction with the soil. Both a test burn ash and the actual fly ash generated from on-line production of the cogeneration plant were analyzed for elemental analysis by the X-ray fluorescence method at the University of Hawaii. Although the locally produced fly ash has significant percentages of total lime already (on the order of 20 percent by dry weight), further addition of lime to the blend when mixed with soils enhances the stabilizing characteristics. The fly ash "blend" itself may be close to the lime retention point (as evidenced by high pH) but when mixed with soil the total percentage of lime is greatly reduced. Thus a further addition of lime may be beneficial when longer-term cementing strength gains are desired.

### Lime Admixture Used

The lime used as a stabilizing agent for these studies was obtained from Brewer Environmental Industries, Inc., on Oahu. The lime is a hydrated commercial grade and was not analyzed.

## TESTS PERFORMED ON HAWAIIAN SOILS

### General Testing Methodology

A series of six types of laboratory tests was performed on each of the soils. These tests were first performed on recompacted soil specimens without admixture followed by additional tests in which fly ash (fly ash blend 75:25) and lime were added in different amounts in order to evaluate the changes in engineering properties of the soils with the addition of these admixtures. Six batches of each soil with admixture were prepared. These mixes consisted of one with 15 percent (by total weight) fly ash, one with 25 percent fly ash, one with 15 percent fly ash plus an additional 3 percent lime, and one each with 3 percent, 5 percent, and 7 percent lime. The test results were compiled and analyzed, and conclusions drawn from them.

Mixing was done without pulverizing either the soil or admixture, to more closely approximate the type of mixing that might be achieved in the field. The soils were mixed with the admixture and water was added (if needed) to raise the moisture content above the plastic limit (PL) of the soil. Pre-curing was allowed for 24 hr, after which the various tests were performed or samples prepared. All recompacted specimens were prepared to approximately 90 percent of the relative compaction defined by Modified Proctor Compaction tests performed on each sample mixture, at a moisture content within 2 percent of the optimum moisture content (OMC).

### Test Results

The tests performed on the soils with and without admixtures included

1. Grain size analyses,
2. Atterberg Limit tests,
3. Modified Proctor compaction,
4. Free swell (expansion with nominal load),

5. CBR: value and swell, and
6. Unconfined compression.

### Grain Size Analyses

Grain size analyses consisted of standard sieve analyses and wet sieving through the #200 sieve in order to properly classify each of the soils. For the soils tested in this study, all were classified as fine grained with only small percentages of coarse-grained fragments. The purpose of performing the #200 sieve analysis was to check the variation in percent fines for the soils with and without admixtures, because lime treatment has previously shown a marked decrease in "fines content." The results for all of the soils were not collected as it became apparent during the testing that the complications of separating the effect of adding the fly ash (which contained a high percentage of -#200 particles) obscured the results.

### Atterberg Limit Tests

The Atterberg Limits assist in soil identification and classification, as well as providing other indicators of possible problems such as swell potential and workability. The PL is generally low and the LL is high for the CH and MH clays tested, which may indicate problems of excessive swell. One of the aims of these experiments was to measure changes of LL and PL with the addition of lime, fly ash, and lime-fly ash admixtures. Previous investigations have shown a marked reduction in PI (the difference between the LL and the PL) with the addition of lime to similar types of soils [Diamond and Kinter (2), and others]. It was speculated that the addition of lime, fly ash, and lime-fly ash mixes should have comparable results, considering the basic reactions involved.

The Atterberg limit tests were performed on the cured soil after a further air drying to a moisture content near or slightly below its expected PL, generally to a moisture content of about 20 percent. In most soils there are substantial time-dependent changes in the PLs (PL) and LLs. The trend for most cases reported appears to be a higher plasticity (PI) after 2 days of curing compared with the value recorded just after the addition of lime, and a subsequent decrease after curing periods of 7 to 28 days (6). Therefore, the reduction in plasticity as a result of admixture addition determined after 2 days of curing—as was generally the case in these experiments—may well be conservative.

The LL for the natural soils ranged from as high as 141 and 123 for the Manoa and Palolo clays, respectively, to 60 for the Kapolei clay. The LL decreased for all of the soils tested with increased amounts of stabilizing admixture. For the CH clays with initially high LL, there was a sharp decrease in LL with the addition of 15 percent fly ash and a smaller additional decrease with 25 percent fly ash. The Kailua soil reacted similarly but from a lower initial LL. For the other silty soils, there was a gradual decrease in LL with the addition of fly ash. The LL for soils treated with lime alone decreased with increased amounts of lime added up to a point, after which further addition of lime tended not to reduce the LL significantly.

The PI for all the soils decreased with increased amounts of lime, and also decreased with increased amount of fly ash added with the exception of Kapolei clay. Addition of fly ash reduced the PI for the CH clays by more than 50 percent, whereas addition

of lime caused two of the three silty-clay soils to become non-plastic. The changes tended to be initially more dramatic, and less so with additional admixture added. For the silty soils, the decrease in PI was more gradual with the addition of fly ash. Although some of the soils showed some decrease in PL with the addition of lime, the change in LL was more than enough to offset that decrease, so that the overall plasticity (PI) continually decreased. The decrease in plasticity is shown in Figure 1 as changes in the PI for the varied amounts of lime and fly ash added to the soils.

With the decrease in PI and LL, the engineering properties of the high-plasticity soils are improved. Additionally, the change in Atterberg Limits along with changes in apparent grain size distributions resulted in altering the USCS classification of the CH clays to MH, and some MH soils to ML (inorganic silts).

#### Modified Proctor Compaction

Many of the engineering properties of a soil, such as shrink and swell potential, compressive strength, and CBR value, permeability, compressibility, and stiffness, are dependent on the moisture and density at which the soil is compacted. Generally a high level of compaction of the soil enhances the most important soil parameters of the soil. Therefore, achieving the desired degree of relative compaction necessary to meet specified or desired properties of a soil is of great importance.

A common problem encountered with the tropical soils is that of a natural water content much higher than optimum. For soils in the field that have such a high moisture content, the increase in OMC and reduction of maximum dry density of the soil with the addition of lime or fly ash admixture, allows the desired relative compaction to be more easily achieved. There is less of a need for the soil to be dried to a lower moisture content before compaction, which in many cases is impractical if not nearly impossible. In addition, the typical "flattening" of the compaction curves that typically occurs with the addition of lime or fly ash admixtures makes it easier to achieve this minimum required density over a wider range of possible moisture contents. This change

in the shape and characteristics of the peak of the compaction curve can allow for significant savings in time, effort, and energy.

Some of the tropical soils of Hawaii (typically the andisols) have compaction properties that vary with "the gradation, crushing strength of the coarse factor, method of pre-treatment or sample preparation, mineral composition and compactive effort" (7). Mitchell and Sitar listed four different moisture-density curves for the same soil for compaction of samples: from the natural state, air dried with each point representing a fresh sample, air dried and using the same sample, and oven dried. The procedure chosen in the laboratory to compact the soil should be representative of the same method in which it is compacted in the field. Ideally the soil in the field should be allowed to dry to within a specified range of moisture content before it is compacted. Therefore the most appropriate method for laboratory test preparation is to air dry the moist sample to the desired moisture and use a fresh batch to plot each point on the curve.

The soils and soil mixtures prepared by remolding for testing in this study were first mixed with fly ash (and water if needed) while moist, and then allowed to cure for a period of up to 2 days before compaction. The gradual decrease in maximum dry density and increase in OMC with the addition of greater amounts of lime and fly ash to the various soils tested are shown in Figure 2. Significant changes were noted for each of the soils with the addition of fly ash, whereas only modest changes were seen for those soils tested with lime admixture.

#### Free Swell Test

The free swell test was performed on remolded specimens of soil and soil mixtures in the laboratory with a nominal load of approximately 7 kPa in order to measure the maximum amount of swell (swell potential) for the soil. Free swell tests were performed by compacting the soils at the OMC in standard 6.35-cm-diameter consolidation molds in five layers with a Harvard miniature compactor by delivering approximately the same energy to each layer as that used in the modified Proctor test, to 90 percent of the maximum dry density as attained by the modified Proctor test.

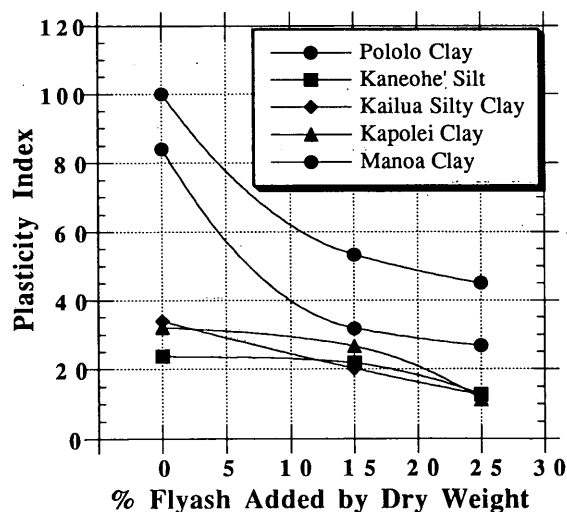
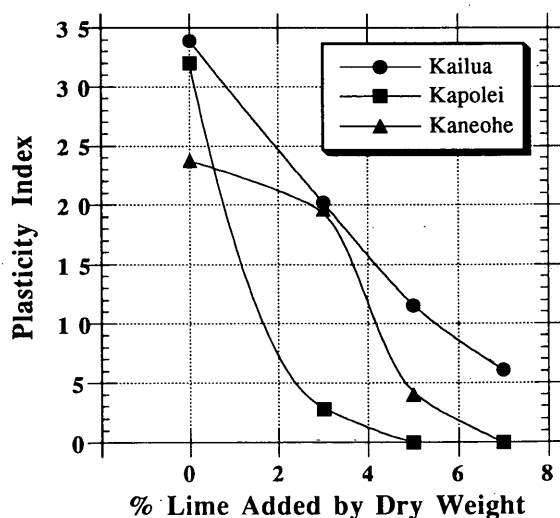


FIGURE 1 Variation of plasticity index with varied amounts of lime and fly ash.



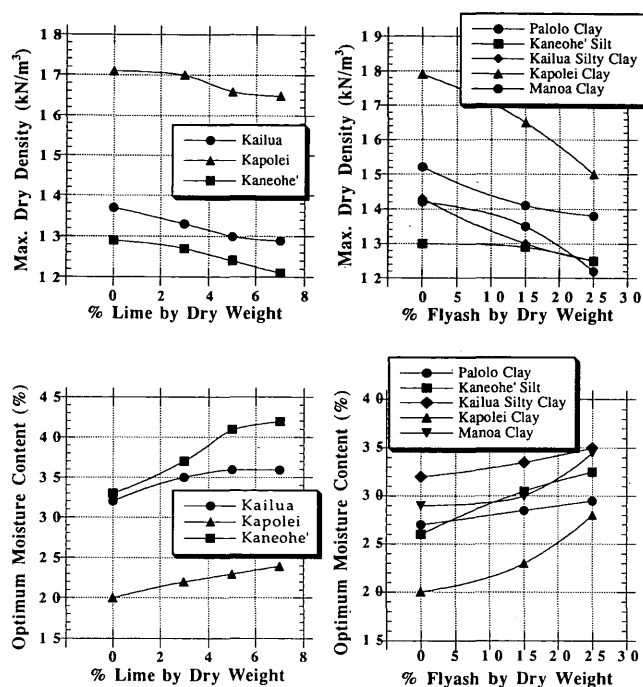


FIGURE 2 Variation of maximum dry density and optimum water content with varied amounts of lime and fly ash.

Tests were performed on specimens after approximately 4 days of curing. During the tests a continuous supply of water was maintained so that water had access to the sample bottom and that water was drawn in through the base of the cell to the soil. The soil specimens were allowed to swell for 2 to 4 days or until the daily measured displacement was less than 3 percent of the total displacement measured, after which the percent swell was calculated.

As expected, there was a decrease in swell potential for all the soils tested with admixtures. The results of the free swell tests for

the soils with varied amounts of admixtures are shown in Figure 3. Results of the tests performed in this study showed that the addition of fly ash greatly reduced the swell for the smectite clays and to a lesser degree for the other soils tested. Lime added to the various soils all but eliminated the free swell measured for each of the soils tested with as little as 3 to 5 percent lime by dry weight of the soil. When using fly ash as an admixture, the most notable decrease was for the smectite clays for which the swell was reduced to less than 25 percent of that of the untreated soil. A further reduction of the swell potential was observed for all the soils tested, with the addition of lime to the fly ash and soil mixture.

The limited reduction in swell for the Kailua silty clay with fly ash alone may indicate incomplete reactions because of a shortage of lime. Addition of lime to the soil or the use of fly ash with a higher lime content may result in a reduction of swell because of further reaction with the pozzolans present in the soil and fly ash.

### California Bearing Ratio

The CBR value is an indicator of soil strength and bearing capacity that is widely used in the design of the base and subbase material for pavement. Lime-fly ash-stabilized soils are often used for the construction of these pavement layers and also for embankments. The CBR is therefore a familiar indicator test used to evaluate the strength of soils for these applications.

According to the state-of-the-art report on lime stabilization by the Transportation Research Board (8), the CBR is "not appropriate for characterizing the strength of cured soil-lime mixtures," can only be used as a comparison, and has little practical significance or meaning as a measure of strength of stability other than as a relative indicator test.

The measurement of swell is an integral part of the CBR test. The CBR swell value differs from the free-swell value in that there is a significant surcharge on the soil specimen. The CBR swell values measured during this study consistently decreased with the addition of lime.

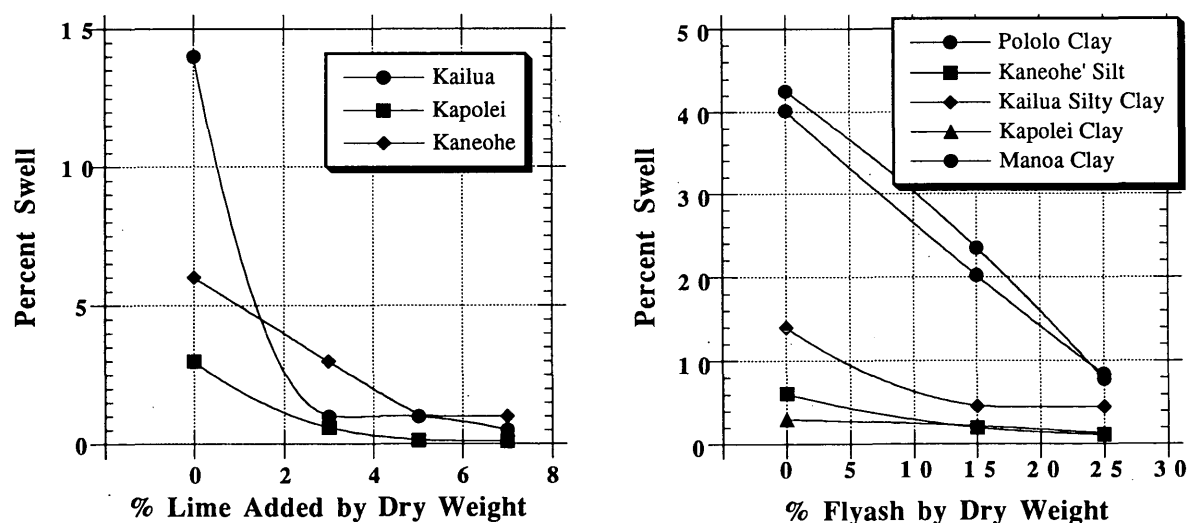


FIGURE 3 Variation of free swell with varied amounts of lime and fly ash.

To simulate the compaction carried out in the field, the soil-lime-fly ash mixtures were compacted to 90 percent of the maximum dry density as obtained from the modified Proctor compaction after curing at the OMC. Specimens were then soaked in water for a further 96 hr under a surcharge weight of 5.72 kg. After swell was measured, the CBR values were then recorded according to ASTM standards (method D-1883).

All of the soils tested had initially very low CBR values. With the addition of fly ash there was a gradual increase for all the soils, although the fly ash alone did not increase the CBR value by much. The most significant increase using fly ash admixture was for the Kapolei clay, for which the CBR increased to 10.8 from 5. A deficiency in the lime content of the fly ash-soil mixtures may be the reason for the low CBR values. When 3 percent lime was added to the 15 percent fly ash and soil mixture, there was a dramatic increase in CBR. For the soils tested with the addition of lime, dramatic increases in CBR were noted with as little as 3 percent lime, and much smaller increases with further addition of lime.

The CBR swell was reduced nearly linearly with the addition of different amounts of fly ash, and when lime or lime-fly ash mixtures were used with only 3 percent lime, the swell was reduced to 1 percent or less for all the soils.

The variation of CBR values obtained for the various soils and admixture combinations tested is shown in Figure 4.

#### Unconfined Compression Test

The compressive strength of a soil is an important factor in evaluating the design criteria for use as a pavement construction material. The lime and fly ash stabilization of soil in most cases tends to increase the strength of the soil and therefore it becomes not only a cost-effective and efficient material for use in embankment construction and earth fills, but also compares favorably with asphalt construction as an approach to upgrading unpaved roads.

The gain in strength of lime and fly ash-stabilized soil is primarily caused by the formation of various calcium silicate hydrates and calcium aluminate hydrates. The exact products

formed, however, vary with the kind of clay mineralogy and the reaction conditions, including temperature, moisture, and curing conditions.

In undertaking a study of the optimum amount of fly ash to be used for the best strength gain results, two papers were used as guidelines. One study (9) used eight different fly ashes and two limes to study the variation in strength properties of four natural soils (a dune sand, a friable loess, an alluvial clay, and a highly plastic gumbotil) with different mixes of lime and fly ash. A second study was performed using lime and industrial wastes for the stabilization of volcanic ash soils or loams in Japan with lime mixed with industrial waste ash (10). The soils tested in the second study may be similar in many regards to some of the regional soils found in Hawaii. The changes in properties for different mixes were correlated to the intensities measured through the X-ray diffraction method (10).

When lime is to be mixed with fly ash, it has been suggested that for "a given ratio of lime to fly ash, the compressive strength of the lime-fly ash-soil mixture will increase with an increase in the amount of lime and fly ash used" (11), although there has been some discussion that there may be an upper limit at which no further strength gain should be expected.

Strength gains for clayey soils treated with lime have been reported through many case studies for roadways and airport runway subgrades. The strength gains have typically been reported as comparative CBR values and as increased unconfined compressive strengths, as used for soil cements.

The unconfined compressive strength tests in this study were performed on soils compacted to 90 percent RC based on the modified Proctor compaction results. The soils were first mixed with the lime and fly ash, to which water was then added. The soil mixtures were allowed to cure for one day, after which the soil specimens were compacted at optimum moisture. Samples were the same size as the mold used for the modified Proctor compaction (101.6 mm diameter, 116.43 mm height). ASTM method, designation D-5102, was followed in tests in which specimens were cured at a temperature of approximately 22°C. Each specimen was sealed in airtight polythene sheets. Cured specimens

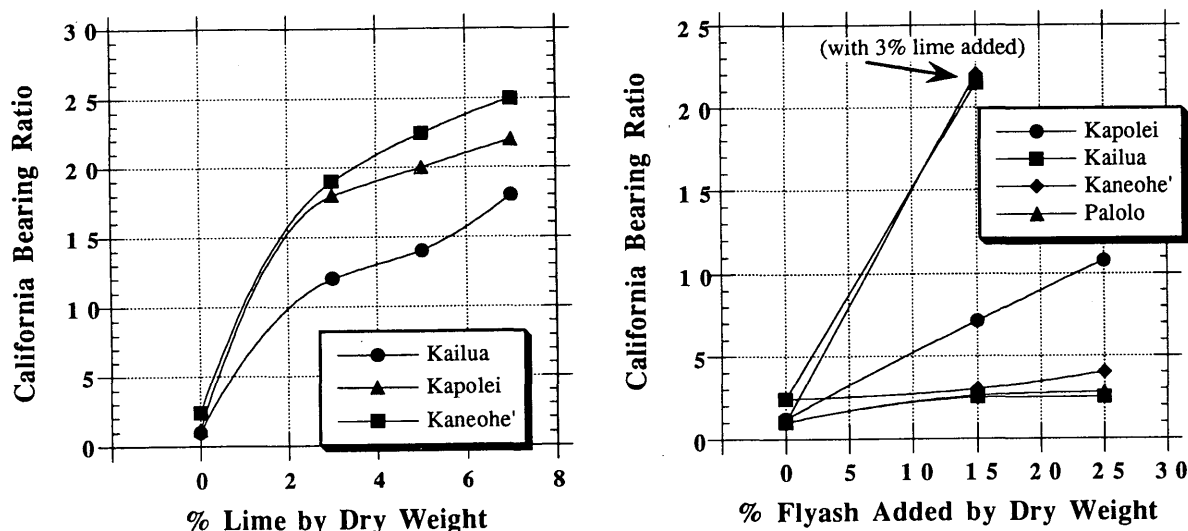


FIGURE 4 Variation of CBR values with varied amounts of lime and fly ash.

TABLE 1 Unconfined Compressive Strengths (kPa) for Soils Tested With and Without Lime and Fly Ash

	Palolo				Kaneohe								Manoa			
%Ash	0	15	25	15	0	15	25	15	0	0	0	0	0	15	25	15
% Lime	0	0	0	3	0	0	0	3	3	5	7	0	0	0	0	3
1-Day	347	200	98	358	517	245	209	862	352	400	414	349	120	203	332	
7-Day		349	289	388		302	249	861	461	517	1117		307	259	395	
28-Day		651	395	470		397	299	1676	862	1082	1862		599	350	484	

	Kapolei							Kailua						
%Ash	0	15	25	15				0	15	25	15			
% Lime	0	0	0	3	3	5	7	0	0	0	3	3	5	7
1-Day	444	523	962	885	272	173	184	433	451	195	572	291	332	330
7-Day		914	1368	1599	433	465	839		500	396	951	323	417	753
28-Day		1134	1993	1951	1143	1276	2306		659	520	1238	577	728	1110

were then randomly picked for testing after 1, 7, and 28 days. Maximum stresses recorded for the soils are presented in Table 1.

For some of the soils there was an initial loss in compressive strength with the addition of fly ash, but strength was typically regained and increased with time. Studies have shown that fly ash-stabilized soils continue to gain significant strength at a fairly steady rate for at least 90 days. It is suggested that further aging would also provide significantly greater strength gains for these soils. An explanation for this initial loss in unconfined compressive strength is that as the soils are altered into more friable, "less clayey" form, their cohesive strength may decline while their frictional strength is increased. This hypothesis was supported by performing a few undrained triaxial tests on those soils for which there was a significant loss of unconfined strength reported. The results of the triaxial tests confirmed that the treated soils had an initial strength gain when confined and that the strength continually increased with time.

Some additional tests were performed with the 3 percent lime added to the 15 percent fly ash and soil mixtures (3:15:82). Tests were also performed on soils stabilized with 3, 5, and 7 percent lime. The results of those additional tests showed that a significant increase in the unconfined strengths could be expected for the 3:15:82 mixtures (typically twice that of the 15 percent fly ash mixtures), and that those strengths achieved were considerably greater than those achieved for the mixtures with up to 7 percent lime without fly ash.

## CONCLUSION

These studies have demonstrated the potential for stabilization and improvement of a variety of "poor to marginal" quality tropical soils with locally available materials. The local Hawaiian soils tested appear to be especially well suited for improvement by lime admixture stabilization, exemplified by dramatic improvements in critical geotechnical properties shown by laboratory tests. The studies also showed potential for dramatic improvement with a low-cost, high-quality admixture generated as an industrial by-product from a coal-burning electrical cogeneration plant. Although the locally available fly ash by itself is lime rich with more than 20 percent total lime content by weight, when used as a soil admixture at 15 percent by dry weight of the soil, the lime content

is dramatically diluted to 3 to 4 percent. Using a blend of the fly ash with a small percentage of additional lime produces even more dramatic results while still providing a cost-effective alternative to designing with (or disposing of) these soils. Test results show that treatment with lime, fly ash, or a combination of fly ash and lime, can be an effective and cost-efficient method of soil stabilization. The study also shows that to attain desired attributes and engineering properties for some of the tropical soils, use of the fly ash may provide better results than a much more expensive treatment by lime alone where more than double the amount of lime was added to the soil. This result is most likely because of the source of pozzolans provided by the fly ash that may not be available from the natural soils.

Although many projects have been completed and approved on the basis of past experience and research done on lime, fly ash, and lime-fly ash admixture stabilization in other geologic and climatic environments, these stabilization methods have not yet been generally accepted or widely applied in Hawaii. These preliminary tests represent the beginning of the verification of applicability of lime and the locally generated ash as practical and cost-efficient soil improvement admixtures to the local soils.

## ACKNOWLEDGMENTS

The tests performed as part of this study were sponsored by grants from Fewell Geotechnical Engineering, Ltd., and AES Barbers Point, Inc., and that support is gratefully appreciated.

## REFERENCES

1. Uehara, G. Soil Science for the Tropics. In *Proc., American Society of Civil Engineers Geotechnical Engineering Division Specialty Conference, Engineering and Construction in Tropical and Residual Soils*, New York, N.Y., 1982, pp. 13.
2. Diamond, S., and E. B. Kinter. Mechanisms of Soil-Lime Stabilization: An Interpretive Review. In *Highway Research Record 92*, HRB, National Research Council, Washington, D.C., 1965, pp. 83-96.
3. Usmen, M. A., and J. J. Bowders, Jr. Stabilization Characteristics of Class F Fly Ash. In *Transportation Research Record 1288*, TRB, National Research Council, Washington, D.C., 1990, pp. 59-60.
4. Glenn, G. R., and R. L. Handy. Lime-Clay Mineral Reaction Products. In *Highway Research Record 29*, HRB, National Research Council, Washington, D.C., 1963, pp. 70-82.